Advances in Understanding High-Mass X-ray Binaries with *INTEGRAL* and Future Directions

Peter Kretschmar[*,a], Felix Fürst[b], Lara Sidoli[c], Enrico Bozzo[d], Julia Alfonso-Garzón[e],
Arash Bodaghee[f], Sylvain Chaty[g,h], Masha Chernyakova[i,j], Carlo Ferrigno[d],
Antonios Manousakis[k,l], Ignacio Negueruela[m], Konstantin Postnov[n,o], Adamantia Paizis[c],
Pablo Reig[p,q], José Joaquín Rodes-Roca[r,s], Sergey Tsygankov[t,u], Antony J. Bird[v],
Matthias Bissinger né Kühnel[w], Pere Blay[x], Isabel Caballero[y], Malcolm J. Coe[v], Albert Domingo[e],
Victor Doroshenko[z,u], Lorenzo Ducci[d,z], Maurizio Falanga[A], Sergei A. Grebenev[u],
Victoria Grinberg[z], Paul Hemphill[B], Ingo Kreykenbohm[C,w], Sonja Kreykenbohm né Fritz[D,C],
Jian Li[E], Alexander A. Lutovinov[u], Silvia Martínez-Núñez[F], J. Miguel Mas-Hesse[e],
Nicola Masetti[G,H], Vanessa A. McBride[I,J,K], Andrii Neronov[h,d], Katja Pottschmidt[L,M],
Jérôme Rodriguez[g], Patrizia Romano[N], Richard E. Rothschild[O], Andrea Santangelo[z],
Vito Sguera[G], Rüdiger Staubert[z], John A. Tomsick[P], José Miguel Torrejón[r,s], Diego F. Torres[Q,R],
Roland Walter[d], Jörn Wilms[C,w], Colleen A. Wilson-Hodge[S], Shu Zhang[T]

[a] *European Space Astronomy Centre (ESA/ESAC), Operations Department, E-28692 Villanueva de la Cañada (Madrid), Spain*
[b] *Quasar Science Resources S.L for ESA, European Space Astronomy Centre (ESA/ESAC), Operations Department, E-28692 Villanueva de la Cañada (Madrid), Spain*
[c] *INAF – IASF, Istituto di Astrofisica Spaziale e Fisica Cosmica, Via A. Corti 12, I-20133 Milano, Italy*
[d] *Department of Astronomy, ISDC, University of Geneva, Chemin d'Ecogia 16, CH-1290 Versoix, Switzerland*
[e] *Centro de Astrobiología – Departamento de Astrofísica (CSIC-INTA), E-28692 Villanueva de la Cañada (Madrid), Spain*
[f] *Department of Chemistry, Physics and Astronomy, Georgia College and State University, Milledgeville, GA 31061, USA*
[g] *AIM, CEA, CNRS, Université Paris-Saclay, Université de Paris, F-91191 Gif-sur-Yvette, France*
[h] *Université de Paris, CNRS, Astroparticule et Cosmologie, F-75006 Paris, France*
[i] *School of Physical Sciences and CfAR, Dublin City University, Dublin 9, Ireland*
[j] *Dublin Institute for Advanced Studies, 31 Fitzwilliam Place, Dublin 2, Ireland*
[k] *Department of Applied Physics & Astronomy, University of Sharjah, Sharjah, UAE*
[l] *Sharjah Academy of Astronomy, Space Sciences, and Technology (SAASST), Sharjah, UAE*
[m] *Department of Applied Physics, University of Alicante, E-03080 Alicante, Spain*
[n] *Sternberg Astronomical Institute, Moscow State University, 119234, Moscow, Russia*
[o] *Kazan Federal University, Kazan, Russia*
[p] *Institute of Astrophysics, Foundation for Research and Technology-Hellas, 71110 Heraklion, Crete, Greece*
[q] *University of Crete, Physics Department & Institute of Theoretical & Computational Physics, 70013 Heraklion, Crete, Greece*
[r] *Department of Physics, Systems Engineering and Signal Theory, University of Alicante, E-03690 Alicante, Spain*
[s] *University Institute of Physics Applied to Sciences and Technologies, University of Alicante, E-03690 Alicante, Spain*
[t] *Department of Physics and Astronomy, FI-20014 University of Turku, Finland*
[u] *Space Research Institute of the Russian Academy of Sciences, Profsoyuznaya Str. 84/32, Moscow 117997, Russia*
[v] *School of Physics and Astronomy, Faculty of Physical Sciences and Engineering, University of Southampton, Southampton SO17 1BJ, UK*
[w] *Erlangen Centre for Astroparticle Physics (ECAP), Erwin-Rommel-Strasse 1, 91058 Erlangen, Germany*
[x] *Universidad Internacional de Valencia - VIU, C/Pintor Sorolla 21, 46002, Valencia, Spain*
[y] *Aurora Technology B.V. for ESA, European Space Astronomy Centre (ESA/ESAC), Operations Department, E-28692 Villanueva de la Cañada (Madrid), Spain*
[z] *Institut für Astronomie und Astrophysik, Universität Tübingen, Sand 1, 72076 Tübingen, Germany*
[A] *International Space Science Institute (ISSI), Hallerstrasse 6, CH-3012 Bern*
[B] *MIT Kavli Institute for Astrophysics and Space Research, Massachusetts Institute of Technology, Cambridge, MA 02139, USA*
[C] *Dr. Karl Remeis-Sternwarte, Friedrich-Alexander-Universität Erlangen-Nürnberg, Sternwartstr. 7, D-96049 Bamberg, Germany*
[D] *Franz-Ludwig-Gymnasium, Franz-Ludwig-Strasse 13, 96047 Bamberg*
[E] *Deutsches Elektronen Synchrotron DESY, D-15738 Zeuthen, Germany*
[F] *Instituto de Física de Cantabria (CSIC-Universidad de Cantabria), E-39005, Santander, Spain*
[G] *INAF – OAS, Osservatorio di Astrofisica e Scienza dello Spazio, via Gobetti 93/3, I-40129 Bologna, Italy*
[H] *Departamento de Ciencias Físicas, Universidad Andrés Bello, Fernández Concha 700, Las Condes, Santiago, Chile*
[I] *South African Astronomical Observatory, Observatory Road, Observatory, 7925, Cape Town, RSA*
[J] *Inter-University Institute for Data-Intensive Astronomy, Department of Astronomy, University of Cape Town, Private Bag X3, Rondebosch 7701, South Africa*

[*] Corresponding author.

[K] *IAU-Office of Astronomy for Development, P.O. Box 9, 7935 Observatory, South Africa*

[L] *CRESST, Department of Physics, and Center for Space Science and Technology, UMBC, Baltimore, MD 21250, USA*

[M] *NASA Goddard Space Flight Center, Greenbelt, MD 20771, USA*

[N] *INAF – Osservatorio Astronomico di Brera, Via E. Bianchi 46, I-23807 Merate, Italy*

[O] *Center for Astrophysics and Space Sciences, University of California, San Diego, 9500 Gilman Drive, La Jolla, CA 920093-0424, USA*

[P] *Space Sciences Laboratory, 7 Gauss Way, University of California, Berkeley, CA 94720-7450, USA*

[Q] *Institute of Space Sciences (ICE, CSIC), Campus UAB, Carrer de Can Magrans s/n, E-08193 Barcelona, Spain; Institut d'Estudis Espacials de Catalunya (IEEC), Gran Capitá 2-4, E-08034 Barcelona, Spain*

[R] *Institució Catalana de Recerca i Estudis Avançats (ICREA), E-08010 Barcelona, Spain*

[S] *ST12 Astrophysics Branch, NASA Marshall Space Flight Center, Huntsville, AL 35812, USA*

[T] *Key Laboratory of Particle Astrophysics, Institute of High Energy Physics, Chinese Academy of Sciences, 19B Yuquan Road, Shijingshan District, 100049, Beijing, China*

ABSTRACT

High mass X-ray binaries are among the brightest X-ray sources in the Milky Way, as well as in nearby Galaxies. Thanks to their highly variable emissions and complex phenomenology, they have attracted the interest of the high energy astrophysical community since the dawn of X-ray Astronomy. In more recent years, they have challenged our comprehension of physical processes in many more energy bands, ranging from the infrared to very high energies.

In this review, we provide a broad but concise summary of the physical processes dominating the emission from high mass X-ray binaries across virtually the whole electromagnetic spectrum. These comprise the interaction of stellar winds with the high gravitational and magnetic fields of compact objects, the behaviour of matter under extreme magnetic and gravity conditions, and the perturbation of the massive star evolutionary processes by presence in a binary system.

We highlight the role of the INTEGRAL mission in the discovery of many of the most interesting objects in the high mass X-ray binary class and its contribution in reviving the interest for these sources over the past two decades. We show how the INTEGRAL discoveries have not only contributed to significantly increase the number of high mass X-ray binaries known, thus advancing our understanding of the population as a whole, but also have opened new windows of investigation that stimulated the multi-wavelength approach nowadays common in most astrophysical research fields.

We conclude the review by providing an overview of future facilities being planned from the X-ray to the very high energy domain that will hopefully help us in finding an answer to the many questions left open after more than 18 years of INTEGRAL scientific observations.

1. Introduction

In High-Mass X-ray Binaries (HMXBs) a compact object – most frequently a neutron star (NS) – accretes matter from a binary companion star with a mass above $\sim 10 M_\odot$. They form a sub-class of X-ray Binaries (XRBs), hosting very massive donors ($M_{donor} \gtrsim 10\,M_\odot$). Galactic HMXBs were among the earliest sources detected by the new field of X-ray astronomy in the 1960's (see, e.g., Giacconi et al., 1962; Chodil et al., 1967; Schreier et al., 1972; Webster and Murdin, 1972) and have remained an intense subject of study ever since. These systems can form during the joint evolution of a pair of massive stars in a sequence involving mass transfer between the companions also before the first supernova explosion (van den Heuvel and Heise, 1972; Tauris et al., 2017). Massive stars influence their environment significantly, through their strong, ionizing ultraviolet radiation, as well as by their strong winds and final explosions which provide a significant input of energy and chemically enriched matter into the interstellar medium (Kudritzki, 2002). Some of these systems may develop further into double compact objects, i.e., future sources of gravitational wave events (see, e.g., van den Heuvel, 2019, and references therein).

Accretion in HMXBs can occur in different ways, as described in Section 2. Observationally, one usually distinguishes between disc-fed systems, showing Roche-Lobe overflow, wind-accreting Supergiant X-ray Binaries (sgHMXBs), with stellar type O or B mass donors – including the sub-class of peculiar Supergiant Fast X-ray Transients (SFXTs) – and Be X-ray Binaries (BeXRBs), in which accretion is driven by the interaction between the compact object and the decretion disc around the mass donor. Another, special class are the Wolf-Rayet X-ray Binaries with only 7 known examples, 6 of which are in other galaxies (Esposito et al., 2015). The very well-known, but peculiar X-ray binary Cyg X-3 is the only example in our Milky Way and has been studied

frequently by *INTEGRAL* (e.g. Beckmann et al., 2007; Zdziarski et al., 2012a; 2012b).

Due to the large field of view of the *INTEGRAL* instruments and their sensitivity, especially in the hard X-ray band, as well as an observing programme concentrating in particular on regions in the Galactic disc, the number of known HMXBs has grown very significantly with *INTEGRAL* and new types of HMXBs have been identified. Specifically, *INTEGRAL* observations led to the detection of very highly absorbed sources (see Sect. 3.2) and to the identification of SFXTs as a new class (see Sect. 3.4). In addition, *INTEGRAL* observed almost all major outbursts from BeXRBs and discovered eight new such systems (see Sect. 3.5). Studies of accreting X-ray pulsars with long pulse periods, have also benefited from the long, uninterrupted observations possible due to the highly-elliptic orbit of *INTEGRAL*. The relatively high fraction of sgHMXBs among the sources found with *INTEGRAL* (see also Table A.1) has led to a more even distribution of known source types and allowed us to fill the parameter space in the spin-period (P_s) over binary (P_b) period diagram (Figure 1), often referred to as "Corbet-Diagram".

While for obvious reasons detections of new HMXB systems were especially frequent in the early years of *INTEGRAL*, when certain areas of the sky where covered in depth for the first time by its instruments (see Table A.1 and its references), the number of identified sources has been steadily growing, also due to the transient nature of many systems. For catalogues of *INTEGRAL* surveys see Revnivtsev et al. (2004); Bird et al. (2006, 2007, 2010); Krivonos et al. (2010, 2012), while results from the Optical Monitor Camera have been published by Alfonso-Garzón et al. (2012). An extensive review of HMXBs in the Milky Way and *INTEGRAL*'s contribution was published by Walter et al. (2015).

In the following, we first summarize in Section 2 the physics and observable phenomena which are behind the rich phenomenology seen in HMXBs by *INTEGRAL* and other satellites. Section 3 summarizes key

results obtained for the different classes of sources and specific example cases. In Section 4 we discuss the distribution of HMXB systems in the Galaxy and their contribution to the overall luminosity of the Galaxy in these wavelengths. Finally, Section 5 focuses on the future of HMXB observations with *INTEGRAL* and other observatories.

2. Physics and observable phenomena

In this Section, we give a short overview of the most important observable phenomena and their physical interpretation. We discuss flux variability, which is linked to variations in the accretion rate (Sects. 2.1, 2.2, 2.3), super-orbital variability (Sect. 2.4), interactions at the magnetosphere (Sect. 2.5), X-ray continuum emission properties of neutron stars (Sect. 2.6), the formation of Cyclotron Resonant Scattering Features (CRSFs, Sect. 2.7), and X-rays from black hole systems (Sect. 2.8).

2.1. X-ray binaries accreting from stellar winds

In the majority of sgHMXBs, the compact object accretes directly from the stellar wind of its companion. Therefore the physical state, structure, and density of the wind has an immediate effect on the accretion rate and hence on the observed X-ray luminosity. A large fraction of the observed aperiodic variability can be qualitatively explained by accretion from a "clumpy" stellar wind; however, quantitative calculations are more difficult to obtain, as outlined below.

2.1.1. Acceleration of stellar winds

The winds of hot luminous stars are mainly driven and accelerated by ultra-violet (UV) resonance lines (like ions of C, N, O, Fe, etc), therefore they are known as line driven winds. The theory of radiatively driven stellar winds was first developed by Castor et al. (1975) (CAK hereafter) and refined in many subsequent publications, see e.g. Kudritzki and Puls (2000); Puls et al. (2008). The acceleration depends on the ionization, excitation, and chemical composition of the stellar wind (see e.g., Eq. 7 in Castor et al., 1975). The amount of ionization is strongly affected by the stellar parameters (e.g. effective temperature, T_{eff}) and in X-ray binary systems also by the X-ray emission of the compact object (see e.g., Sander et al., 2018; Krtička et al., 2018, for recent studies).

From the phenomenological point of view, the stellar wind can be characterized by two parameters: i) the mass loss rate ($\dot{M}$) per unit of time and ii) the terminal velocity (v_∞) at large distances from the star, where wind acceleration becomes insignificant. Typical mass loss rates of massive stars are of the order of $\dot{M} \sim 10^{-6}\,\text{M}_\odot\,\text{yr}^{-1}$. Typical values of the terminal velocity in massive stars are of the order of $v_\infty \sim 500 - 2000\,\text{km s}^{-1}$ (Kudritzki and Puls, 2000; Puls et al., 2008).

Assuming a spherically symmetric (non-rotating) stellar wind, the mass loss rate can be derived from $\dot{M} = 4\pi r^2 \rho(r) v(r)$, where r is the distance from the center of the star, $\rho(r)$ is the density and $v(r)$ is the velocity at that distance. The radial density profile is commonly parametrized assuming a so-called β-velocity law (CAK):

$$v(r) = v_\infty (1 - R_\star/r)^\beta, \tag{1}$$

where $R_\star$ is the stellar radius and β describes the steepness of the wind velocity profile. Both wind terminal velocity (v_∞) and the β-parameter are obtained mainly through spectral fitting of optical/UV data. Typical values of β parameters are in the range between 0.5 and 1 (Kudritzki and Puls, 2000).

2.1.2. Inhomogeneous (clumpy) winds

It was recognized early (Lucy and Solomon, 1970; Lucy and White, 1980) that line driven wind acceleration is likely to be unstable, leading to the formation of shocks and inhomogeneous regions in the wind, commonly referred to as clumps (Owocki and Rybicki, 1984; Owocki et al., 1988). This phenomenon is usually described as line-

deshadowing (or just line-driven) instability (LDI), which will lead to a very unstable outer wind, but which may be damped close to the stellar surface, although Sundqvist and Owocki (2013) also found an unstable wind in near photospheric layers. For most of the wind mass, the dominant overall effect of the instability is to concentrate material into dense clumps, leading to a density contrast up to 10^{4-5} (Puls et al., 2008).

Accounting for clumpy winds can affect the interpretation of observable quantities for the stellar wind (e.g. mass-loss rates derived from spectral line fits) by large factors. LDI simulations tend to favour relatively small clump sizes and masses, compared to some values assumed in studies of X-ray binaries, see Martínez-Núñez et al. (2017) for a detailed discussion.

2.1.3. Corotating interaction regions

The existence of large structures in OB supergiant winds, beyond the typical size expected for the clumps, was suggested already in the 1980s by Mullan (1984), and confirmed later by the observational detection of so-called discrete absorption components (DACs; see, e.g., Underhill, 1975, and references therein). These DACs are understood to be generated by corotating interaction regions (CIRs) induced by irregularities on the stellar surface, related either to dark/bright spots, magnetic loops, or non-radial pulsations (Cranmer and Owocki, 1996). CIRs are spiral-shaped density and velocity perturbations in the stellar wind that can extend outward up to several tens of stellar radii, and the physical properties of such structures (thickness, inclination, velocity and density profiles, number of spiral arms, rotational period) can be determined from the characteristics assumed for the irregularity(ies) from which they originate (see also Fig. 2). Unfortunately, there is a paucity of observational data on DACs in supergiant stars, with all evidence obtained with the IUE satellite (Boggess et al., 1978), due to the lack of an UV facility with comparable or better sensitivity. But their existence is further supported by modulations of the X-ray
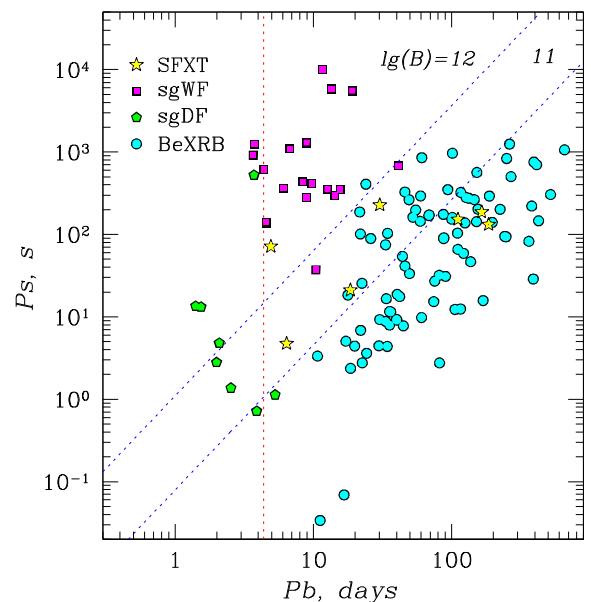

Fig. 1. Spin-period (P_s) over binary (P_b) period diagram ("Corbet diagram") for HMXBs. The different classes are distinguished by colour and symbol shape: SFXTs, disc-fed (sgDF) supergiant binaries (including ultra-luminous X-ray sources (ULXs)), wind-fed (sgWF) supergiant binaries, as well as Be X-ray Binaries (BeXRB). The vertical line indicates the binary period at which a 20 $R_\odot$, 22 $M_\odot$ supergiant fills its Roche lobe. Below the blue lines quasi-spherical accretion from the stellar wind for two different dipole magnetic field strengths B is inhibited by the centrifugal barrier (see Section 2.5), assuming a wind speed of 800 km s^{-1}. Updated from Fig. 4 in Grebenev (2009).
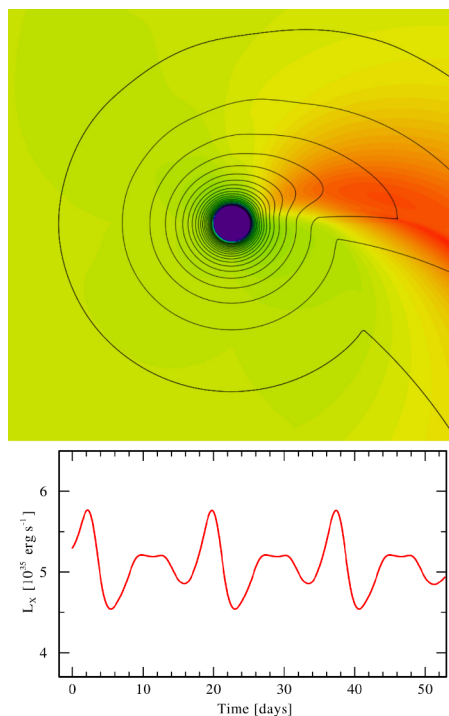
Fig. 2. Top: an example of a single-arm CIR presented by Bozzo et al. (2017a) and obtained from the hydrodynamic code developed by Lobel and Blomme (2008). In this case, the CIR is generated by a bright spot on the stellar surface and it has a period of 10.3 days. The colors code the wind density of the CIR model relative to the density of the supergiant star unperturbed, smooth wind. The maximum over-density in the CIR is by a factor 1.22 (red colors). The black solid lines show 20 overplotted contours of equal radial velocity in the hydrodynamic rotating wind model. Bottom: Simulated long-term light curve of IGR J16493 - 4348, assuming that the superorbital period of ~ 20 days is produced by a single-arm CIR in the top figure.
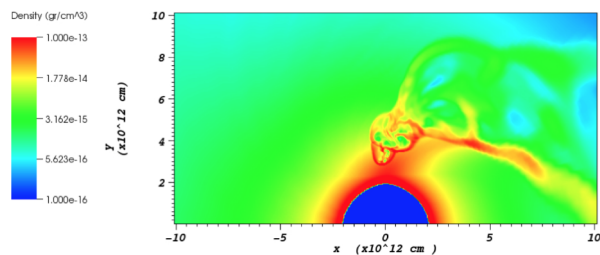

Fig. 3. Snapshot of a hydrodynamic simulation of a model of the Vela X-1 system using the VH1 code developed by John Blondin. Originally Fig. 7.5 in Manousakis (2011).

emission observed in single OB stars (Oskinova et al., 2001; Nazé et al., 2013; Massa et al., 2014).

2.1.4. The influence of the compact object

In wind accreting HMXBs, the presence of the compact object moving through the dense stellar wind close to the massive star significantly influences the wind flow. The gravity of the compact object will focus the wind towards the orbital plane and the position of the accretor; the orbital movement of the companion will lead to the formation of a bow shock and a trailing accretion wake; and finally the X-ray emission will ionize the local environment, changing the availability of resonance lines for acceleration. The ionization state of the wind is defined as ($\xi(r) = L_X/Nr^2$), where L_X is the average X-ray luminosity and N is the gas density at the distance r from the NS (Tarter et al., 1969). X-ray photoionization and heating can lead to the

formation of a Strömgren sphere, where the wind is not accelerated anymore. At the boundary of this a shock is formed and sheets of gas trailing the X-ray source result (Fransson and Fabian, 1980). In extreme cases, wind accretion might be inhibited, leading to a feedback process (e.g. Blondin et al., 1990; Krtička et al., 2018).

In general, in a sgHMXBsystem an accretion wake develops around and behind the compact object and evolves with time, showing fluctuations. Even when assuming a smooth wind as starting condition, the wind is likely to be heavily disrupted due to the hydrodynamical effects, accounting for high X-ray variability even in the absence of clumps (Manousakis and Walter, 2015a). First steps to model the accretion of clumps from a realistic clumpy wind model (Sundqvist et al., 2018) were done by El Mellah et al. (2018), but with a simplified treatment of the impact of photoionization.

We note that most studies relating wind density and X-ray emission effectively assume immediate Bondi-Hoyle accretion of the matter reaching the vicinity of the NS. As shown in Section 2.5, the detailed physics of accretion close to or at the magnetosphere will further modulate the variability, e.g., by "magnetic gating", possibly dampening or enhancing the intrinsic density fluctuations. Simulations combining all these multi-scale, multi-physics effects are still in the future.

2.2. Potential Roche-lobe Overflow systems

While wind accretion is the main mechanism to feed X-ray emission in HMXBs, for a limited subset of these sources the presence of an accretion disc is inferred from their substantially higher luminosity, their position in the spin period over orbital period (Corbet) diagram (Corbet, 1986), marked trends in their spin periods, or their optical lightcurves. Well-known examples are LMC X-4 (Heemskerk and van Paradijs, 1989), Cen X-3 (Tjemkes et al., 1986) and SMC X-1 (Hutchings et al., 1977). Other systems in which transient discs have been reported and/or strongly suggested due to observationally indirect evidences include OAO 1657 - 415 (Jenke et al., 2012; Sidoli and Paizis, 2018), 4U 0114650 (Hu et al., 2017), GX 301 - 2 (Nabizadeh et al., 2019), and possibly IGR J08408 - 4503 (Ducci et al., 2019b); see also Taani et al. (2019) for a recent compilation of possible evidence of disc accretion in HMXBs.

In the spin-period (P_s) over binary (P_b) period diagram (a.k.a. "Corbet diagram", Figure 1) a group of bright X-ray binaries occupies a distinct position in the lower left part of the diagram and these are generally considered to be accreting from a disc. The very high and persistent X-ray flux has an effect on the mass donors, which are "bloated" – their luminosity class and brightness is higher than expected for their mass (which has been accurately measured, unlike in almost all other HMXBs). There may even be X-ray heating of the stellar surface, and this may have an effect on wind acceleration, connected to, but not quite the same as, the effects discussed in Section 2.1.4 above for fainter X-ray sources.

The disc formation has often been ascribed to Roche-lobe Overflow (RLO). Fully-developed RLO will lead to mass transfer on the thermal timescale of the donor, at a rate of about $10^{-3} M_\odot$ yr^{-1}, which will completely extinguish the X-ray source. However, it was shown by Savonije (1978, 1983) that prior to filling the Roche lobe, already a phase of beginning atmospheric RLO may set in, which in the case of a core-hydrogen-burning donor may last many thousands of years and supply mass-transfer rates below $10^{-8} M_\odot$ yr^{-1}. In addition, Quast et al. (2019) showed that a stable RLO phase with mass-transfer rates below $10^{-5} M_\odot$ yr^{-1} – as observed in ULXs – may last for > 200 000 yrs, before full thermal-timescale RLO sets in. On the other hand, recent theoretical publications (El Mellah et al., 2019; Karino et al., 2019) indicate that under certain conditions, especially for slower wind speeds than assumed in the past, also accretion discs may form at least temporarily in wind-accreting systems without the need to invoke Roche-lobe Overflow.

We only briefly mention the well-known X-ray binary SS 433, discussed in its own review as part of this collection (Cherepashchuk et al., 2019). The accreting X-ray pulsar Her X-1 (e.g. Staubert et al., 2017), an intermediate mass system and disc accretor, is also discussed in another review in this volume (Sazonov et al., 2020, Sect. 6.1).

2.3. Be X-ray Binaries and their outbursts

When the optical counterpart in an HMXB is not an evolved (supergiant) star but a Be star, then the system is called Be/X-ray binary (BeXRB, Maraschi et al., 1976; Reig, 2011; Paul and Naik, 2011). The Be components are early-type B (earlier than B3) or late-type O (later than O8) stars with masses in the range 8 – 15 $M_\odot$ whose most prominent property is the presence of a disc around the star's equator. The disc is formed by material ejected from the photosphere, due to the star's rapid rotation in addition to stellar activity (e.g., Balona and Ozuyar, 2020) and not by accretion from an external source. Since material is transported outwards by the same viscosity mechanism that drags matter inwards in an accretion disc, the disc is referred to as a decretion disc. The disc provides the reservoir of material that is accreted by the compact object, in contrast to the stellar wind in sgHMXBs, and is ultimately responsible for the variability observed in these systems at all frequency bands. In the optical and infrared, Be stars show emission lines in their spectra, excess flux that increases with wavelength (with respect to a canonical B star of the same spectral type), and polarization. The emission lines and infrared excess are formed by recombination in the disc. Linear polarization results from Thomson scattering, when photons from the Be star scatter with electrons in the Be disc (Poeckert et al., 1979; Wood et al., 1996; Yudin, 2001; Halonen et al., 2013; Haubois et al., 2014). In the X-rays, BeXRBs show two distinct types of outbursting behaviour: an orbitally-modulated increase in X-ray flux, normally coincident with periastron passage (type I), and giant and long-lasting outbursts (type II). During type I outbursts, the X-ray luminosity is generally below a few 10^{37} erg s^{-1}, while in type II outbursts the luminosity may reach a few 10^{38} erg s^{-1}, close to the Eddington value (Stella et al., 1986; Okazaki and Negueruela, 2001)

The Be phenomenon, i.e., the presence of a circumstellar disc, was first observed in isolated Be stars, without NS companions. In principle, one could turn to the vast amount of studies on classical Be stars to shed light on the properties of BeXRBs since the variability in BeXRBs is closely linked to the evolution of the decretion disc. The disc forms, grows and dissipates on time scales of years. However, it turns out that the presence of a compact companion affects the characteristics and evolution of the disc. Discs in BeXRBs are smaller and denser than in isolated systems (Reig et al., 1997; Zamanov et al., 2001; Okazaki et al., 2002; Reig et al., 2016). The reason is that discs in BeXRBs are truncated at the outer rim (Okazaki and Negueruela, 2001; Okazaki et al., 2002). Disc truncation was also proposed as a natural explanation for the existence of the two different types of outbursts (Okazaki and Negueruela, 2001).

Observational evidence for disc truncation stems from the various correlations of disc parameters with the size of the orbit, expressed as the orbital period P_b, eccentricity e, or orbital separation a. Circumstellar discs in narrow-orbit systems are naturally more affected by the tidal torque exerted by the NS than systems with longer orbital periods. Thus, we expect faster and larger amplitude variations of the observables in systems with tighter orbits. The following correlations support the disc truncation idea:

– *Orbital separation and disc size*. The correlation between the orbital period and the highest historical value of the equivalent width of the Hα line (EW(Hα)) was the first to be suggested as evidence for disc truncation (Reig et al., 1997) and confirmed in subsequent studies (Reig, 2007; Antoniou et al., 2009; Coe and Kirk, 2015; Reig et al., 2016). Because the equivalent width is directly related to the size of the disc (Quirrenbach et al., 1997; Grundstrom and Gies, 2006), these

correlations imply that large discs can only develop in systems in which the two components are far apart. In systems with small orbital separation, the tidal torque exerted by the NS prevents the disc from expanding freely.

– *Orbital period and variability*. Systems with small orbital periods are more variable both in the continuum and line optical emission (Coe et al., 2005; Reig et al., 2016). A similar result was found by analysing the variability in the X-ray band (Reig, 2007). Because the discs in systems with short orbital periods suffer strong tidal torques exerted by their NS, they cannot reach a stable configuration over long timescales.

– *Disc recovery after dissipation*. Systems with shorter orbital periods display larger growth rates after a disc-loss episode. Owing to truncation, the disc becomes denser more rapidly in shorter orbital period systems, and so the equivalent width of the Hα line increases faster. Not only the disc formation, but also the entire formation and dissipation cycle appears to be faster in systems with short orbital periods, while longer timescales are associated with longer orbital periods (Reig et al., 2016).

Disc truncation has implications for theories that explain type II (giant) outbursts. X-ray outbursts are caused by the mass transfer from the Be star's disc to the NS. But if the disc is truncated, how can large amounts of matter be transferred to the NS? The current idea is that the giant outbursts occur when the NS captures a large amount of gas from a warped and eccentric Be disc, highly misaligned with respect to the orbital plane (Okazaki et al., 2013; Martin et al., 2011; 2014). The models show that highly distorted discs result in enhanced mass accretion when the NS gets across the warped part. Observational evidence for misaligned discs comes from optical spectra (Moritani et al., 2011; 2013) and polarization (Reig and Blinov, 2018).

In Be stars, the Hα line can display very different shapes, from single peaked to double-peaked. These varied flavours in the emission line appearance are attributed to the different inclinations of the line of sight with respect to the circumstellar disc (Hanuschik, 1995; Hummel, 1994). Single-peaked profiles are seen (generally showing flank inflections due to non-coherent scattering, producing the wine-bottle profile) in low inclination systems. For intermediate inclinations, Doppler broadening gives rise to double-peaked profiles. For large inclination systems, the outer cooler regions of the disc intercept the line of sight and produce shell profiles (deep narrow absorption cores that go below the continuum level). But, what if all the types of profiles described above are seen in the same source, as in the BeXRB 4U 0115 + 63 (Negueruela et al., 2001; Reig et al., 2007)? Because the spin axis of the Be star cannot change on time scales of days, the appearance of different profiles in the same star can only imply that the disc axis is changing direction. This phenomenon is then interpreted as evidence for a precessing and warped disc. A similar interpretation has been used to explain the complex, three-peaked Hα profiles shown by 1A 0535 + 262 and AX J0049.4-7323 (Moritani et al., 2011; Ducci et al., 2019a). The warping of the disc may be caused by the tidal interaction with the NS (Martin et al., 2011) or by radiation from the central star (Porter, 1998)

Further evidence for warped discs comes from polarization. The light coming from a Be star is polarized. The net polarization is perpendicular to the scattering plane (the plane containing the incident and scattered radiation). Since the photons that get scattered come from the Be star and the scattering medium is the disc, the polarization angle is expected to be perpendicular to the major elongation axis. Therefore, if the disc precesses, we should expect the polarization angle to change. Changes in the optical polarization angle on time scales comparable to the orbital period were reported for the first time during a giant X-ray outburst in the BeXRB 4U 0115 + 63 and were interpreted as variation in the orientation of the disc (Reig and Blinov, 2018).

As with the supergiant systems, BeXRBs in the Milky Way are generally affected by heavy extinction. Advances in our understanding of the class have come through the detailed analysis of a few representative systems (e.g. Reig et al., 2007; Monageng et al., 2017, and

references therein). In contrast, the Small Magellanic Cloud (SMC) contains a very large number of BeXRBs (approaching 100), almost free of interstellar absorption (at a moderately large distance, though), which can be used to perform population studies (Coe and Kirk, 2015). This large number of BeXRBs is unexpected in such a small galaxy, and likely related to a recent burst of star formation due to interaction with the Large Magellanic Cloud (LMC) (Antoniou et al., 2010). Thanks to these properties, the SMC has become the prime laboratory for the study of BeXRBs (Haberl and Sturm, 2016). Optical properties (McBride et al., 2008) and X-ray properties (Galache et al., 2008) can be studied statistically, providing valuable input for the investigation of the accretion process (e.g. Yang et al., 2017), formation mechanisms (e.g. Townsend et al., 2011a) or even strict constraints on models for the production of gravitational wave emitting systems (e.g. Vinciguerra et al., 2020).

2.4. Superorbital modulations

Superorbital modulations are periodic variations of the X-ray luminosity observed from several HMXBs on time-scales longer than their orbital period (typically a factor of 3–10 longer; see, e.g., Kotze and Charles, 2012, and references therein). In a few disc-fed HMXBs, as SMC X-1 and LMC X-4, superorbital variations have been known for decades, and have been clearly detected in all long-term monitoring data collected with *RXTE, INTEGRAL*, and *Swift* (see, e.g., Dage et al., 2019, and references therein). These modulations can be interpreted as being caused by irradiation from the X-rays emitted by the compact object onto a tilted and/or warped accretion disc, which is then forced to precess and periodically obscures the X-ray source (see, e.g., Pringle, 1996; Ogilvie and Dubus, 2001).

Superorbital modulations have also been more recently discovered in several wind-fed sgHMXBs, mainly by using *Swift* data and then confirmed in a few cases also in the *INTEGRAL* and *RXTE* data (see Corbet and Krimm, 2013; Corbet et al., 2018); in some occurrences, only promising indications are found and confirmations are expected in the future when more data will be available. The interpretation of super-orbital modulations in wind-fed systems is less straightforward than in disc accreting binaries. It is unlikely that the presence of temporary accretion discs in wind-fed sgHMXBs could be the cause of the super-orbital modulations, as these periodicities require a mechanism stable over years to produce variations that are detected by folding the decade-long data-sets collected with *INTEGRAL, Swift*, and *RXTE*. The interpretation put forward to explain the super-orbital variability in sgHMXBs involves either the variability of the mass-loss rate from the donor star induced by tidally-regulated oscillations of its outer layers (Koenigsberger et al., 2006), or the presence of a third star in a hierarchical system (Chou and Grindlay, 2001). The problem with these two interpretations is that the first has been shown to work only for strictly circular orbits, while a stable triple hierarchical system implied by the second interpretation would require the presence of a third body in a very distant orbit that is not compatible with the fact that super-orbital modulations in sgHMXBs have a period that is in general not longer than roughly three times the orbital period of these sources (Corbet and Krimm, 2013).

More recently, Bozzo et al. (2017a) proposed an alternative idea according to which superorbital modulations could be related to the interaction between the CIRs of the supergiant (see Sect. 2.1) and the NS orbiting the companion. When the NS encounters the CIR, the different velocity and density of this structure compared to the surrounding stellar wind produces the required long-term variation of the mass accretion rate to give rise to a super-orbital modulation with the observed intensity. As the CIRs do not necessarily have the same rotational period of the supergiant star and their number as well as geometrical properties are not yet well known, different combinations of a single or multiple CIR arms can be invoked in the different sgHMXBs in order to obtain the observed super-orbital periods. Fig. 2 shows an

example of applying this idea to interpret the ∼ 20 days-long superorbital modulation observed from the sgHMXB IGR J16493 - 4348 (with an orbital period of 6.78 days; see, e.g., Corbet and Krimm, 2013, and references therein). In this case, the superorbital modulation is produced by a single-arm CIR with a rotational period of 10.3 days.

Coley et al. (2019) presented an attempt to observationally understand the nature of the superorbital modulation in IGR J16493 - 4348. They combined an analysis of long-term intensity changes traced via *Swift* BAT with a broad-band spectral analysis combining two quasi-simultaneous *Swift* XRT and *NuSTAR* observation at the maximum and minimum phase of the superorbital modulation within a single 20 days cycle. They did not observe any significant differences between the spectral parameters of the two sets, apart from the overall flux change and could not firmly identify the mechanism causing the modulation. Despite the limitation of the short amount of time during which the broad-band spectral properties are measured, mechanisms where a significant change in the neutral hydrogen column density would be expected were considered unlikely. More observations covering much longer integration time scales, e.g., folding data covering many superorbital cycles, are clearly needed in order to advance our understanding on the intriguing superorbital variability of wind-fed sgHMXBs.

2.5. Interactions at the magnetosphere

In the case of accreting NSs their usually strong magnetic fields add another level of complexity to the accretion physics. Note that this is often happening at the scale of a single pixel within the grids of models describing the system at a whole and thus tends to be handled in a very simplified manner in the kind of models described previously.

Interaction of plasma accreting onto a magnetized NS is usually described using an ideal magneto-hydrodynamic (MHD) approximation. In this approximation, the accreting plasma flow is significantly disturbed by the NS magnetic field at the radius (the Alfvén radius, R_A) determined by the balance between accreting plasma pressure (thermal and dynamical) and magnetic pressure. For example, for a spherically symmetric flow characterized by a mass accretion rate $\dot{M}$ onto a NS with mass M_x and dipole magnetic moment μ, one obtains (Elsner and Lamb, 1977):

$$R_A = \left(\frac{\mu^2}{\dot{M}\sqrt{(2GM_x)}} \right)^{2/7}$$

(2)

This is a convenient reference formula to which real values of the magnetospheric boundary R_m, different by different factors in each particular source, can be normalized. It is convenient to write $R_m = \zeta R_A$, where the coefficient ζ is generally a function of $\dot{M}$, μ and other parameters and geometry of the flow (see, e.g., Lai 2014 but also the criticism to this approach expressed by Bozzo et al. 2009b; 2018). Note that the dependence of the Alfvén radius on accretion rate $R_A \propto \dot{M}^{-2/7}$ was indirectly checked by the analysis of aperiodic X-ray variability of bright accreting NSs (Revnivtsev et al., 2009) and is confirmed by the disc accretion torque-luminosity dependence in transient X-ray pulsars with Be components (Sugizaki et al., 2017; Filippova et al., 2017).

Magnetospheric interaction differs for disc or quasi-spherical accretion. The type of accretion (disc or quasi-spherical) is determined by the specific angular momentum of captured matter j_m at the magnetospheric boundary R_m. A disc is formed around the magnetosphere if j_m exceeds the specific Keplerian value at the magnetospheric boundary, $j_m(R_m) > j_K(R_m) = \sqrt{GM_x R_m}$. This is always the case for Roche-lobe overflow, but more rarely occurs in wind-fed systems (see above in Section 2.2). In the opposite case, the accretion flow arriving at the magnetosphere is quasi-spherical.

2.5.1. Disc accretion and propeller effect

In the case of disc accretion, the inner disc radius $R_d = \zeta_d R_A$ is the key parameter directly related to observational phenomena (spin-up/

spin-down transitions in HMXB X-ray pulsars, the propeller effect, etc.). Presently, there are a number of models effectively describing R_d, which is determined by plasma microphysics and the model of plasma-magnetospheric interaction. For example, assuming a purely diamagnetic Shakura-Sunyaev $\alpha-$disc (Shakura and Sunyaev, 1973), one readily finds $\zeta_d \approx \alpha^{2/7}$ (Aly, 1980). In other models (see, e.g., Ghosh and Lamb (1979a,b); Lovelace et al. (1995); Kluźniak and Rappaport (2007), among many others), different effective values of ζ_d are obtained (Bozzo et al., 2009b; Lai, 2014).

From an observational point of view, the plasma-magnetospheric interaction can be probed by spin-up/spin-down studies of X-ray pulsar spin periods and by analysis of non-stationary phenomena (X-ray outbursts). The torques acting on a NS are usually split into spin-up (K_{su}) and spin-down (K_{sd}) parts so that the angular momentum balance implies $I\dot{\omega}_\star = K_{su} - K_{sd}$, where $\omega_\star = 2\pi/P_s$ is the NS spin frequency, I is the NS moment of inertia. The spin-up torque can be written as $K_{su} = \dot{M}\omega_m R_m^2$, where ω_m is the angular frequency of matter at the magnetospheric boundary. The spin-down torque includes the magnetic part $\sim \mu^2/R_m^3$ (which generally may have different sign depending on the twisting of the magnetic field lines) and the part due to the possible mass outflow from the inner disc radius $\sim \dot{M}_{ej}R_m^2\omega_\star$. Note that adding the matter ejection part provides an explanation for the observed strong spin-down episodes in Her X-1 (Klochkov et al., 2009).

A widely accepted approach is to consider, in the first approximation, an equilibrium spin period P_s^{eq} obtained from the balance $K_{su} = K_{sd}$. Obviously, this is a model-dependent quantity, $P_s^{eq}(\dot{M}, \mu, \zeta_d,)$. The notion of an equilibrium spin period is frequently used for indirect estimation of the NS magnetic field from observations of P_s and the X-ray luminosity produced near the NS surface – the latter is related to $\dot{M}$ as $L_x \approx \dot{M}c^2$. This period is close (but not identical) to the critical NS spin period derived from the condition for accretion to be centrifugally allowed, which is obtained by equating the corotation radius to the inner disc radius: $R_c = (GM_x/\omega^{*2})^{1/3} = \zeta_d R_A$. In the first approximation by assuming $\zeta_d = $ const, we get $P_s^{crit} \propto \dot{M}^{-3/7}$. In other words, with decreasing $\dot{M}$ the inner disc radius increases, and once at a given P_s it reaches the corotation radius, accretion is centrifugally inhibited, and the NS enters the so-called 'propeller' state (Illarionov and Sunyaev, 1975). At this stage, the matter can be centrifugally expelled along open magnetic field lines, and magnetically dominated Poynting jets can be formed (Lii et al., 2014). Nevertheless, a residual, strongly reduced X-ray luminosity (compared to the accretion state), can still be sustained by an inefficient plasma entry rate into the magnetosphere caused by diffusion, cusp instabilities, etc., as discussed e.g. by Elsner and Lamb (1984), or can be due to thermal emission from the magnetospheric accretion with $L_{x,m} \simeq GM_x\dot{M}/R_m$, as in the model developed for γ Cas stars by Postnov et al. (2017a).

Variable accreting X-ray sources offer the possibility to probe the accretion-propeller transitions during rise and decay of outbursts. The propeller mechanism is frequently invoked to explain a variety of transient phenomena in HMXBs, including SFXT outbursts (Grebenev and Sunyaev, 2007; Bozzo et al., 2008a), luminosity changes in bright transient X-ray pulsars (Tsygankov et al., 2016a; Lutovinov et al., 2017; Tsygankov et al., 2018) and in ultra-luminous X-ray pulsars (ULXPs) (Tsygankov et al., 2016b).

2.5.2. Quasi-spherical accretion: supersonic (Bondi) vs subsonic (settling)

In the case of quasi-spherical accretion, interaction of plasma at R_m can be responsible for different steady-state and non-stationary phenomena in wind-fed HMXBs (see Section 3.4 below). Here a new important parameter appears – the plasma cooling time at the magnetospheric boundary, which determines the type of magnetosphere inflow and the torques that apply to the NS.

It has long been recognized that plasma entry into the NS magnetosphere in accreting X-ray binaries occurs via an interchange instability – Rayleigh-Taylor (RT) in the case of slowly rotating NSs (Arons and Lea, 1976; Elsner and Lamb, 1977) or Kelvin-Helmholtz

(KH) in rapidly rotating NSs (Burnard et al., 1983). In the case of disc accretion, the plasma entry into the magnetosphere via the RT instability was compellingly demonstrated by multi-dimensional numerical MHD simulations (Kulkarni and Romanova, 2008). However, global MHD simulations of large NS magnetospheres ($\sim 10^9$ cm) have not been performed as yet, and information about physical processes near NS magnetospheres should be inferred from observations.

During quasi-spherical wind accretion onto slowly rotating NSs, there is a characteristic luminosity, $L^* \simeq 4 \times 10^{36}$ erg s^{-1}, that separates two physically distinct accretion regimes: the free-fall Bondi-Hoyle supersonic accretion occurring at higher X-ray luminosity, when the effective Compton cooling time of infalling plasma t_{cool} is shorter than the dynamical free-fall time t_{ff} (Elsner and Lamb, 1984), and subsonic settling accretion at lower luminosities, during which a hot convective shell forms above the NS magnetosphere (Shakura et al., 2012; 2018). In the latter case, a steady plasma entry rate is controlled by plasma cooling (Compton or radiative) and is reduced compared to the maximum possible value determined by the Bondi-Hoyle-Littleton gravitational capture rate from the stellar wind of the optical companion, $\dot{M}_B \simeq \rho_w R_B^2/v_w^3$, by a factor $f(u)^{-1} \approx (t_{cool}/t_{ff})^{1/3} > 2$. Here ρ_w and v_w are the stellar wind density and the velocity relative to the NS, respectively, and $R_B = 2GM_x/v_w^2$ is the Bondi gravitational capture radius. The necessary conditions for settling accretion are met at low-luminosity states in HMXBs (Postnov et al., 2017b).

Settling accretion, unlike supersonic Bondi-Hoyle accretion, enables angular momentum transfer from the magnetosphere, which makes it possible to find an equilibrium NS spin period from the torque balance $K_{su} = K_{sd}$. However, unlike in the disc case, the equilibrium period for a standard NS magnetic field turns out to be proportional to the binary orbital period P_b, and can be very long: $P_s^{eq} \approx P_b(R_m/R_B)^2 \approx 1000$ s $P_{10} \mu_{30}^{12/11} L_{36}^{-4/11} v_8^4$. Here $P_{10} = P_b/10$ d, $L_{36} = L_x/(10^{36}$erg s$^{-1})$, $v_8 = v_w/(1000$ km s$^{-1})$. This can explain the existence of very long-period X-ray pulsars without invoking a super-strong magnetic field for the NSs (Marcu et al., 2011; Sidoli et al., 2017a). Further implications and population synthesis modeling of HMXBs at the settling accretion stage are discussed in Postnov et al. (2018).

At the settling accretion stage, in a rather narrow X-ray luminosity range between $\sim$ a few $\times 10^{35}$ erg s^{-1} and L^*, Compton cooling is still effective enough to enable steady plasma entry at a rate $\dot{M}_x = f(u)_{Comp}\dot{M}_B$ via the RT instability. The classical persistent X-ray pulsars Vela X-1 and GX 301-2 provide suitable examples (Shakura et al., 2012). With decreasing X-ray luminosity, radiative cooling becomes more effective than the Compton one. However, it is unclear whether the RT-mediated plasma entry into the magnetosphere can be steadily sustained by radiative cooling. Indeed, observations of 'off'-states in Vela X-1 show abrupt decreases in the observed X-ray flux by more than an order of magnitude during which X-ray pulsations are clearly visible, suggesting a temporary transition to the radiative cooling regime (Shakura et al., 2013). Similar changes were observed in the SFXT IGR J11215 - 5952 (Sidoli et al., 2007). The application of the settling accretion model to SFXTs is further discussed below in Section 3.4.

2.5.3. Magnetic and centrifugal inhibition of accretion in wind-fed NS HMXBs

Bozzo et al. (2008a) proposed a different approach to identify the diverse accretion regimes in NS HMXB, especially SFXTs, expanding on Burnard et al. (1983), Davies et al. (1979), and Davies and Pringle (1981). Compared to the previous sub-section, this also considers the case of fast rotating NSs, for which plasma penetration into the magnetosphere through the KH instability can be more effective than the RT instability.

This description is based on the relative sizes of three essential radii defined in wind accretion (see Bozzo et al., 2008a, for detailed equations and definitions):

- the accretion radius: R_a is the distance at which the inflowing matter is gravitationally focused toward the NS;
- the magnetospheric radius: R_M, at which the pressure of the NS magnetic field ($\mu^2/(8\pi R_{NS}^6)$, with μ the NS magnetic moment) balances the ram pressure of the inflowing matter;
- the corotation radius: R_{co}, at which the NS angular velocity equals the Keplerian angular velocity.

Assuming typical values for the NS and the stellar wind, these three radii are all of the order of a few times 10^{10} cm.

Changes in the relative position of these radii result into transitions across different regimes for the NS. In particular, the accretion radius and magnetospheric radius depend on the wind parameters ($R_a \propto v_w^{-2}$, $R_a \propto v_w^{-1/6}$, with the wind velocity v_w), which can vary on a wide range of timescales (from seconds to months) and are usually assumed to trigger the transition between the different regimes, together with the corresponding variations in the X-ray luminosity. Below the different regimes of a magnetic rotating NS, subject to a varying stellar wind, are summarised (see also Bozzo et al., 2008b).

Outside the accretion radius: magnetic inhibition of accretion ($R_M > R_a$).

In systems with $R_M > R_a$ the mass flow from the companion star interacts directly with the NS magnetosphere without significant gravitational focusing, forming a bow shock at R_M. The power released in this region L_{shock} is estimated to be relatively low luminosity – a few times 10^{29} erg s^{-1} – and is mainly radiated in the X-ray band. Two different regimes of magnetic inhibition of accretion can be distinguished:

1. *The super-Keplerian magnetic inhibition regime ($R_M > R_a$, R_{co}):* In this case the magnetospheric radius is larger than both the accretion and corotation radii. Matter that is shocked and halted close to R_M cannot proceed further inward, due to the rotational drag of the NS magnetosphere which is locally super-Keplerian. Since magnetospheric rotation is also supersonic, the interaction between the NS magnetic field and matter at R_M results in rotational energy dissipation and thus, NS spin down. This process releases energy at a rate L_{sd}, again of the order of a a few times 10^{29} erg s^{-1} for typical parameters, which adds to the shock luminosity.

2. *The sub-Keplerian magnetic inhibition regime ($R_a < R_M < R_{co}$):* In this case the magnetospheric drag is sub-Keplerian and matter can penetrate the NS magnetosphere through the KH instability. The mass inflow rate across the magnetospheric boundary R_M resulting from this instability depends on the efficiency factor $\eta_{KH} \sim 0.1$, the shear velocity v_{sh} at R_M, and the densities ρ_i and ρ_e inside and outside R_M, respectively. The luminosity released by accretion of this matter onto the NS is estimated differently (see Bozzo et al., 2008a, for details), depending on the choice of the post shock gas velocity or the rotational velocity of the NS magnetosphere, but is estimated to be of the order of a a few times 10^{34} erg s^{-1} for typical parameters.

Inside the accretion radius: $R_M < R_a$.

Once R_M is inside the accretion radius, matter flowing from the companion star is shocked adiabatically at R_a and halted at the NS magnetosphere. In the region between R_a and R_M this matter redistributes itself into an approximately spherical configuration (resembling an "atmosphere"), whose shape and properties are determined by the interaction between matter and NS magnetic field at R_M. A hydrostatic equilibrium ensues when radiative losses inside R_a are negligible; the atmosphere is stationary on dynamical timescales, and a polytropic law of the form $p \propto \rho^{1+1/n}$ can be assumed for the pressure and density of the atmosphere. The value of the polytropic index n depends on the conditions at the inner boundary of the atmosphere, and in particular on the rate at which energy is deposited there. Three different regimes can be distinguished:

1. *The supersonic propeller regime ($R_{co} < R_M < R_a$):* In this case the rotational velocity of the NS magnetosphere at R_M is supersonic; the interaction with matter in the atmosphere leads to dissipation of some of the star's rotational energy and thus spin-down. Turbulent motions are generated at R_M, which convect this energy up through the atmosphere, until it is lost at its outer boundary. Matter that is shocked at $\sim R_a$, reaches the magnetospheric boundary at R_M, where the interaction with the NS magnetic field draws energy from the NS's rotation. According to Pringle and Rees (1972), this gives the largest contribution to the total luminosity in this regime, L_{sd}, of the order of a a few times 10^{31} erg s^{-1} for typical parameters.

2. *The subsonic propeller regime ($R_M < R_a$, R_{co}, $\dot{M}_w < \dot{M}_{lim}$):* The break down of the supersonic propeller regime occurs when the magnetosphere rotation is no longer supersonic with respect to the surrounding material. The structure of the atmosphere changes and the transition to the subsonic propeller regime takes place. Since the rotation of the magnetosphere is subsonic, the atmosphere is roughly adiabatic ($n = 3/2$). In the subsonic propeller regime, the centrifugal barrier does not operate because $R_M < R_{co}$, but the energy input at the base of the atmosphere is still too high for matter to penetrate the magnetosphere at the capture rate $\dot{M}_{capt}$ at which it flows towards the magnetosphere. Nevertheless, a fraction of the matter inflow at R_a is expected to accrete onto the NS, mainly due to the KH instability, leading to a luminosity $L_{KH} > 10^{35}$ erg s^{-1} for typical parameters. The rotational energy dissipation at R_M gives a small contribution L_{sd} of order of 10^{30} erg s^{-1} under the same assumptions.

   The subsonic propeller regime applies until the critical accretion rate $\dot{M}_{lim}$ is reached, at which the gas radiative cooling completely damps convective motions inside the atmosphere. If this cooling takes place, direct accretion at the rate $\dot{M}_{capt}$ onto the NS surface becomes possible.

3. *The direct accretion regime ($R_M < R_a$, R_{co}, $\dot{M}_w > \dot{M}_{lim}$):* If $R_M < R_{co}$ and matter outside the magnetosphere cools efficiently, accretion onto the NS takes place at the full capture rate $\dot{M}_{capt}$. The corresponding luminosity

$$L_{acc} = GM_{NS}\dot{M}_{capt}/R_{NS}$$
$$\simeq 2 \times 10^{35}\dot{M}_{15} \text{ erg s}^{-1}, \tag{3}$$

where $\dot{M}_{15} = \dot{M}_{capt}/10^{15}$ g s^{-1}. This is the standard accretion regime, identified in some of the previous sections as the Bondi-Hoyle accretion.

2.5.4. Accretion regimes in SFXTs

Supergiant Fast X-ray Transients (SFXT) have been established as a class by INTEGRAL and are discussed in detail in Section 3.4 later. Their behaviour is characterized by transient emission and a huge dynamical range during outbursts. This suggests inhibition of accretion between the flares, which can be due to physically different mechanisms. Chronologically, the first model invoked the *magnetospheric gating* due to the magnetic and/or centrifugal propeller effect in a wind-fed system discussed above in Section 2.5 (Grebenev and Sunyaev, 2007; Bozzo et al., 2008a). Indeed, for a fixed value of the mass accretion rate $\dot{M}$, if a NS spins fast enough and/or if its magnetic field strength is sufficiently intense, the magnetospheric radius can end up being either larger than the corotation radius but inside the accretion radius, or larger than both the accretion and corotation radii. Under these circumstances, the system might end up either in the supersonic propeller regime or even in the super-Keplerian propeller regime, where the largest inhibition of accretion occurs due to the magnetic and centrifugal gate. In this regime, the system is expected to be characterized by a low luminosity state ($\lesssim 10^{33}$ erg s^{-1}). Temporary increases in $\dot{M}$, for example related to the clumps in the winds of OB-supergiants (Bozzo et al., 2016b; 2017a), can 'open' the magnetospheric/centrifugal gates and induce transitions to the other different accretion regimes introduced earlier in this

section. Among them, the subsonic propeller or the direct accretion regimes allow a much higher accretion rate onto the compact object to take place, thus explaining the brightest X-ray states observed from the SFXTs ($\gtrsim 10^{36}$–10^{37} erg s^{-1}).

A first attempt to simulate the transitions between different accretion regimes in SFXTs using an hydrodynamically calculated supergiant clumpy wind model has been presented by Bozzo et al. (2016b). The

authors have shown that the effect of the NS rotation coupled with a strong magnetic field can significantly reduce the average luminosity of a sgHMXBand qualitatively explain the difference between classical systems and SFXTs. This is shown in Fig. 4.

The system parameters adopted in the simulation are shown on the top of each figure (for the parameters and circular orbits assumed in this work a separation of $5\,R_\star$ corresponds to an orbital period of
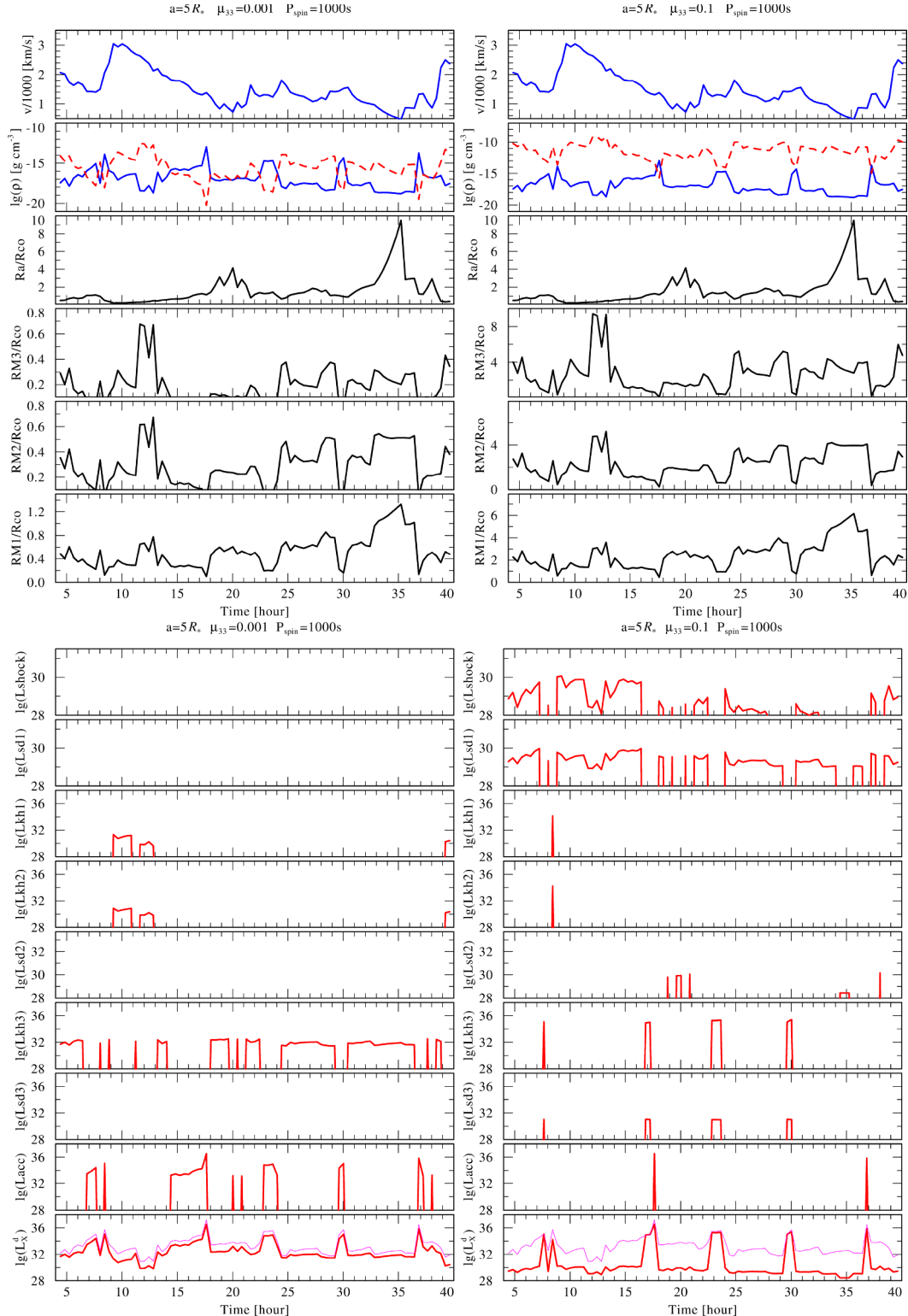

Fig. 4. Results of the simulations of the accretion onto a NS using an hydrodynamically calculated supergiant clumpy wind model and taking into account the gating accretion mechanisms described in Sect. 2.5. This figure combines Figures 7 and 8 of Bozzo et al. (2016b). See text for details.

25.6 days). The top figures both on the left and on the right report the wind velocity and density as a function of time, and all relevant radii to be determined in the gating accretion model (see Sect. 2.5). The bottom figures show the luminosity in each regime that is achieved by the system triggered by the variations of velocity and density in the stellar wind.

The top panel of the top figures shows the instantaneous density of the supergiant wind, while the second panel displays the corresponding density. The red dashed line in these panels represents a critical value of the wind density above which the mass inflow rate toward the compact object becomes large enough to trigger the switch to the direct accretion regime.

In the other panels, $RM1$ corresponds to the magnetospheric radius as defined at the start of Section 2.5.3, $RM2$ to the radius in the supersonic propeller regime, $RM3$ to the subsonic propeller regime. $L_{\rm shock}$ is as above. $L_{\rm sd1}$ corresponds to the spin-down luminosity in the super-Keplerian magnetic inhibition regime, $L_{\rm sd2}$ and $L_{\rm sd3}$ to those in the supersonic and subsonic propeller regimes, respectively. $L_{\rm kh1}$ and $L_{\rm kh2}$ are the two somewhat different estimates for the KH-fueled accretion luminosity in the sub-Keplerian magnetic inhibition regime, while $L_{\rm kh3}$ is the corresponding luminosity in the subsonic propeller regime.

The bottom panels of the bottom figures show the summed X-ray luminosity (red solid line) compared to the luminosity that a system would have if it was always in the direct accretion regime (solid magenta line). The top and bottom figures on the left differ from the corresponding ones on the right only for the assumed NS magnetic field strength. The figures on the left show a representative case of a classical sgHMXB, where the NS magnetic field as a "standard" value close to 10^{12} G and the system in virtually always in the direct accretion regime. The figures on the right show the case where a much stronger NS magnetic field is assumed ("magnetar"-like, 10^{14} G) and how this leads to a very different behaviour in the X-ray domain with a more extreme variability that is closer to what is observed in the SFXTs. With this stronger magnetic field, the velocity and density variations of the stellar wind are able to cause frequent switches among the different accretion regimes due to the fact that the magnetospheric radius, the accretion radius, and the corotation radius are closer to one another.

In a wind-fed system there are also different models to explain the instability of the accretion flow onto the compact object and to interpret the correspondingly induced X-ray variability. As discussed earlier in this section, if we assume the specific case of a "slow" rotating NS, it can be shown that subsonic (settling) accretion onto the NS magnetosphere occurs at X-ray luminosities below $\sim 10^{36}$ erg s^{-1}. In this regime, the entry rate of accreting plasma into the NS magnetosphere is determined by plasma cooling. At low accretion rates, the cooling is radiative (inefficient compared to Compton cooling operating at higher $\dot{M}$), which hampers the development of the RT instability at the magnetospheric boundary. Neglecting the KH instability due to the slow rotation, the mass accretion rate drops down to low values corresponding to luminosities of $\sim 10^{33} - 10^{34}$ erg s^{-1}, which are comparable to those recorded during the SFXT 'low' states.

It is quite possible that in the low-luminosity states of SFXTs no RT-mediated plasma entry into the NS magnetosphere occurs at all. This could be the case if the plasma cooling time is longer than the time a plasma parcel spends near the magnetosphere because of convection in the magnetospheric shell: $t_{\rm cool} > t_{\rm conv} \sim t_{\rm ff}(R_{\rm B}) \sim 300 - 1000$ s. Once this inequality is violated, RT instability can start to develop. Interestingly, the rich phenomenology of X-ray flares of SFXTs as derived from the *XMM-Newton* EXTraS project can naturally be explained by the development of RT instability at low accretion rates (Sidoli et al., 2019).

Additionally, within the context of the settling accretion model, in SFXTs the magnetospheric boundary itself can be made unstable for different reasons. For example, it was conjectured (Shakura et al., 2014) that giant flares in SFXTs are due to a sudden break of the magnetospheric boundary caused by the magnetic field reconnection with the

field carried along with stellar wind blobs. This can give rise to short strong outbursts occurring in the dynamical (free-fall) time scale during which the accretion rate onto the NS reaches the maximum possible Bondi value from the surrounding stellar wind. A tentative evidence for the presence of magnetic fields in the OB supergiant in IGR J11215-5952 was found from ESO-VLT FORS2 spectropolarimetric observations (Hubrig et al., 2018). Another reason for the instability can be due to stellar wind inhomogeneities which can disturb the settling accretion regime and even lead to free-fall Bondi accretion episodes.

So far, only one outburst observed from the SFXTs is difficult to be reconciled with a wind-fed accretion scenario. Independently of the specific assumptions considered for the plasma penetration inside the magnetosphere, the giant outburst observed in 2014 from the SFXT IGR J17544-2619 (Romano et al., 2015) reached an unprecedented X-ray peak luminosity of 3×10^{38} erg s^{-1} that is virtually impossible to achieve in a wind-fed system due to the limitations on the amount of material captured by the NS for any reasonable value of the supergiant companion mass loss rate. Romano et al. (2015) suggested that this event resulted from the temporary formation of a short-lived accretion disc around the NS hosted in this system. Accretion from an even temporary accretion disc can, indeed, lead to much higher luminosities than those achieved in a wind-fed system due to the larger mass accretion rate that can be transported through the disc by viscosity. As of today, this was the only case in which a disc accretion scenario was adopted for an SFXT, but short-lived accretion discs have also been invoked to explain bright X-ray luminosity states in classical sgHMXBs (see, e.g., the case of OAO 1657-415; Xu and Stone, 2019, and references therein)

2.6. Continuum spectrum

Soon after the discovery of X-ray binaries, it became clear that Compton scattering in the hot and dense medium close the compact object leads to the shaping of X-ray radiation (Davidson and Ostriker, 1973). In neutron-star high-mass X-ray binaries, plasma flowing from the limit of the magnetically dominated region (the magnetosphere) is funneled along the magnetic field lines and then falls onto the NS on the magnetic poles forming two or more "accretion columns". The accretion column radius depends on the magnetic field strength and on the accretion rate as (Lamb et al., 1973) $r_{\rm ac} \approx 600 L_{37}^{1/7} B_{12}^{-2/7}$ m, where we have assumed a one solar mass NS with radius of 10 km, luminosity is expressed in units of 10^{37} erg s^{-1}, and the magnetic field in units of 10^{12} G. The spectrum emerging from a hot, dense plasma with a more rarefied medium above is dominated by Compton scattering of some thermal seed photons. At first approximation it has, thus, the spectral shape of an absorbed power-law with an exponential roll-over at high energy. Several empirical functional shapes have been used to describe the spectral energy distribution of these systems (cutoff power law, Fermi-Dirac cutoff, NPEX, etc.; see Coburn et al., 2002, for a collection of model shapes). However, in all of them, the cutoff energy is indicative of the plasma temperature in the accretion column and is of the order of 10 keV or more. At lower energy, for most systems, photoelectric absorption in the local and Galactic medium prevents the investigation of the spectrum. However, for less absorbed systems, such as Her X-1, additional components due to the accretion disc may appear (e.g. Fürst et al., 2013).

Basko and Sunyaev (1976) realized that a high accretion rate would naturally lead to a halt of the infalling material by radiation in the column and identified a critical luminosity at which the formation of a radiatively-induced collisionless shock at some height above the NS surface is unavoidable:

$$L^{\star} \approx 4 \times 10^{36} \frac{r_{\rm ac}}{10^5\,{\rm cm}} \frac{\sigma_{\rm T}}{\sigma_{\rm s}} \frac{10^6\,{\rm cm}}{R} \frac{M}{M_{\odot}}\,{\rm erg\,s^{-1}}, \tag{4}$$

where $r_{\rm ac}$ is the accretion column radius, $\sigma_{\rm s}$ is the cross section in the vertical direction, and M is the neutron star mass. At first

approximation, below this critical luminosity, the plasma is stopped very close to the surface and radiation can escape vertically forming a "pencil beam", while for brighter systems plasma will sink subsonically below the shock and radiation is emitted from the sides of the accretion column in a "fan beam".

In that seminal work, it was noted that a crucial role is played by the value of the opacity due to electron scattering, which is strongly energy dependent in a magnetized plasma, especially at energies comparable to the cyclotron energy in the magnetic field ($E_{cyc} \sim 11.57B_{12}$ keV, see Sect. 2.7). If we indicate with $\sigma_\parallel$ the cross section for electron scattering parallel to the magnetic field lines and with $\sigma_\perp$ the cross section component perpendicular to it, for $E < < E_{cyc}$ one finds $\sigma_\perp \sim \sigma_T$ and $\sigma_\parallel < < \sigma_\perp$ (Canuto et al., 1971). When approaching the cyclotron energy, resonances in the cross section play a crucial role and the extraordinary mode polarization dominates with an angle-dependent cross section which can exceed 10^4 times the Thompson value. Around the cyclotron energy, we thus expect features in the spectrum: the ones that are most known are the cyclotron resonant scattering features, described in Sect. 2.7, which appear in absorption. However, also the continuum formation is influenced by such a strong energy dependency of the cross section.

With the high-sensitivity of the Rossi X-ray Timing Explorer proportional counter array (*RXTE*/PCA), it was noted that there were wiggles appearing around 10 keV on the top of a smooth continuum. However, it was with the giant outburst of EXO 2030 + 375 in 2007 that the issue of whether a broad absorption or emission feature is most appropriate became evident. As depicted in Fig. 5, Klochkov et al. (2007) showed that during a giant outburst, the continuum of this source could be equally described by adding a broad Gaussian feature centered at ~ 14 keV (a "bump") or by two absorption lines at ~ 10 and ~ 20 keV. Spin-phase-resolved analysis revealed a possible absorption feature at much higher energy (~ 60 keV; Klochkov et al., 2008). Since then, more cases arose with such a behaviour: particularly relevant is that of 4U 0115 + 63, for which Müller et al. (2013) showed that the simultaneous presence of emission and absorption features is important for the cyclotron line centroid energy determination. However, the emission feature in this source is

centered at ~ 9 keV, while the absorption line is at about 11 keV, these values significantly differing between each other (see also Ferrigno et al. 2009).

The energy difference between emission and absorption features in 4U 0115 + 63, but also in EXO 2030 + 375 and other sources, disfavors the interpretation of cyclotron scattering being responsible for both features or at least generating them in the same region around the NS. Moreover, the emission region is intrinsically broad and in general broader than the absorption ones. Thus, such emission should originate in a region with lower magnetic field and possibly higher optical depth.

Pioneering works by Meszaros and Nagel (1985a,b) described the spectrum of magnetized accreting NSs as a function of the pulse phase. They exploited the main interactions between matter and radiation in the column to produce the first energy-dependent beam patterns that could qualitatively reproduce the observed properties of pulse profiles and spectra of pulsating HMXBs. Further refinements were focused on the light bending in the strong gravity regime (Riffert and Meszaros, 1988; Meszaros and Riffert, 1988; Leahy and Li, 1995).

A breakthrough in understanding of the spectral characteristics came from the work by Becker et al. (2005) and Becker and Wolff (2007) who managed to find an analytical model to describe the spectral continuum of magnetized XRBs. To understand their work, it should be first noted that there are two regions of the system where photons can be originally generated: the base of the column, where an optically thick thermal mound emits as a black body at 1–2 keV, and the accretion column in which the flowing plasma, in an optically gray regime, emits bremsstrahlung radiation with a temperature of several keV. However, in presence of a magnetic field with cyclotron energy of the order of the plasma temperature, the collisional excitation of the Landau levels around the magnetic field lines strongly modifies the emission spectrum with a prominent angle-dependent spike at the cyclotron energy produced at the expense of higher-energy photons (Riffert et al., 1999). This spectrum is very complex, but it can be simplified by assuming that the cyclotron emission is a delta function and the bremsstrahlung is not modified. In this approximation, seed photons are thus of three kinds: black-body from the base of the column, thermal bremsstrahlung and cyclotron emission (delta-function) from the vertical column body.

Seed photons are then up-scattered in the Compton process. In the presence of a strong magnetic field, the Compton cross section is heavily modified because photons have two polarization states and these interact differently with the electrons bound to the magnetic field lines. To make the problem viable it can be noted that, below the cyclotron energy, the cross section parallel to the magnetic field is heavily suppressed, while perpendicularly it remains essentially the Thompson one. The effective cross section can thus be treated in the model as an angle-average. With these assumptions, it is then possible to compute the transfer function for seed photons as they diffuse along the accretion column: which is a Green function (Becker and Wolff, 2007). The model is substantially analytical and it can be used to fit the spectra of accreting X-ray binaries. This was done by Ferrigno et al. (2009) for 4U 0115 + 63 using *BeppoSAX* data, where it was necessary to introduce an additional emission component at low energy, and by Wolff et al. (2016) for Her X-1 using *NuSTAR* data. Model limitations include the assumption of a cylindrical shape of the accretion column, of an analytical plasma velocity profile decoupled from radiation, of a constant magnetic field and electron temperature in the column. Farinelli et al. (2016) managed to relax the assumptions on the vertical dependency on the magnetic field and on the plasma velocity profile; they also introduced a Gaussian profile of the cyclotron emission instead of a delta function. This allowed them to describe the spectra of three X-ray binaries (4U 0115 + 63, Cen X-3 and Her X-1) without the need for any additional component.

Despite these theoretical efforts, a comprehensive description of the X-ray spectrum of pulsating HMXBs still eludes our complete understanding, due to the inherent difficulties in treating the coupled MHD
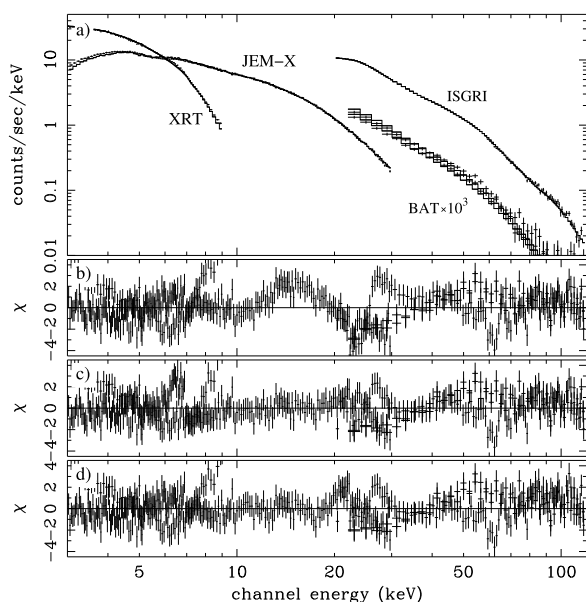

Fig. 5. The broad band spectrum of EXO 2030 + 375 from simultaneous fits of *INTEGRAL* and *Swift* data of the 2007 giant outburst with `highecut` (a) and residual plots after fitting it without additional features (b), adding a "bump" around 15 keV (c), or alternatively including two absorption lines at ~ 10 and ~ 20 keV (d) (from Klochkov et al., 2007). See Camero-Arranz et al. (2005) for a broadband spectrum from an earlier, normal outburst.

problem of a plasma that is emitting near the local Eddington limit. However, with the models proposed so far, it has become clear that the commonly used power law with exponential rollover can only describe the thermal part of the emission, i.e. the Compton upscattering of thermally produced photons. Additional components in the emission are thought to be due to the Compton broadening from collisional excitation of the Landau level (cyclotron emission). Once a continuum is formed, there is a transition from an optically gray regime to free streaming. In this phase, scattering features, mainly in absorption, can be imprinted on the spectrum (see the next section). These features are quite broad and sometimes it becomes impossible to disentangle between emission and absorption (see Bozzo et al., 2017b; Ferrigno et al., 2019, for recent cases).

2.7. Cyclotron Resonant Scattering Features

Electrons moving in a magnetic field are forced onto cyclic paths in the direction perpendicular to the magnetic field. If the magnetic field is strong enough, their cyclotron energy becomes comparable to their rest mass, requiring a quantum mechanical and relativistic treatment (e.g., Daugherty and Harding, 1986; Canuto et al., 1971; Harding and Daugherty, 1991). In fields that are strong, the movement of the electrons perpendicular to the magnetic field axis can be described by quantized Landau levels, whose energies are the Eigenvalues of the electron's Hamiltonian and can be approximated when integrating over all angles and polarization as

$$E_{\mathrm{Landau},n} = n\frac{\hbar e B}{m_e} \tag{5}$$

These quantized levels change the cross-section between electron and photons, and hence strongly influence the observed X-ray spectrum. Calculating these cross-sections, however, requires detailed fully relativistic QED-based calculations. The most recent work on this topic was presented by Schwarm et al. (2017b,a), building on work by, e.g., Sina (1996); Harding and Daugherty (1991); Isenberg et al. (1998); Araya and Harding (1999); Schönherr et al. (2007).

The cross-sections show two important properties: first of all, they are very strongly peaked close to the Landau level energies, implying that the plasma becomes optically thick at these energies. Secondly, because the energy of the electrons is only quantized in the direction perpendicular to the magnetic field, the angle between the magnetic field and the photon becomes relevant. For large angles, the cross-sections become thermally broadened and shift to higher energies for the harmonic levels, as shown in Fig. 6.

Because the optical depth is so large at the resonant energies for cyclotron scattering, photons with the exact amount of momentum in the direction perpendicular to the magnetic field cannot escape the line forming region, and we can observe absorption like features in the hard X-ray spectrum. These features are referred to as Cyclotron Resonant Scattering Features (CRSFs) or cyclotron lines for short. The CRSF central energy can directly be related to the magnetic field strength in the line forming region via

$$E_{\mathrm{CRSF},n} = E_{\mathrm{Landau},n}\frac{1}{1+z} \approx \frac{n}{1+z}11.6 \times B_{12}\ \mathrm{keV} \tag{6}$$

where B_{12} is the magnetic field strength in 10^{12} G and z is the gravitational redshift. Equation 6 is commonly known as the "12-B-12"-rule and works well for different geometries in the case of $B \lesssim 10^{13}$ G.

CRSFs are the only way to directly measure the magnetic field strength close to the surface of a NS. Currently, 36 CRSF are known. For a recent in-depth review about them and their history, see Staubert et al. (2019, and references therein).
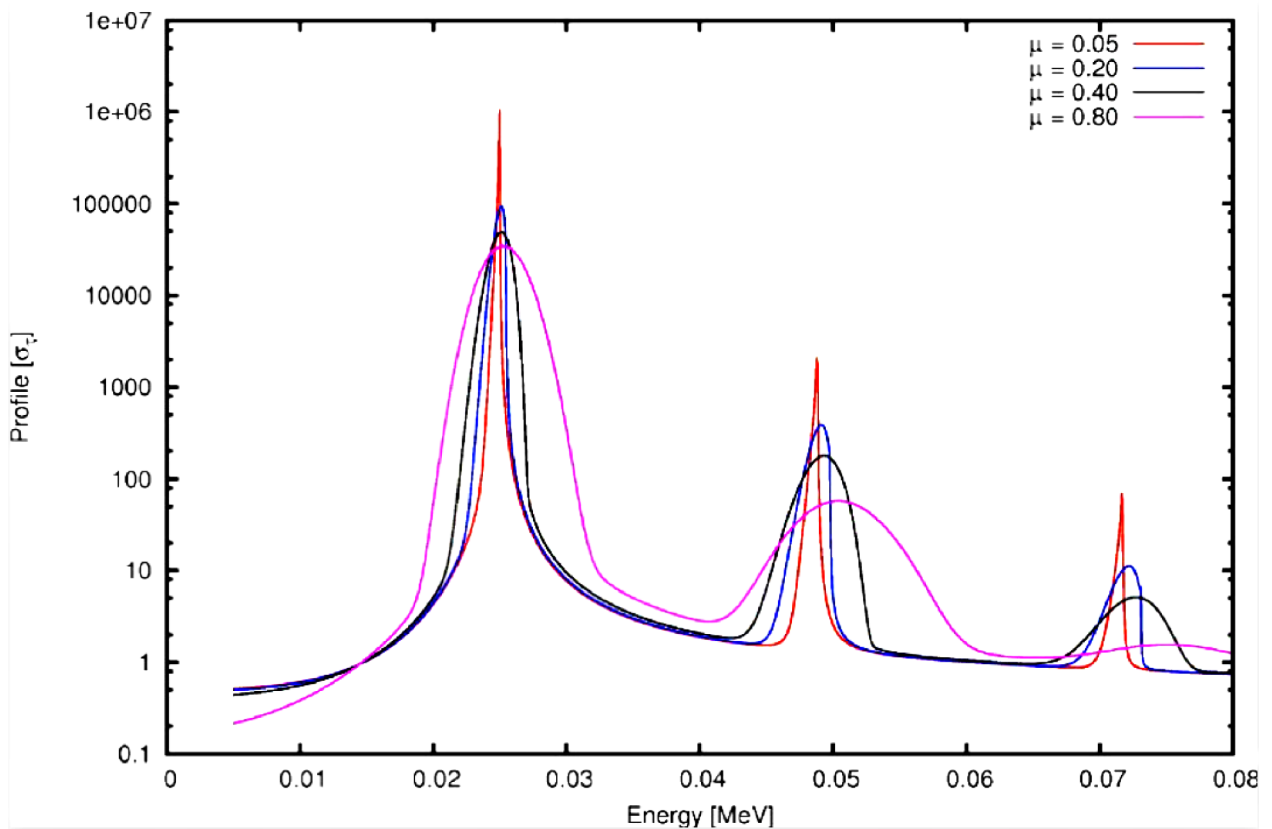

Fig. 6. Averaged cyclotron cross-sections in units of the Thomson cross-section calculated by Schwarm et al. (2017b,a). The different colors indicate different angles ϑ between the photon path and the magnetic field, where $\mu = \cos\vartheta$. The calculations were done for a magnetic field strength of $B = 2 \times 10^{12}$ G and a plasma temperature of $kT = 3$ keV.
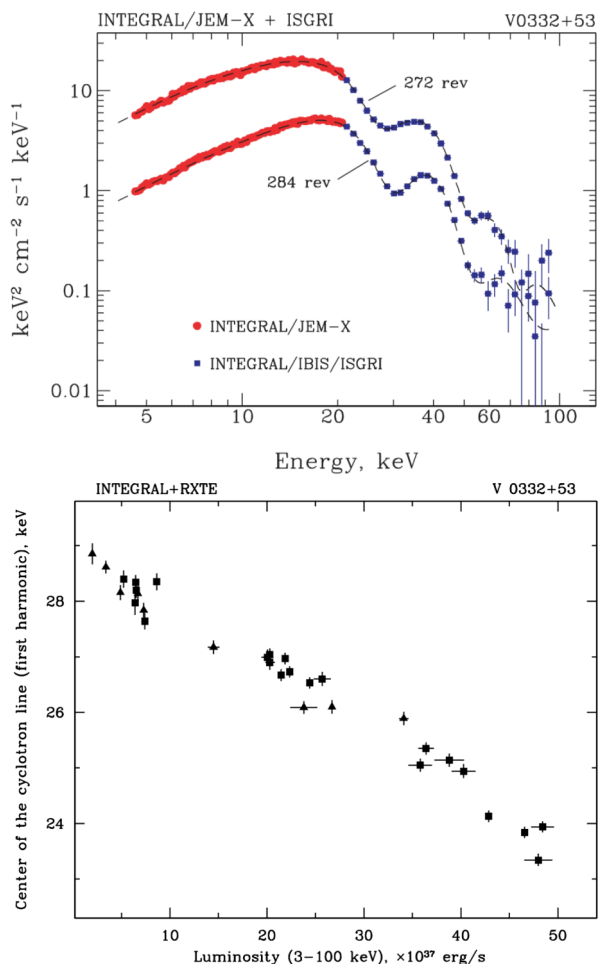
Fig. 7. Upper panel: Energy spectra of V0332 + 53 measured with *INTEGRAL* for two different brightness states, with an immediately visible shift of the cyclotron lines. Lower panel: Dependence of the cyclotron line energy on the source luminosity (3–100 keV); Triangles and squares mark *INTEGRAL* and *RXTE* results, respectively. (Originally Figures 3 and 4 of Tsygankov et al. (2006a)).

Among the open questions in CRSF research is the fact that model calculations (Araya and Harding, 1999; Schwarm et al., 2017b; 2017a) tend to predict asymmetrical lines, frequently showing "emission wings" at energies below and above the central energy, while observed features tend to be broad and without a marked asymmetry.

In order for discrete CRSFs to be observable, the sample magnetic field has to be confined to a very narrow range, indicating a closely confined region within the accretion column, possibly a shock region in the column or close to the poles (Becker et al., 2005; Becker and Wolff, 2007, and references therein). Broad and shallow observed CRSF might be caused by multiple line forming regions contributing (Nishimura, 2008). Another possibility is that CRSFs are formed due to reflection of the downwards beamed radiation from the accretion column on the NS surface around the poles (Poutanen et al., 2013).

2.7.1. Luminosity dependence of the CRSF energy

It is observationally clearly established that the CRSF energy may change as function of luminosity. The sources exhibiting such behaviour can be divided into two groups: the first, where the centroid energy of CRSF is positively correlated with accretion luminosity, and the second, where an anti-correlation is observed. The sources with detected positive correlation tend to be less bright than the sources with negative correlation (Becker et al., 2012; Mushtukov et al., 2015a).

Different models which are able to explain the observed CRSF energy behaviour have been proposed.

Becker et al. (2012) defined three different accretion regimes, depending on luminosity and magnetic field strength. At the lowest luminosities the infalling material is only stopped at the NS surface and the line is formed there. In this case, no change of the line energy with luminosity is expected. At intermediate luminosities a Coulomb-dominated shock is formed in which the line is formed. With increasing luminosity the shock is expected to move closer to the NS surface, sampling higher magnetic field strengths and increasing the observed line energy. At the highest luminosities, above a critical luminosity, the infalling material is decelerated in a radiation dominated shock (Inoue, 1975; Basko and Sunyaev, 1976). This shock is expected to rise in height with increasing luminosity, decreasing the observed line energy (see Sect. 2.6).

In the line formation model of Poutanen et al. (2013) a higher luminosity leads to a higher accretion column and a larger fraction of the NS surface being illuminated by this column. A larger area includes regions of a lower magnetic field closer to the NS equator, resulting in a decrease of the observed cyclotron energy with increasing luminosity. Mushtukov et al. (2015b) explain the case of positive correlation for sub-critical luminosities via the Doppler effect of a mildly relativistic falling plasma in the column.

2.7.2. Pulse phase dependence of the CRSF profile

The observed line profiles and energies depend strongly on the angle under which we see the line forming region. Because the rotational axis is typically not aligned with the magnetic field axis (or with our line-of-sight), our viewing angle of the CRSF region changes as function of pulse phase. The possible changes are very complex and predictions depend strongly on the assumptions about the magnetic field geometry and emission pattern of each column. Energy shifts of the CRSF could for example be explained by different observed relativistic boosting factors of the infalling plasma (Fürst et al., 2018).

In case of a perfectly symmetric accretion geometry, with two opposed accretion columns, a lot of the expected variability as function of pulse phase is considerably suppressed (Falkner, 2018). Because of the relativistic light-bending, at most phases both columns are visible and their flux variations as function of the viewing angle almost cancel each other.

The beaming function, and therefore flux and CRSF profile variations with the pulse phase, can be strongly affected by the material moving from the accretion disc to the NS surface. The influence of magnetospheric accretion flow is expected to be stronger in the case of super-critical accretion, when the gravitationally lensed flux from the accretion columns passes the regions of relatively high density of magnetospheric flow (Mushtukov et al., 2018).

2.7.3. Secular changes of the CRSF energy

Because accretion is a dynamic process during which the NS gains mass, it is also expected that the accretion geometry might slowly change over time. Because the CRSF is so sensitive to the magnetic field, we might expect a secular change of the CRSF energy, for example if the magnetic field slowly decays. However, expected decay times of magnetic fields are of the order of 10^6 years (e.g., Bhattacharya et al., 1992), much longer than the history of CRSF science. However, other effects, like screening or burying of the surface magnetic field due to accumulation of the accreted material might occur, but a clear theoretical picture has so far not emerged (see also the discussion in Staubert et al., 2014).

2.8. X-rays from black hole HMXB systems

The *INTEGRAL* view on Galactic black-hole (BH) binaries is discussed elsewhere in a dedicated chapter, and we refer the reader to this for a more detailed discussion (Motta et al., this volume). Most of these

sources are in low-mass X-ray binaries (e.g., McClintock and Remillard, 2006). Only a few confirmed BH HMXBs are known, but among them is one of the most prominent X-ray sources in the sky, Cygnus X-1, that has been observed by *INTEGRAL* for over 11 Ms of dead-time corrected exposure (Cangemi et al., 2019). Although thought to be wind-accretors, BH HMXBs usually exhibit a stable accretion disc.

Observationally, BHs in XRBs can be found in two main states: *hard state*, where the total energy output is driven by a hard power law component above 10 keV with an exponential cutoff at a few hundred keV, and *soft state*, where soft thermal emission from a ~ 1 keV accretion disc dominates and a weak, very steep power law component with a cutoff above ~ 500 keV may be present. Changing between the states, the source evolves through the hard/soft intermediate state that shows intermediate spectral characteristics (e.g. Fender et al., 2004; Belloni, 2010). Radio emission is detected in the hard state but it is strongly suppressed or absent in the soft one; radio jets can be resolved in several sources and radio flares are often associated with state transitions. The states further show distinct X-ray timing characteristics (e.g. Belloni, 2010). BH X-ray binary states correspond to different accretion/ejection geometries, but in particular the exact origin of the Comptonized hard emission is still controversial (Nowak et al., 2011; Zdziarski et al., 2014). Additionally, sources sometimes show an excess beyond the hard cutoff, the so-called hard tail.

Cygnus X-1 is a key source to understanding BH X-ray binaries: as a HMXB, it is a persistent accretor and thus easy to observe. Additionally, it often transits between the states, crossing the so-called 'jet line' where we expect the strongest changes in accretion geometry to take place (Grinberg et al., 2013). *INTEGRAL*'s unique capabilities at highest energies have contributed in several ways to a better understanding of this system: in particular, the hard tail above 400 keV in Cygnus X-1 has been shown to be polarized (Laurent et al., 2011; Jourdain et al., 2012; Rodriguez et al., 2015), hinting at a jet origin for this component. For the spectrum of the hard tail, see also Walter and Xu (2017). Cabanac et al. (2011) analyzed power spectra and time lags up to ~ 130 keV, for the first time assessing the energy-dependence of variability properties at such high energies, giving strict constrains on models that try to reproduce properties of hard X-ray emission.

2.9. Gamma-ray binaries

The population of Galactic X-ray sources above 2 keV is dominated by the X-ray binaries, see e.g. Grimm et al. (2002). At gamma-ray energies, however, the situation is drastically different. While current Cherenkov telescopes have detected around 80 Galactic sources (see the TeVCat catalogue at http://tevcat2.uchicago.edu/), less than 10 binary systems are regularly observed at TeV energies as non-extended gamma-ray sources (Dubus, 2013; Chernyakova et al., 2019). The properties of PSR B1259 - 63, LS 5039, LS I +61˚ 303, HESS J0632 + 057 and 1FGL J1018.6 - 5856 are reviewed in Dubus (2013). Since 2013, three more Galactic binaries, PSR J2032 + 4127 (Mirzoyan and Mukherjee, 2017), HESS J1832 - 093 (Eger et al., 2016; Martí-Devesa and Reimer, 2020), 4FGL J1405.1 - 6119 (Corbet et al., 2019), and one extragalactic – LMC P3 (Corbet et al., 2016), have been discovered at TeV energies, but still the number of binaries observed in the TeV sky is extremely small; the reason why these systems are able to accelerate particles so efficiently is not known yet. These systems are called gamma-ray binaries as the peak of their spectral energy distribution lies in the gamma-ray range above 1 MeV, sometimes in the GeV–TeV range.

All gamma-ray binaries host compact objects orbiting around massive young stars of O or Be spectral type. This leads to the suggestion that the observed gamma-ray emission is produced as the result of interactions between the relativistic outflow from the compact object and the non-relativistic wind and/or radiation field of the massive companion star. However, neither the nature of the compact object (BH or NS?) nor the geometry (isotropic or anisotropic?) of the relativistic

wind from the compact object are fully understood. Only in PSR B1259 - 63 and PSR J2032 + 4127, is the compact object known to be a young rotation-powered pulsar which produces a relativistic pulsar wind. The interaction of the pulsar wind with the wind of the Be star leads to the observed high energy emission, and in particular to the huge GeV flare observed in PSR B1259 - 63 (Abdo and (Fermi LAT Collaboration), 2011; Chernyakova et al., 2015; Caliandro et al., 2015; Johnson et al., 2018).

In all other cases the source of the high-energy activity of gamma-ray binaries is uncertain. It can be either dissipation of rotation energy of the compact object (e.g. Dubus, 2006; Sierpowska-Bartosik and Torres, 2008; Torres et al., 2012), or emission from a jet (e.g. Bosch-Ramon and Paredes, 2005; Zimmermann and Massi, 2012a). In these other systems the orbital period is much shorter than in PSR B1259 - 63 and PSR J2032 + 4127, and the compact object spends most of the time inside the dense wind of the companion star. The optical depth of the wind due to free-free absorption is high enough to suppress most of the radio emission within the orbit, including the pulsed signal of the rotating NS (Zdziarski et al., 2010), hampering a direct detection of the possible pulsar. Super-orbital variability has also been found in at least one of these sources, e.g., see the GeV detection of LS I +61˚ 303 in Ackermann and (Fermi LAT Collaboration) (2013); we refer more about this below.

Massi et al. (2017) tried to deduce the nature of the compact source in LS I +61˚ 303 by studying the relation between the X-ray luminosity and the photon index of its X-ray spectrum. It turned out that existing X-ray observations of the system follow the same anti-correlation trend as BH X-ray binaries. Under the hypothesis of a microquasar nature for LS I +61˚ 303, they were able to explain the observed radio morphology (Bosch-Ramon and Paredes, 2005) and interpret the observed superorbital period as a beat frequency between orbital and jet-precession periods (Massi and Torricelli-Ciamponi, 2016). This is further supported by the presence of 55-minute and 2-hour long quasi-periodic oscillations in radio and X-rays, respectively, which are stable over a few days (Nösel et al., 2018). Conversely, Zdziarski et al. (2010) showed that the model in which the compact source is a pulsar allows a natural explanation of the keV – TeV spectrum of LS I +61˚ 303. These authors argued that the radio source has a complex, varying morphology, and jet emission is unlikely to dominate the spectrum through the whole orbit. Within this model, the superorbital period of the source is explained as the timescale of the gradual build-up and decay of the disc of the Be star. Li et al. (2012a) and Chernyakova et al. (2012) demonstrated the presence of superorbital variability in X-rays, the latter publication showed that a constant time delay between the drifting orbital phases of X-ray and radio flares could be naturally explained if one takes into account the time needed for electrons to reach regions transparent to radio emission.

Cyclical variations in the mass-loss of the Be star are supported by optical observations confirming the superorbital variability of the Be-star disc (Paredes-Fortuny et al., 2015); this is also an explanation for superorbital variability in an alternative flip-flop model (Zamanov et al., 2001; Torres et al., 2012; Papitto et al., 2012; Ahnen and (MAGIC Collaboration), 2016). This model assumes the compact object in LS I +61˚ 303 to be a magnetar and implies a change from a propeller regime at periastron to an ejector regime at apastron. During the periastron the pressure of matter from the Be star outflow compresses and disrupts the magnetosphere of the NS, which leads to the disappearing of the pulsar wind. In this case electrons are accelerated at the propeller shock, which accelerates electrons to lower energies than the inter-wind shock produced by the interaction of a rotationally powered pulsar and the stellar wind of the Be star. A magnetar-like short burst caught from the source supports the flip-flop model and the identification of the compact object in LS I +61˚ 303 with a NS (Barthelmy et al., 2008; Burrows et al., 2012; Barthelmy et al., 2019). However, RXTE observations of LS I +61˚ 303 demonstrated the presence of a few, several second long, flares (Smith et al., 2009), which

were compared by those authors to the flares typically found in the accretion-driven sources; see also Li et al. (2011b) for a further analysis covering a wider range of orbital cycles. In principle, neither BAT nor RXTE observations can exclude the possibility that the observed flares are coming from another source located close to the line-of-sight (Smith et al., 2009), although similar observations of instruments with better spatial resolution indicate that it is likely they are from the gamma-ray source (Paredes et al., 2007; Rea et al., 2010).

Other possible scenarios for the super-orbital modulation in LS I +61° 303are related to the precession of the Be star disc (Saha et al., 2016), or to a non-axisymmetric structure rotating with a period of 1667 days (Xing et al., 2017).

During its orbital motion around the optical companion, the environment of the compact source changes a lot from periastron to apastron. This leads to the observed spectral variability on very different time scales, from hours to the orbital and superorbital periodicities. The typical X-ray flux from gamma-ray binaries is at the level of few mCrabs, so it is not possible to study with *INTEGRAL*the spectral variability on short time scales (few hours). Still, *INTEGRAL*is sensitive enough to study the properties of gamma-ray binaries on longer time scales.

2.10. Ultraluminous X-ray sources

Ultraluminous X-ray sources (ULXs) have been defined as a class of extragalactic point-like objects, outside the nucleus of their respective galaxies and with a luminosity exceeding the Eddington limit for a 10 M$_\odot$black hole. Originally often thought to be intermediate-mass black holes with masses > 100M$_\odot$, further studies rather indicated "stellar mass" compact objects accreting at super-Eddington rates for at least most ULXs (e.g., Sazonov et al., 2014). The discovery of X-ray pulsations from the ULX M82 X-2 (Bachetti et al., 2014) demonstrated that ULXs can host accreting neutron stars and further examples have been found subsequently. Due to their distance, the nature of the mass donor is not well determined for most ULXs and only for NGC 7793 P13 (Israel et al., 2013) this has been clearly identified as a high mass star (Motch et al., 2011). A few more pulsating ULX have been tentatively identified as HMXBs, but, for example, in the case of NGC 300 ULX1, Heida et al. (2019) reclassified the mass donor as red supergiant. As noted also in Bachetti et al. (2014), very luminous outbursts of BeXRB systems can also reach super-Eddington luminosities and different Be transients like SMC X-3 (Tsygankov et al., 2018) or the recently found transient Swift J0243.6 + 6124 (Kennea et al., 2017; Jenke and Wilson-Hodge, 2017; Wilson-Hodge et al., 2018) are now being labeled as ultraluminous sources, demonstrating a continuum of behaviour from classical accretors to ULXs (Mushtukov et al., 2015a; Kaaret et al., 2017; Grebenev, 2017).

3. *INTEGRAL*'s role in HMXB studies

3.1. Persistent wind-accreting Supergiant HMXBs

Persistent wind-accreting supergiant HMXBS (sgHMXBs) are systems with an early type (O or B-star) supergiant companion, losing large amounts of mass through a stellar wind. The compact objects in these systems accrete from this dense wind, and, while they tend to show a large variability (up to a factor of 100), they are always active and some were among the first HMXBs discovered. *INTEGRAL*contributed to the knowledge about this source class by the merit of long observations of fields containing these sources – frequently not directly targeting the sources themselves. *INTEGRAL*data in the hard X-ray band have also been important to disentangle intrinsic variations of the X-ray source flux from the effects of absorption when studying X-ray variability. For eclipsing systems, the accumulated long-term data has allowed to refine eclipse parameters and thus derive new constraints on the masses of the binary companions, as detailed in Section 3.3. In the
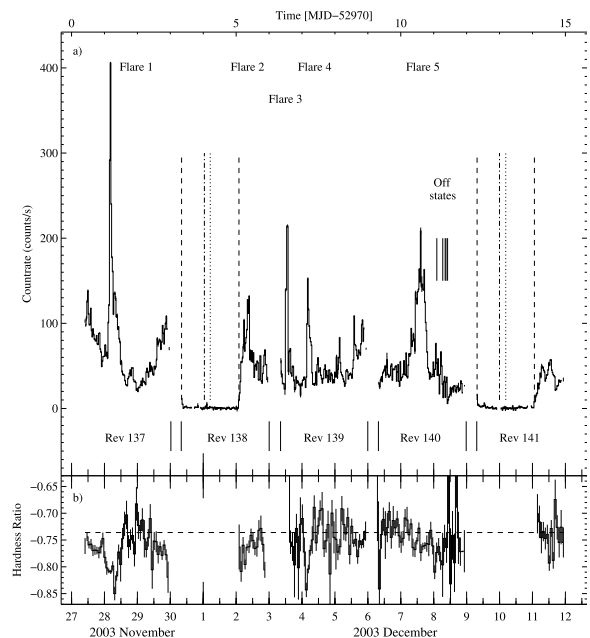

Fig. 8. Variability of Vela X-1 for the complete Vela region observation from Revolution 137 to 141. a) ISGRI 20–40 keV light curve (time resolution 1 SCW, i.e. ~ 1800 s) and b) 20–30 keV vs. 40–60 keV hardness ratio. Short vertical lines below the X-ray light curve show *INTEGRAL*'s perigee passages, during which the instruments are switched off. The long dashed vertical lines show the eclipse ingress and egress times. The dotted vertical line indicates the derived eclipse center, while the dash-dotted line indicates the time of mean longitude T90. Originally Fig. 2 in Kreykenbohm et al. (2008).

following, we give a few specific examples of *INTEGRAL*results for this source class.

The sgHMXBVela X-1is among the best studied objects in the X-ray sky and often taken as a prototype supergiant X-ray binary in order to study the physics of HMXB or as baseline case for modeling and simulation efforts (see Kretschmar et al., 2019, for an overview). Long-term X-ray monitor data show on average a clear orbital profile (Fürst et al., 2010; Falanga et al., 2015), driven by the mean absorption in the dense material present in the system, especially in the accretion and photoionization wakes (Grinberg et al., 2017, and references therein). Erratic flux variations on timescales from days to minutes have been reported since early deep observations of the system (e.g., Forman et al., 1973; Watson and Griffiths, 1977; Ögelman et al., 1977). During an extended observation of the Vela region for five consecutive *INTEGRAL*revolutions in November/December 2003 (Fig. 8), covering almost two orbital periods of Vela X-1, *INTEGRAL*found especially intense flaring, as well as off-states, which during the flux dropped below the detection limit of *INTEGRAL*for 1–2 rotations of the neutron star (Staubert et al., 2004; Kreykenbohm et al., 2008). Fürst et al. (2010) found that the *INTEGRAL*flux distribution closely followed a log-normal distribution. Early studies of the accretion flow (Taam and Fryxell, 1988) identified strong time-dependent behaviour as well as indications of a highly asymmetric flow. Other studies (starting with Blondin et al., 1990) revealed indeed highly asymmetric structures caused by the photoionization and accretion wakes. Pushing these studies further, Manousakis and Walter (2015a,b) found time-dependent holes in the simulated mass flow, which may explain the off-states observed by Kreykenbohm et al. (2008) and others, without requiring intrinsic clumpiness of the wind.

4U 1907 + 09 is a less studied source, a wind-accreting sgHMXBon a moderately eccentric, close orbit. *INTEGRAL*observations (Fritz et al., 2006) found a clear spin-down after almost 20 years of constant spin-up and confirmed CRSFs at ~ 19 and ~ 40 keV, consistent with earlier
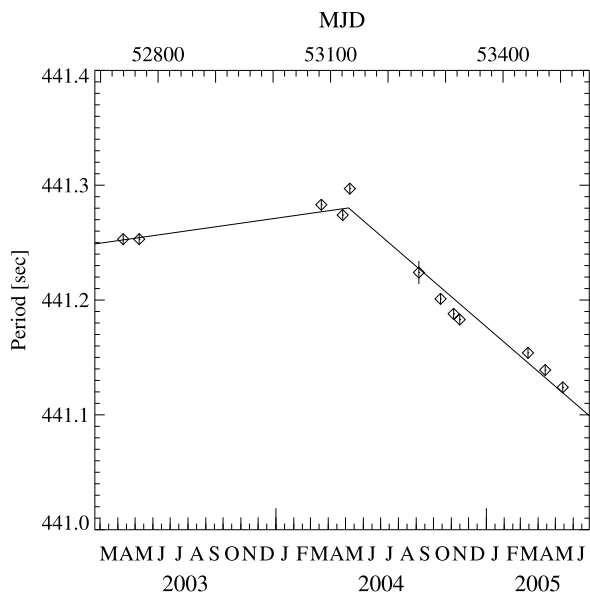
Fig. 9. A torque reversal of 4U 1907 + 09 found in *INTEGRAL* observations. Originally Fig. 6 in Fritz et al. (2006).

results (Figure 9). The spin-down trend reversed later (Şahiner et al., 2012). Long-term spin period change trends like in this source contrast with the "random walk" changes in pulse period observed, e.g., in Vela X-1. This source also shows dips or off-states. Using a *Suzaku* observation, Doroshenko et al. (2012a) found that the source continues to pulsate in the off-state and that the transitions may be explained by "gated accretion" (see Section 2.5.3), which might make 4U 1907 + 09 an interim source between SFXTs and ordinary accreting pulsars.

The somewhat unusual system 2S 0114 + 650 harbours one of the slowest spinning pulsars ($P_s \approx 2.65$ h) in a close orbit ($P_b \approx 11.6$ d) around a supergiant star. *INTEGRAL* observations (Bonning and Falanga, 2005; Wang, 2011) have confirmed the previously observed long-term spin-up trend with shorter variations. Noting stronger short-term variations and super-orbital variations, Hu et al. (2017) propose the formation of a transient disc (see also Section 2.2), while Sanjurjo-Ferrrín et al. (2017) consider quasi-spherical settling accretion (see Section 2.5) on a magnetar to explain the observed behaviour.

3.2. Highly absorbed HMXBs

Highly absorbed systems do not define a class themselves: the physics and the nature of the sources are clearly the same as non-absorbed ones. It is, however, worth pointing out that due to its unprecedented coverage, and, at that time, the best angular resolution at hard X-rays, we could hope that *INTEGRAL* could see sources otherwise undetected at lower energies, for various reasons: sensitivity, hard spectra, confusion, high absorption, etc. On 2003 January 29th, during the first Galactic Plane Scan of the Norma region (after a few weeks spent on the other side of the Galaxy in the Cygnus region), *INTEGRAL* detected its first such system, and one of the most extreme of all *INTEGRAL* sources (IGRs): IGR J16318 - 4848. This object is indeed the most absorbed HMXB (10 times higher than previously known absorbed systems such as 4U 1700 - 37 or GX 301 - 2) with N_H in excess of 10^{24} cm^{-2} (Walter et al., 2003). This results in a featureless, continuumless spectrum below $4 - 5$ keV, huge Fe K$_\alpha$, K$_\beta$ and Ni K$_\beta$ lines in the soft X-ray spectrum (Matt and Guainazzi, 2003; Walter et al., 2003), and variable hard X-ray emission (Barragan et al., 2010), see Figure 10. Multi-wavelength follow-ups (mainly from near-to-mid infra-red spectroscopy) have shown the companion to be a peculiar supergiant (a so-called sgB[e]), while the system is enshrouded in a dense cocoon

(Filliatre and Chaty, 2004). This material also shows up in the X-rays, where the strongly absorbed spectrum can be self-consistently explained with a combination of gas and dust absorber (Ballhausen et al., 2020). Later observations with the ESO-VLT VISIR instrument suggested that the compact object (of unknown nature) is orbiting within or behind the rim of a torus of matter encircling the supergiant star (Chaty and Rahoui, 2012). Recently, Fortin et al. (2020) presented new ESO-VLT X-shooter broad-band spectroscopic observations from optical to near infra-red of this source, and compared it with models made with the POWR code for atmospheres of massive stars.

It was still surprising that the following IGRs (e.g. IGRT J16320 - 4751, IGR J16393 - 4643, IGR J17252 - 3616, IGR J18325 - 0756) also were quite absorbed objects with $N_H \sim 10^{23}$ cm^{-2} (Rodriguez et al., 2003; Bodaghee et al., 2006; Zurita Heras et al., 2006; Walter et al., 2006; Tomsick et al., 2008), more in line, however, with older sources. The strength of the absorption can vary as function of the orbital phase. García et al. (2018) followed the spectral evolution and changes in column density of IGR J16320 - 4751 along its orbit with a series of *XMM-Newton* observations, describing the changes in a simple geometrical model.

3.2.1. Infra-red identification of highly absorbed IGR sources

After the highly absorbed archetype IGR J16318 - 4848, *INTEGRAL* found some more sources with similar X-ray spectral properties. Some of these systems seem to be persistent sources, such as IGR J16320 - 4751 (Rodriguez et al., 2003), and some of them are clearly transient, such as IGR J16358 - 4726 (Patel et al., 2004) and IGR J16465 - 4507 (Lutovinov et al., 2005a). Kuulkers (2005) reviewed the X-ray and optical and infra-red (IR) properties of highly absorbed IGR sources and suggested that these are HMXBs containing either a NS or a BH in orbit around a (super)giant donor. Here we will concentrate on this class of sources and the IR analysis to identify and characterize the counterparts.

Before *INTEGRAL*, the small number of sgHMXBs was explained by the short-lived supergiant phase. The distribution of this kind of systems was reproduced well by population synthesis models. However, the *INTEGRAL* survey of the Galactic plane and central regions has revealed the existence of more than 900 sources in the energy range 17–200 keV (Bird et al., 2016), with a location accuracy of 0.5′–4′, depending on count rate, position in the field of view and exposure. The observing strategy of *INTEGRAL* allowed the detection of new kinds of
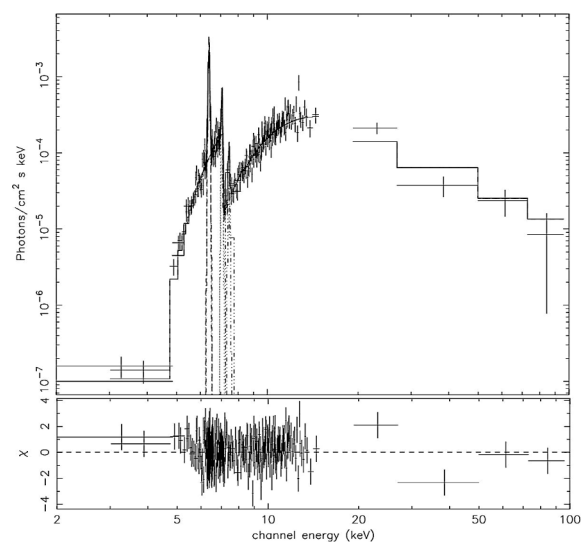

Fig. 10. XMM-Newton and ISGRI unfolded photon spectra of IGR J16318–4848, the first new source detected by *INTEGRAL* and an extremely absorbed HMXB. From Walter et al. (2003).

sources that had been missed in the past due to the very short transient nature (see Section 3.4) or the very high absorption. A large fraction of these newly discovered sources belongs to the sgHMXBclass, resulting in a substantial increase of its members. Often the highly absorbed sources are not accessible in the optical band due to the high interstellar extinction or would require extremely long exposure times on large optical telescopes.

Under these circumstances, infrared spectroscopy is an alternative tool to characterize these systems in a multiwavelength context. The detection and study of counterparts in the infrared is possible with the IR instrumentation on a 4-m class telescope. Combining it with available IR photometry and the X-ray properties, the nature of the binary system can be established unambiguously. Follow-up X-ray observations by *XMM-Newton* (e.g. Bodaghee et al., 2006; Rodriguez et al., 2006; Bozzo et al., 2012b), *Chandra* (e.g. Tomsick et al., 2008; Paizis et al., 2011; Nowak et al., 2012) or *Swift* (e.g. Kennea et al., 2005; Rodriguez et al., 2009; Pavan et al., 2011) lead to the reduction of the error circle to a few arcseconds and, consequently, the correct identification of the IR counterpart (e.g. Chaty et al., 2008).

To establish or constrain the nature of the companions through IR spectroscopy, IR atlases of Hanson et al. (1996, 1998, 2005) are used for comparing the spectral features present in the IR spectrum. The IR counterpart of IGR J19140 + 0951, 2MASS J19140422 + 0952577 (in't Zand et al., 2006), was classified as a B0.5-1 supergiant (Hannikainen et al., 2007; Nespoli et al., 2008). Nevertheless, Torrejón et al. (2010) showed that the 2MASS companion was formed by two stars. They performed the photometry on images of higher spatial resolution that allowed them to clearly separate both stars. Using their photometry and the spectral type B0.5 Ia, they estimated a distance of 3.6 kpc. The companion of IGR J16207 - 5129, 2MASS J16204627 - 5130060 (Tomsick et al., 2006a), was classified as a B1 supergiant from its IR spectrum (Nespoli et al., 2008), confirming the spectral type derived from optical observations (Negueruela and Schurch, 2007). *Suzaku* observations confirmed that this object belongs to the class of absorbed HMXB (Bodaghee et al., 2010). Pellizza et al. (2011) obtained optical and IR observations of the field of IGR J16283 - 4838 (Rodriguez and Paizis, 2005) in order to unveil the nature of its counterpart (2MASS J16281083 - 4838560). They demonstrated that this source is a highly absorbed HMXB with a blue supergiant companion.

Torrejón et al. (2010) also investigated the nature of the counterpart to IGR J18027 - 2016, a HMXB candidate identified as 2MASS J16204627 - 5130060 (Masetti et al., 2008), by combining IR spectra in the *I, J, H* and *K* bands with *JHK* photometry. They concluded that this IGR source is a persistent X-ray source with a B1 Ib companion, i.e. a highly absorbed sgHMXBsystem (see also Pradhan et al., 2019; Aftab et al., 2016).

Although Walter et al. (2006) did not use IR spectroscopy, they studied 10 IGR sources (8 persistent and 2 transient systems), obtained follow-up observations with *XMM-Newton* and proposed IR counterparts from existing catalogues. They confirmed or demonstrated that 8 out of the 10 sources are intrinsically absorbed and 7 of them are persistent sources. Moreover, they suggested that the companions of these persistent systems are very likely supergiants.

AX J1910.7 + 0917, discovered by ASCA (Sugizaki et al., 2001), was also detected by *INTEGRAL* in the hard X-ray band. Pavan et al. (2011) analysed all archival *INTEGRAL*, ASCA, *XMM-Newton* and *Chandra* observations around the position of this object. These authors associated the IR counterpart of the source with 2MASS J19104360 + 0916291, but could not firmly establish the nature of the system. However, using IR spectroscopy and new photometric analysis provided by UKIDSS, Rodes-Roca et al. (2013) were able to resolve the 2MASS candidate into two different components (see Fig. 11). Their conclusion was that the companion of this source is most likely an early B supergiant located at a distance of ∼ 16.0 kpc, placing it in the Outer arm. This system would also belong to the class of obscured HMXBs containing the slowest pulsar found to date (Sidoli et al., 2017a).

Overall, *INTEGRAL* has increased the number of sgHMXBsystems dramatically. The proportion of confirmed sgHMXBrelated to HMXBs is now around 42%, and so, almost ten times higher than before *INTEGRAL* (Coleiro et al., 2013).

3.3. Masses of eclipsing high-mass X-ray binaries

Only in a few sources among more than one hundred HMXBs is the inclination of the system high enough for the compact star to be periodically occulted along our line of sight by the companion, giving rise to X-ray eclipses. For these eclipsing HMXB systems, LMC X-4, Cen X-3, 4U 1700 - 377, 4U 1538 - 522, SMC X-1, IGR J18027 - 2016, Vela X-1,
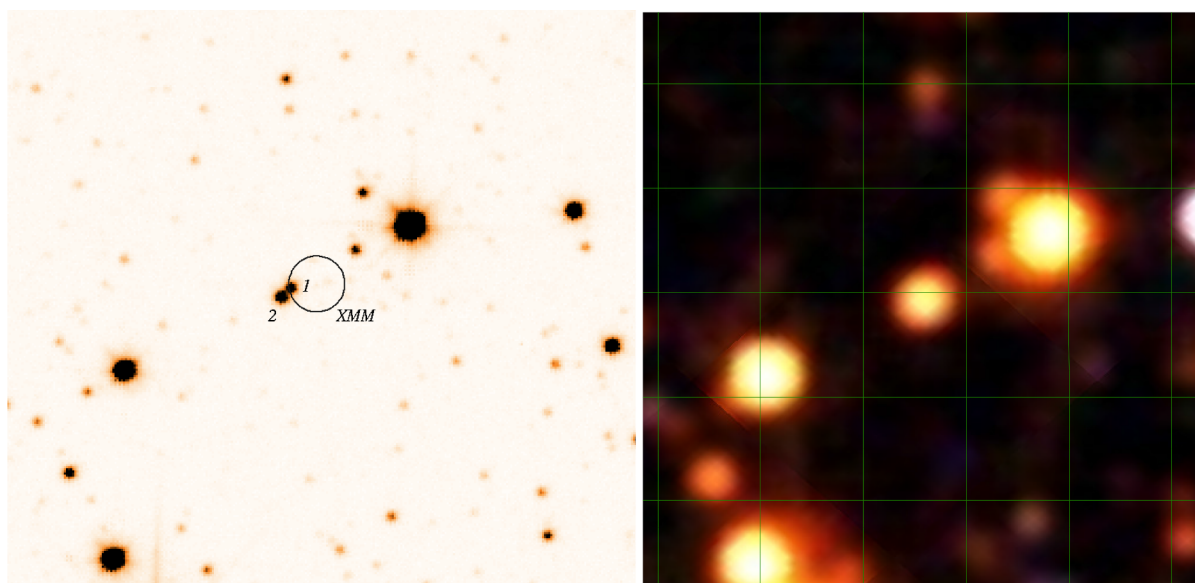

Fig. 11. *Left panel*: 1.2′ × 1.0′ *K* finding chart for 2XMM J191043.47 + 091629.4 obtained with the UKIDSS. The black circle is centred on the *XMM-Newton* position of 2XMM J191043.47 + 091629.4, with the radius indicating the 2.13″ positional error. *Right panel*: 50″ × 50″ 2MASS coloured map. The images are displayed with north up and east to the left. We note that the two NIR UKIDSS sources appear unresolved in the 2MASS image.
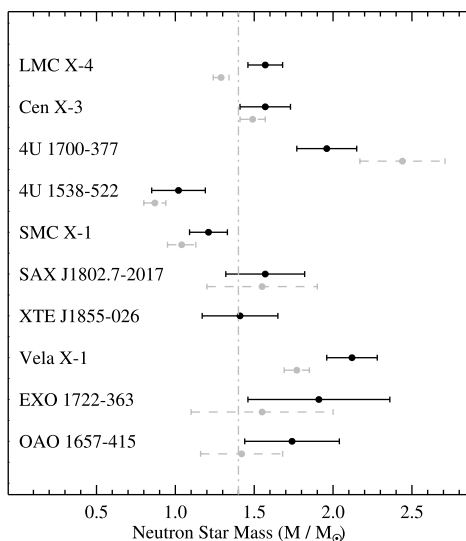
Fig. 12. Masses of the ten eclipsing HMXBs. The NS masses determined using 10 years *INTEGRAL* data are shown with solid lines. Values from the literature are represented with dashed lines. The error bars correspond to uncertainties at 1σ c.l. The dashed vertical line indicates the canonical NS mass of 1.4 $M_\odot$ (see Falanga et al., 2015, for more details).

IGR J17252 - 3616, XTE J1855 - 026, and OAO 1657 - 415, with the help of more than ten years of monitoring with the *INTEGRAL* and *RXTE*/ASM, the ephemeris, including the duration of the eclipse, orbital decay, and for eccentric systems the angle of periastron and the apsidal advance has been derived (Falanga et al., 2015). Additionally, updated values for the masses of the NS hosted in these ten HMXBs were also provided, as well as the long-term light curves folded on the best determined orbital parameters of the sources. The energy-dependent profile of the X-ray light curve during the eclipse ingress and egress also reveals details of the OB stellar wind structure (see e.g., White et al., 1995). These light curves reveal complex eclipse ingresses and egresses that are understood mostly as being caused by accretion wakes. These results constitute a database to be used for population and evolutionary studies of HMXBs and for theoretical modeling of long-term accretion in wind-fed X-ray binaries.

Determining the equation of state (EoS) of matter at densities comparable to those inside NSs is one of the most challenging problems of modern physics and can only be addressed based on observations of astrophysical sources. Models proposed in the past years can be tested against observational results, especially by evaluating the highest NS mass that each EoS model is able to sustain (see e.g., Lattimer and Prakash, 2001). Very soft EoSs predict highest NS masses in the 1.4–1.5 $M_\odot$ range (this occurs when the NS core is made of exotic matter such as kaons, hyperons, and pions), whereas stiff EoSs can reach up to 2.4–2.5 $M_\odot$. More massive NSs can thus provide stronger constraints on the EoS models. As discussed by Rappaport and Joss (1983), eclipsing HMXBs hosting X-ray pulsars provide a means to measure the NS mass and thus place constraints on their EoS. *INTEGRAL* data at high energy band measured semi-eclipse angle smaller than the values reported in the literature, and thus for the ten eclipsing HMXBs NS masses we estimated are generally higher, see Figure 12.

3.4. Supergiant Fast X-ray Transients

INTEGRAL has proved an excellent tool for the discovery of transients. Its combination of large field of view, fine angular resolution and excellent instantaneous sensitivity, coupled with long exposures as part of regular monitoring of the Galactic Plane, makes it far superior to classical all-sky monitors at this task. In particular, one of the major

outcomes of the mission has been the detection of several unidentified fast X-ray transients (Sguera et al., 2005; 2006). Although some of these objects were already known at the time of launch, they had not been studied in depth (Figure 13). Several more fast transients were quickly discovered, characterised by strong activity on very short time-scales. Their identification with OB supergiant counterparts (Negueruela et al., 2006b) changed our view of the overall HMXB population, by adding a new, distinct class of wind-accreting sources: a totally unanticipated result.

3.4.1. Discovery and optical identification

While classical wind-fed supergiant HMXBs are, as described in Sect. 3.1, persistent or mildly variable in X-rays, but always detectable around $L_X \sim 10^{36}$ erg s^{-1}, these new sources were characterised by their transient nature. Early in the mission, 5 such objects had been identified, namely XTE J1739 - 302 (IGR J17391 - 3021; Smith et al. 2006), IGR J17544 - 2619 (Sunyaev et al., 2003b; Grebenev et al., 2003; Pellizza et al., 2006), IGR J16465 - 4507 (Lutovinov et al., 2004; Chaty et al., 2016), AX J1845.0 - 0433 and AX J1841.0 - 0536 (Negueruela et al., 2006b). Given the low duty cycles (see next subsection), previous detections were rare. Only XTE J1739 - 302 had been characterised with *RXTE* (Smith et al., 2006). An accurate localisation by *Chandra* allowed the identification of its counterpart, and follow-up optical spectroscopic observations obtained in May 2004 with VLT/FORS1 showed it to be an O8 Iab(f) star, at a distance of ∼ 2.6 kpc (Negueruela et al., 2006a), with interstellar absorption much lower than that implied by X-ray spectral fits. By then, the long stares by *INTEGRAL* during the first few years of operation had already permitted the discovery and characterization of a handful of new systems. Intensive work by different groups (e.g. Masetti et al., 2006a; 2008; Negueruela and Schurch, 2007) led to the localisation of counterparts to many of these sources, both persistent and transient.

One of the new transient sources, IGR J17544 - 2619, was unambiguously identified with an optical counterpart thanks to *XMM-Newton* and *Chandra* positions, allowing Pellizza et al. (2006) to take spectra with NTT/EMMI, and identify the counterpart as an O9 Ib supergiant, at a distance of ∼ 3 kpc, with a variable amount of absorbing material. Similarly, the counterpart to IGR J16465 - 4507 was unambiguously identified thanks to the small *XMM-Newton* error circle, containing only one star. NTT/EMMI spectra of this object taken in 2005 and VLT/X-shooter spectra obtained in 2012 allowed its identification as an early B0.5 to 1 Ib star with moderate mass loss and very broad lines, indicating a high rotational velocity of 320 km s^{-1}, far higher than in most supergiant stars (Chaty et al., 2016). In a few other cases, the infra-red (IR) counterparts of the fast IGR transient sources were identified thanks to the fast repointing and positional capabilities of Swift/XRT (see, e.g., Romano et al., 2016, and references therein).

This serves to illustrate that subsequent follow-up optical/infrared spectroscopy in most cases showed that these sources are associated with blue OB supergiant donor stars, just like the majority of sgHMXBs, with a variable amount of absorbing material, though. It was thus proposed to name this new class of sgHMXB as Supergiant Fast X-ray Transients (SFXT; Sguera et al., 2005; Negueruela et al., 2006b; Smith et al., 2006), because of the fast outbursts and supergiant companions. This new subclass of sgHMXBs, sharing many similarities with other wind-fed sgHMXBs, comprises about 20 sources (including both firm members and candidates), a population size comparable with persistent sgHMXBs.

Although most SFXTs were discovered in the first years of the *INTEGRAL* mission, new members have been uncovered recently (e.g., AX J1949.8 + 2534 and IGR J17503 - 2636; Sguera et al., 2017; Hare et al., 2019; Ferrigno et al., 2019; Sguera et al., 2020), and two candidate SFXTs have also been discovered in other galaxies (Laycock et al., 2014; Vasilopoulos et al., 2018).
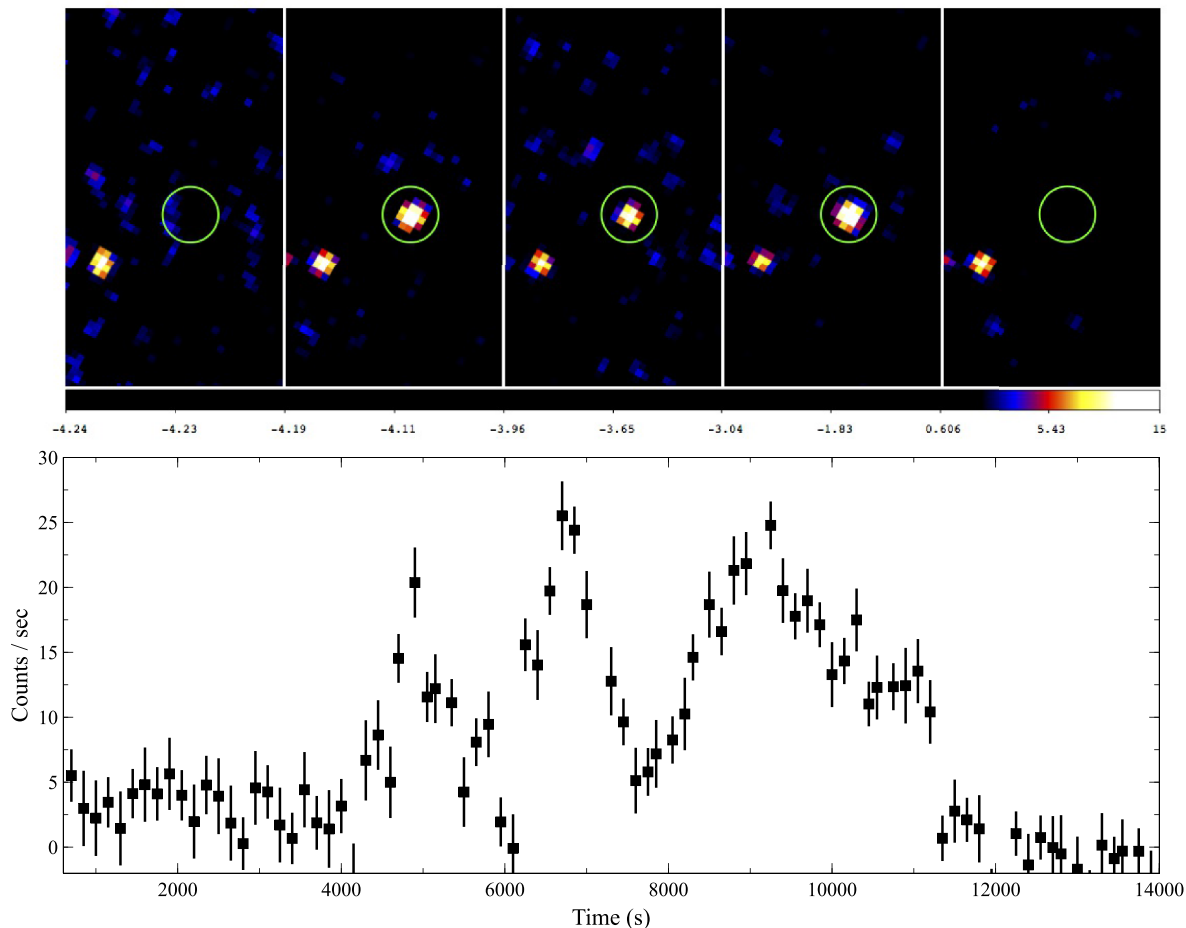
Fig. 13. Top panel: IBIS/ISGRI pointing-by-pointing image sequence (20–60 keV) of a fast X-ray outburst from the SFXT XTE J1739 - 302 (encircled), where each pointing has a duration of about 2000 s. The colour scale used encodes the difference in sigma from the mean reconstructed flux. A weaker persistent source (1E 1740.7 - 2942) is also visible in the field of view. Bottom panel: the corresponding hard X-ray light curve. See Sguera et al. (2005) for more details.

3.4.2. X-ray phenomenology

After the association of SFXTs with early-type supergiant companions, it became evident that these HMXBs are characterized by a remarkable hard X-ray activity: their sporadic high-energy emission caught by *INTEGRAL* only during short duration (a few thousand seconds) flares, put into question the accretion mechanism driving them (see the next subsection), compared with the classical population of supergiant HMXBs (like Vela X-1), known to persistently emit X-rays.

On the timescales typical of SFXT flares ($\sim$ 2 ks), the detection by IBIS/ISGRI occurs at fluxes greater than a few 10^{-10} erg s^{-1} cm^{-2} (18 – 50 keV). This implies luminosities above $10^{35} – 10^{36}$ erg s^{-1} at the known SFXT distances (see Sidoli and Paizis 2018 for a systematic analysis of the *INTEGRAL* archival observations of a sample of 58 HMXBs, from 2002 to 2016). In this bright flaring state, SFXTs spend less than 5% of the time (their duty cycles at hard X-rays range from 0.01% in IGR J17354 - 3255 to 4.6% in IGR J18483 - 0311; Sidoli and Paizis 2018), and their temporal properties (duration and time interval between consecutive flares, as observed by *INTEGRAL*) show power-law like distributions, possibly indicative of a fractal structure of the supergiant wind matter (Sidoli et al., 2016b).

An important observational effort involved several X-ray missions operating at soft X-rays, to investigate the SFXT behaviour outside these outbursts. It consisted of a twofold approach: deep, sensitive pointings at soft X-rays (below 10 keV; from the first studies by in't Zand 2005; González-Riestra et al. 2004; Walter et al. 2006 with *Chandra* and *XMM-Newton*, to the most recent *XMM-Newton* overviews by Bozzo et al. 2017b and Pradhan et al. 2018), alongside long-term monitoring campaigns aimed at characterizing the X-ray properties outside outbursts and at catching new luminous flares (we refer the reader to Romano (2015) and Bozzo et al. (2015) for the most recent reviews of the *Swift*/XRT monitoring of a sample of SFXTs, and to Smith et al. (2012) for the *RXTE* results).

These investigations found that the most extreme SFXTs span a large dynamic range in X-ray luminosity, from quiescence ($L_X \sim 10^{32}$ erg s^{-1}, e.g. Drave et al. 2014) to the peak of the flares ($L_X \sim 10^{36}$-10^{37} erg s^{-1}, reaching 10^{38} erg s^{-1} in IGR 17544 - 2619; Romano et al. 2015), whereas more typical variability amplitudes are between $L_X \sim 10^{33}$-10^{34} erg s^{-1} and $L_X \sim 10^{36}$ erg s^{-1} (Sidoli and Paizis, 2018), with a time-averaged X-ray luminosity $L_X \lesssim 10^{34}$ erg s^{-1} (Sidoli et al., 2008; Bozzo et al., 2015). The comparison of the SFXTs and classical sgHMXBs duty cycles carried out with Swift/XRT highlighted even more the strikingly different behaviours of the two classes of systems in the X-ray domain (see, e.g., Bozzo et al., 2015, and references therein). The SFXT emission is indeed very variable (flaring) at all X-ray luminosities (already evident from the first *XMM-Newton* observation of the SFXT IGR J17544 - 2619; González-Riestra et al. 2004).

The properties of the lowest luminosity state ($L_X \sim 10^{32}$ erg s^{-1}) of SFXTs remain poorly known, although from *Swift*/XRT monitoring it can be estimated as the most frequent state in some members of the class (IGR J08408 - 4503, IGR J16328 - 4726 and IGR J17544 - 2619; Romano 2015).

The bright short ($\sim$ 2 ks duration) flares belong to longer outbursts, lasting a few days (Romano et al., 2007; Rampy et al., 2009; Bozzo et al., 2011b), and usually occur in an unpredictable way, except for

IGR J11215 - 5259: here, a periodicity in the outburst recurrence was found with *INTEGRAL*(Sidoli et al., 2006), later refined to ~ 165 days with *Swift*/XRT (Sidoli et al. 2007, Romano et al. 2009b) and likely associated with the orbital period of the system. This is the longest one, while for other SFXTs the orbital cycle ranges from 3.3 days (Jain et al., 2009a) to 51 days (Drave et al., 2010). Most periodicities have been discovered from the modulation of their long-term light curve observed with *INTEGRAL*(Bird et al., 2009; Zurita Heras and Chaty, 2009; Clark et al., 2009; 2010; Drave et al., 2010; Goossens et al., 2013), *Swift*/BAT (Corbet et al., 2006b; La Parola et al., 2010a; D'Aì et al., 2011) and *RXTE*(Levine and Corbet, 2006; Corbet et al., 2010d). SFXTs display both narrow circular orbits and wide, very eccentric ones, with orbital eccentricities ($e = 0.63$ in IGR J08408 - 4503 and $e > 0.8$ in IGR J11215 - 5952) even higher than in Be/X-ray transients (see the discussion in Sidoli and Paizis 2018). In IGR J17544 - 2619 a high proper motion has been discovered (Maccarone et al., 2014).

In some sources, SFXT flares appear to be more concentrated around periastron (e.g. Romano et al. 2014b; Gamen et al. 2015), but they can occur at any orbital phase and it is crucial to remark that not every periastron passage triggers an outburst (except in the case of IGR J11215 - 5259, where an outburst is present every time the source is observed at the expected times of the periastron passage; e.g. Sidoli et al. 2020).

Super-orbital periods have been discovered in IGR J16418 - 4532 and IGR J16479 - 4514 (Corbet and Krimm, 2013; Drave et al., 2013a) and, tentatively, in IGR J08408 - 4503 (Gamen et al., 2015).

Six SFXTs are X-ray pulsars (including the unconfirmed periodicities in IGR J17544 - 2619 and IGR J18483 - 0311; Drave et al. (2012); Romano et al. (2015); Ducci et al. (2013)), with spin periods reaching ~ 1200 s (Walter et al., 2006), implying that the accreting compact object is a NS. In general, a NS is assumed also in SFXTs where no pulsations have been detected, given the similarity of their broad-band X-ray spectra in outburst with those of accreting pulsars: an absorbed, flat power law within 10 keV (with photon index Γ between 0 and 1), modified by a high energy cutoff in the range of energies 10–30 keV (e.g. Walter et al. 2006; Sidoli et al. 2006; Götz et al. 2007; Filippova et al. 2007; Romano et al. 2008; Sidoli et al. 2009; Zurita Heras and Walter 2009; Ducci et al. 2010). The few SFXTs where both spin and orbital periods are detected are spread over a vast area of the Corbet diagram, overlapping (and bridging) persistent sgHMXBsand Be/X-ray transients.

In a few SFXTs a soft X-ray spectral component has been detected during outbursts (as observed in many accreting pulsars; see e.g. La Palombara and Mereghetti 2006) and was modeled using a hot blackbody with radius of a few hundred meters, compatible with the NS polar caps (e.g. Sidoli et al. 2012). To date, only in the case of the SFXT pulsar IGR J11215 - 5952 a spectral evolution along the spin phase has been observed (Sidoli et al., 2007). In IGR J17544 - 2619, the most extreme transient of the SFXT class, a spectral evolution was observed in the *XMM-Newton*plus *NuSTAR*spectrum across different luminosity states (from 6×10^{33} erg s^{-1}up to the peak of a flare, 1600 times brighter): the combination of a hot (blackbody with $kT \sim 1 - 2$ keV) thermal component (likely emitted from the surface of the NS), together with a non-thermal, Comptonized component up to ~ 40 keV, showed evidence of a more prominent contribution from the blackbody at fainter fluxes (Bozzo et al., 2016a), similar to what is usually observed in HMXB pulsars.

Sometimes the soft excess detected in the same X-ray observation can be accounted for equally well by different models, besides a blackbody: either a partial covering absorption or a ionized absorber (Sidoli et al., 2012; 2017b). The specific case of IGR J08408 - 4503 is notable, as this source has the lowest absorbing column density (10^{21} cm^{-2}) out of all SFXTs. This allowed Sidoli et al. (2009) to uncover two distinct photon populations (during outburst): one with a

temperature of ~ 0.3 keV, possibly associated with a thermal halo around the NS, and a hotter one at ~ 1.6 keV, likely from the accretion column. A clear soft excess has been observed in this SFXT also in low luminosity states (Sidoli et al., 2008; Bozzo et al., 2010), possibly due to thermal X-rays from the donor wind.

The X-ray spectra of SFXTs outside outbursts (at $L_X \sim 10^{33} - 10^{34}$ erg s^{-1}) are usually softer, although still well described by a power law (with photon index Γ ~ 1 – 2, Sidoli et al. 2008; Bozzo et al. 2010; Romano et al. 2014a; Bozzo et al. 2017b), implying ongoing accretion. Sometimes a double component model (non-thermal plus thermal) describes the 1 – 10 keV emission better than a single power law even at these low luminosities. The soft excess can be accounted for by a blackbody or by a thermal plasma model (Zurita Heras and Walter, 2009; Bozzo et al., 2010; Sidoli et al., 2010; Romano et al., 2014a). This ambiguity in the spectral deconvolution of the soft excess translates into inconclusive results about its nature, at present. The X-ray spectrum observed during the lowest luminosity state (~ 10^{32} erg s^{-1}) can be very soft (Γ ~ 6; in't Zand 2005), probably due to thermal X-ray emission from the supergiant wind.

In some sources the local absorbing column density is variable: an increase in the absorption during the rise to the peak of a flare is interpreted as due to and enhancement of the accreting wind matter (Sidoli et al., 2009; Bozzo et al., 2011b; 2016a), otherwise it can be simply due to the passage of a foreground dense clump (Rampy et al., 2009; Boon et al., 2016; Bozzo et al., 2017b). A drop in the column density at the peak of a bright flare is explained with the ionization of the local material (Bozzo et al., 2011b; 2016a; 2017b).

SFXTs have overall lower absorbing column densities than persistent sgHMXBs(Giménez-García et al., 2015; Pradhan et al., 2018). Some exceptions exist, like SAX J1818.6 - 1703, where $N_H \sim 5 \times 10^{23}$ cm^{-2} was observed, similar to what is seen in obscured HMXBs (Boon et al., 2016; Bozzo et al., 2017b). Another diagnostic of the circumsource material is the iron line emission (Bozzo et al., 2011b; Giménez-García et al., 2015; Pradhan et al., 2018), contributed by the supergiant wind illuminated by the X-ray source. The equivalent width (EW) of the 6.4 keV line measured outside eclipses correlates with the absorbing column density and can reach much higher values (EW > 1 keV) in persistent HMXBs than in SFXTs (Giménez-García et al., 2015; Pradhan et al., 2018). This is indicative of an accretion environment less dense in SFXTs than in classical sgHMXBs. Other observations indicate a difference in the donor wind between some members of the two subclasses: in the persistent source Vela X-1 a slower supergiant wind than in the SFXT IGR J17544 - 2619 has been observed (Giménez-García et al., 2016), while a kiloGauss magnetic field has been measured (at 3.8σ) in the supergiant companion of the periodic SFXT IGR J11215 - 5952 (Hubrig et al., 2018), supporting the hypothesis of the presence of a magnetically focused supergiant wind (Sidoli et al., 2007). These findings have important implication for the mechanism triggering bright flares (see next subsection).

NS surface magnetic fields, measured from the detection of a CRSF, are elusive: a hint of a low magnetic field ($B \sim 10^{11}$ G) has been found in IGR J18483 - 0311 (Sguera et al., 2010), while a more typical $B \sim 10^{12}$ G has been measured with *NuSTAR*in IGR J17544 - 2619 (Bhalerao et al., 2015), although not confirmed by a second *NuSTAR* observation (Bozzo et al., 2016a). In the 187 s pulsar IGR J11215 - 5952 only a hint for a CRSF around 17 keV could be found in the *NuSTAR* spectrum of a flare (Sidoli et al., 2017b), but was not confirmed during a second *NuSTAR* observation (Sidoli et al., 2020).

As a final remark, we note that the classification of a source as an SFXT or a classical sgHMXBis by no means clear-cut, and there exist several sources displaying a behaviour which is intermediate between the two subclasses (see, e.g., Walter et al. 2015; Sidoli and Paizis 2018). Thus, we should not expect lists of SFXTs or sgHMXBsproduced by different groups to agree exactly.

3.5. Be X-ray Binaries with INTEGRAL

The large field of view and high sensitivity of the instruments on-board *INTEGRAL* allowed this mission to play a leading role in the detection and study of transient sources, and particularly transient X-ray pulsars (XRPs) in Be-binary systems (BeXRBs; see Sect. 2.3). For over 15 years, almost all major outbursts from systems already known were observed, while eight new Be binaries were discovered by *INTEGRAL*, representing an increase in the total number of such sources up to 60 in our Galaxy (Walter et al., 2015). Pulsations with periods ranging from ∼ 12 to ∼ 700 s were detected in several new systems: IGR J01583 + 6713, IGR J11435-6109, IGR J13020-6359, IGR J19294 + 1816, IGR J22534 + 6243 (Walter et al., 2015), IGR J21343 + 4738 (Reig and Zezas, 2014b) and IGR J06074 + 2205 (Reig and Zezas, 2018), confirming their pulsar nature.

Observations of bright transient XRPs at different mass accretion rates is essential to understand physical processes at the accretion disc - magnetosphere border and in the vicinity of the NS surface. A giant (type II) outburst from the BeXRB V 0332 + 53 starting late in 2004 (Swank et al., 2004; Kreykenbohm et al., 2005) became the first such an event studied with the *INTEGRAL* observatory in great detail. About 400 ks of exposure time were invested to cover the whole outburst and investigate the properties of the source at very different mass accretion rates. As a result of this monitoring, an unexpected negative correlation of the cyclotron energy (see Sect. 2.7) with source luminosity was revealed (Tsygankov et al., 2006b; Mowlavi et al., 2006; Tsygankov et al., 2010; Ferrigno et al., 2016). This discovery led to a surge of interest in the study of cyclotron lines, especially using the *INTEGRAL* observatory in view of its good energy resolution and broad energy coverage (see e.g., Filippova et al., 2005, for the review of spectral properties of XRPs with *INTEGRAL*). Another pulsar possessing a possible negative correlation of the cyclotron energy with luminosity is 4U 0115 + 63, where such a trend was suggested by Mihara et al. (1998). Later, this correlation was confirmed using the *INTEGRAL* and *RXTE* averaged and pulse-amplitude-resolved spectra (Nakajima et al., 2006; Mihara et al., 2004; Tsygankov et al., 2007; Klochkov et al., 2011). On the other hand, some authors explained this behaviour of the cyclotron energy in 4U 0115 + 63 with our poor knowledge of the spectral continuum

(Ferrigno et al., 2009; Müller et al., 2013; Boldin et al., 2013). In less bright sources ($L_X \lesssim 10^{37}$ erg s^{-1}), a positive correlation of the cyclotron energy with luminosity was discovered using different observations, including some by *INTEGRAL* (Staubert et al., 2007; Yamamoto et al., 2011; Klochkov et al., 2012). For the well known source 1A 0535 + 262, *INTEGRAL* and *RXTE* observations of the first observable outburst after a long period of quiescence fixed the previously debated magnetic field strength and found no correlation with luminosity over the observed range (Kretschmar et al., 2005; Caballero et al., 2007). These and many other results obtained with different X-ray missions (e.g. *RXTE, NuSTAR, Suzaku*) substantially improved our knowledge in the field of cyclotron lines formation and evolution (see Sect. 2.7 and the recent review by Staubert et al. 2019).

The good time resolution of the *INTEGRAL* main instruments also permitted studies of temporal properties of emission from XRPs in hard X-rays. In particular, a comprehensive investigation of the pulse profile shapes and pulsed fraction as a function of energy band and flux from the source was performed by Lutovinov and Tsygankov (2009). These authors showed that the pulsed fraction systematically increases with energy and has local peculiarities near the cyclotron energy. Phase-resolved spectral analysis also revealed a significant variability of the emission properties over the pulse phase in several sources. Particularly in EXO 2030 + 375, a hint of the presence of a cyclotron absorption line has been found at ∼ 63 keV in a very narrow phase interval covering less than 10% of the whole spin period (Klochkov et al., 2008).

In addition to transient sources, the BeXRB family contains a few persistent X-ray pulsars (Reig and Roche, 1999). Such objects are characterized by relatively low luminosity ($10^{34} - 10^{35}$ erg s^{-1}) and wide orbits ($P_b \gtrsim 200$ days). Due to the high sensitivity of the IBIS telescope some of these systems were detected and studied in the hard energy range with great detail. For instance, RX J0440.9 + 4431 and X Persei were detected up to ∼ 120 keV (Tsygankov et al., 2012) and ∼ 160 keV (Lutovinov et al., 2012), respectively, which is not typical for X-ray pulsars. In the case of X Persei, the high quality of the spectrum allowed Doroshenko et al. (2012b) to interpret the broad absorption-like feature around 30 keV not as a cyclotron line (Coburn et al., 2001), but as an artificial deficit of photons between two distinct spectral components (see also Di Salvo et al., 1998). The latter interpretation was recently confirmed for two other BeXRBs, GX 304 - 1 and 1A 0535 + 262, at low accretion rates (Tsygankov et al., 2019b; 2019a).

Another contribution to BeXRB research with *INTEGRAL* is from the Optical Monitoring Camera (OMC), which provides photometry in the Johnson *V*–band simultaneously with the high-energy observations (Mas-Hesse and (INTEGRAL OMC Consortium), 2003). In this way long-term OMC optical light curves of many HMXBs, along with light curves of many other variable objects (Alfonso-Garzón et al., 2012), are available through the OMC archive[1] (Gutiérrez et al., 2004; Domingo et al., 2010). Long-term optical variability has been observed in the OMC light curves of some BeXRBs, with examples shown in Fig. 14.

Beyond the Milky Way, *INTEGRAL* has made a significant contribution to identifying the BeXRB population in the nearby Magellanic Clouds. A series of deep observations has led to the discovery and identification of several new systems (McBride et al., 2007; Coe et al., 2010a). A good example of the power of the *INTEGRAL* wide field of view is shown in this map of objects detected during one set of observations - see Figure 15. Identifying all the BeXRB systems in external galaxies like the Magellanic Clouds provides us with a very effective tool for understanding recent star formation and X-ray luminosity functions in these galaxies – see, for example, Shtykovskiy and Gilfanov (2005).
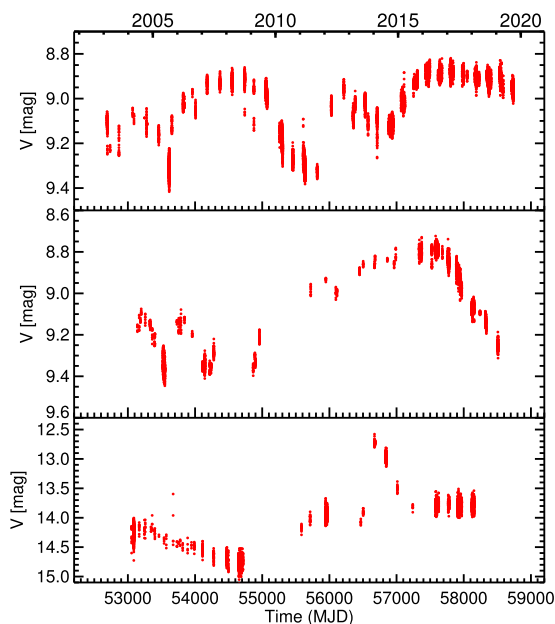

Fig. 14. OMC light curves of BeXRBs. Top: 1A 0535 + 262. Middle: H 1145 - 619. Bottom: GX 304 - 1. The apparent dispersion within the observation windows is due to intrinsic low-amplitude variability, typical of Be systems.
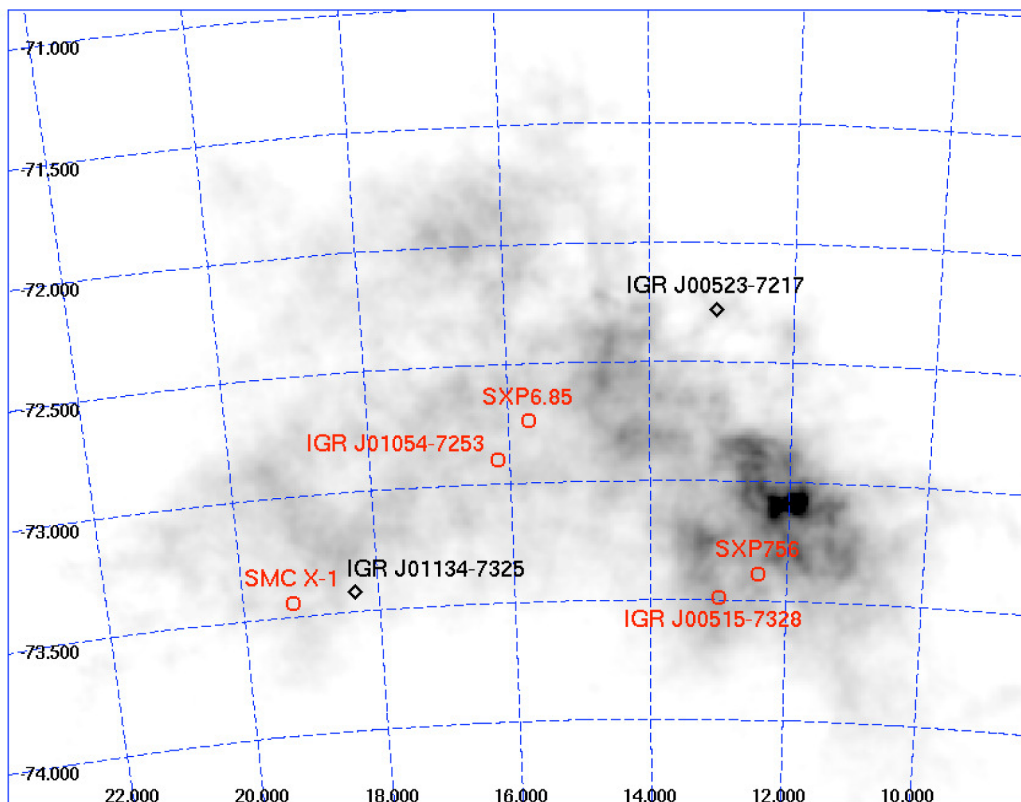
---

[1] http://sdc.cab.inta-csic.es/omc/

Fig. 15. Sources detected by IBIS on *INTEGRAL* overplotted on the SMC H I column density map. Figure from Coe et al. (2010a). The sources in red are definite source detections. The two sources in black are candidate sources.

3.6. Gamma-ray binary studies with INTEGRAL

Joint *INTEGRAL* and *XMM-Newton* observations of LS I +61° 303 demonstrated that the overall spectrum of the system in the 0.5–100 keV energy band is well fit with a featureless power law both at high- and low-flux states, see, e.g., Fig. 16 and Chernyakova et al. (2006); Zhang et al. (2010); Li et al. (2014). Non-observation of a cut–off or a break in the spectrum at 10–100 keV energies, typical of accreting NSs and BHs, favours the scenario in which the compact object is a rotation-powered pulsar. *INTEG-RAL* observations demonstrated that in the hard X-rays LS I +61° 303 is following the overall orbital modulation trend of soft X-rays (Zhang et al., 2010) and also showed hints of a variability similar to the change of the orbital lightcurve on the superorbital time scale observed in the 3–20 keV range (Chernyakova et al., 2012; Li et al., 2014). A joint study of the LS I +61° 303 spectral variability at hard X-rays with

Fig. 16. Broad-band spectrum of LS I +61° 303. This Figure is an adapted extract of Figure 6 in Chernyakova et al. (2006). The solid (dashed) line shows the model fit within the synchrotron-inverse Compton model for the high-flux (low-flux) state of the source.

INTEGRAL and in the radio band was done by Zimmermann and Massi (2012b) and Li et al. (2014) to test the possible microquasar nature of the system. Li et al. (2014) showed that, for most of the *INTEGRAL* observations, LS I +61° 303 had a hard spectrum with $\Gamma \sim 1.5$ while the corresponding radio GBI observations (non-simultaneous, but taken at the same orbital and superorbital phase) had a spectral slope $\alpha < 0$, which is inconsistent with the predictions of the microquasar model (Zimmermann and Massi, 2012b). Still, more observations are needed to reach any firm conclusion on the nature of the compact source in the system.

The study of *INTEGRAL* observations of another gamma-ray binary, LS 5039, revealed that that the source significantly emits at hard X-rays (25–200 keV); this emission varies with the orbit in phase with the very high energy gamma-rays detected with HESS (Hoffmann et al., 2009) and is fully anti-correlated with the GeV emission (Abdo and (Fermi LAT Collaboration), 2009). The spectrum at the inferior conjunction is well described by a power law, while at the superior conjunction the hard X-ray emission is below the sensitivity of *INTEGRAL*. This result indicates that accretion might not be the mechanism for the production of the hard emission in the system, since, in this case, one would expect a rather sharp flux maximum near periastron (Hoffmann et al., 2009). An investigation of the orbital light curve in a broad energy range from classical X-ray to TeV energies revealed a transition energy range of tens to hundreds MeV, in which the dominant emission moves from around apastron region to around periastron (Chang et al., 2016).

A similar behaviour is observed in 1FGL J1018.6 - 5856, another gamma-ray binary with a period of 16.5 days, discovered blindly in Fermi-LAT data (Fermi LAT Collaboration, 2012). Li et al. (2011a) have carried out an analysis of all *INTEGRAL* data available at that time. The total effective exposure extracted on the source amounted to 5.78 Ms, and led to a credible detection of the source at hard X-rays (18–40 keV). The count rate of the source is very low, but hints at an anti-correlation with the 100 MeV–200 GeV emission detected by Fermi-LAT.
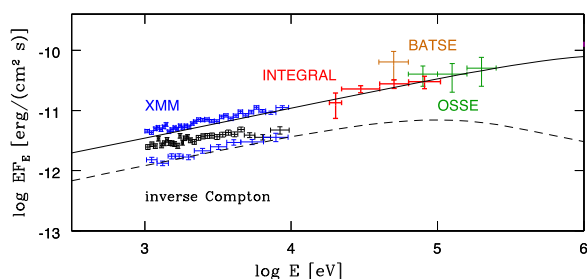
In 2004 *INTEGRAL* performed the first imaging observations of PSR B1259 - 63 in the hard X-ray range (> 20 keV) (Shaw et al., 2004), which allowed separating the emission of PSR B1259 - 63 from the emission of the nearby pulsar 2RXP J130159.6 - 635806 (Chernyakova et al., 2005), which may have contaminated previous hard X-ray observations of this system. Unambiguous measurement of the non-cutoff power law spectrum in the 20–200 keV energy range served as invaluable input for further broad band spectral modeling. *INTEGRAL* also traced the hard X-ray behaviour of PSR B1259 - 63 between 55 and 70 days after its 2014 periastron passage (Chernyakova et al., 2015).

4. Population overview and distribution in the Galaxy (and beyond)

All-sky surveys by *INTEGRAL*-IBIS have lowered the sensitivity limit to 2.2×10^{-12} erg cm^{-2} s^{-1} for a 5σ source detection above 20 keV (Krivonos et al., 2017). This is equivalent to an X-ray luminosity of

2×10^{35} erg s^{-1} for a source located at a distance of 20 kpc, i.e., at the far side of the Milky Way. As a result, *INTEGRAL* doubled the number of HMXBs detected in hard X-rays in the Galaxy, and tripled the number of those with supergiant donor stars (Walter et al., 2015). These HMXBs feature column densities in excess of 10^{22} or even 10^{23} cm^{-2}. The nature of the compact object in these new systems is known, or suspected, to be a NS in almost every case. Many of them exhibit long pulsation periods expected from wind accretors. Therefore, the catalog of *INTEGRAL*-detected HMXBs provides a large (in number), uniform (in exposure), and nearly complete (in luminosity) population for statistical analysis.

4.1. Spatial Distributions

Figure 17 presents the Milky Way as viewed by an outside observer with the locations of 112 HMXBs detected by *INTEGRAL*-IBIS, as well as active sites of massive star formation (Russeil, 2003). There are now 91 HMXBs whose distances, as reported in the literature, place them
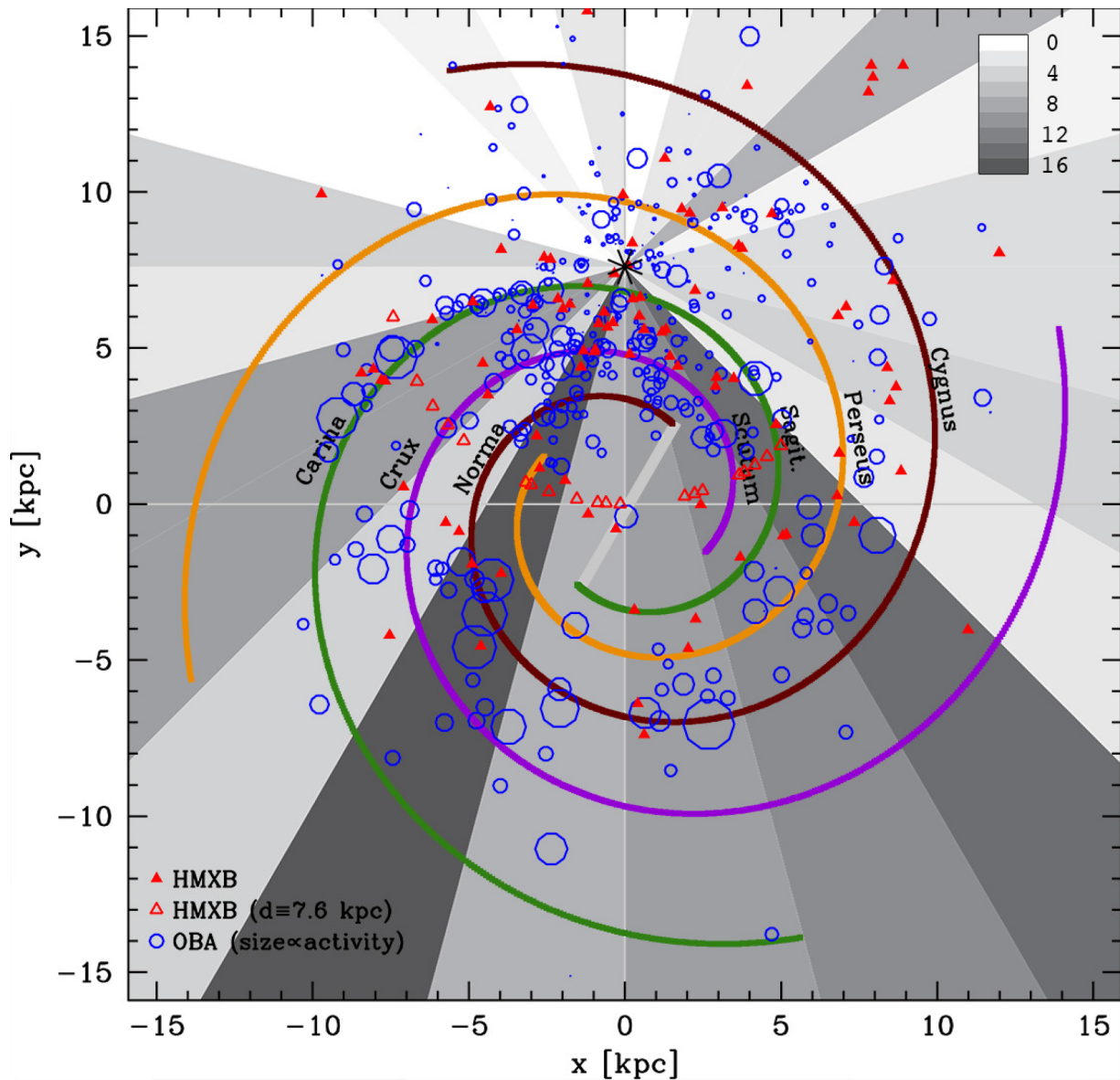

Fig. 17. The distribution of *INTEGRAL*-IBIS-detected HMXBs is shown for an observer situated outside the Milky Way. The closed triangles represent 91 HMXBs whose distances are known. The open triangles denote 21 HMXBs whose distances are not known, so they are placed at the galactocentric distance of 7.6 kpc used in the spiral arm model of Vallée (2002). The largest circles indicate the most active sites of massive star formation (Russeil, 2003). The shaded bands in the background indicate the number of HMXBs per bin of 15° in Galactic longitude, as viewed from the Sun (star symbol). This is an update of the study by Bodaghee et al. (2012b).
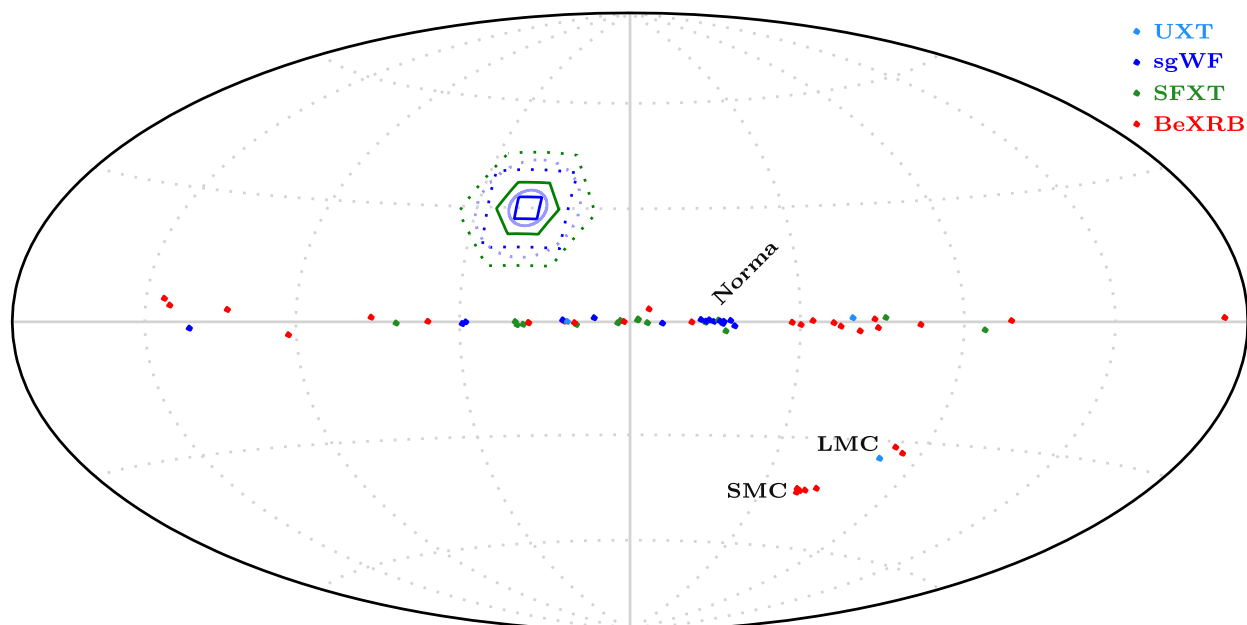
Fig. 18. Sky distribution in Galactic coordinates of HMXBs for which *INTEGRAL* played a significant role (see Table A.1). The overlay contours indicate the fully-coded and maximum fields of view of the *INTEGRAL* instruments.
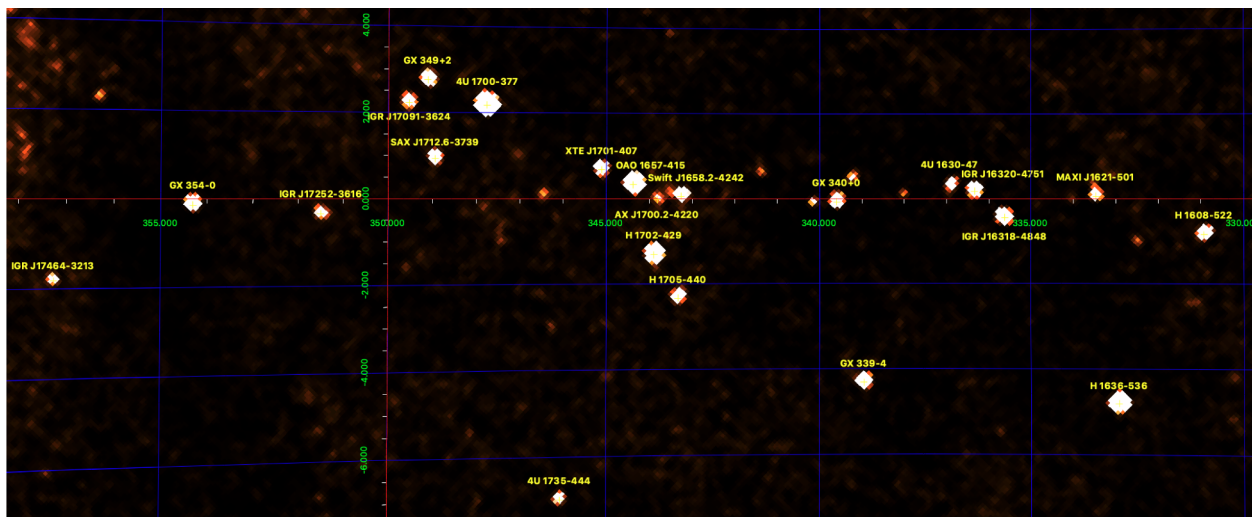

Fig. 19. Deep mosaic image in the 28–80 keV energy range of the Norma region close to the tangent direction, a zone in the Galaxy rich in hard X-ray sources. The mosaic includes 770 individual *INTEGRAL* pointings between 2016 and 2020.

somewhere within our Galaxy. The previous version of this map had 79 such objects (Bodaghee et al., 2012b). Distances to 47 HMXBs were either refined or collected for the first time thanks to measurements of the optical counterpart as part of the 2nd data release from the *Gaia* mission (Gaia Collaboration, 2018; Bailer-Jones et al., 2018). From our perspective within the Galaxy, the direction tangent to the Norma spiral arm continues to feature the highest concentration of HMXBs (the darkest band in Fig. 17). That particular wedge of 15° in longitude contains 16 HMXBs which has motivated X-ray surveys by *Chandra* and *NuSTAR* (Fornasini et al., 2014; Fornasini, 2016; Fornasini et al., 2017) to uncover its faint HMXB population. Figure 19 shows a deep mosaic of this region.

The spatial distribution of HMXBs traces the recent history of massive star formation in the host galaxy. This is because only a few tens of Myr are thought to elapse between the birth of a massive stellar binary in an OB Association (OBA), and the supernova phase that leaves behind a compact object (Schaller et al., 1992). Studies of longitudinal distributions of HMXBs consistently show that they are most abundant near sites where the formation of massive stars is most intense, i.e., towards the tangents to the Galactic Spiral Arms (Grimm et al., 2002; Dean et al., 2005; Lutovinov et al., 2005a; Bodaghee et al., 2007). The surface density of HMXBs is largest for galactocentric distances of 2–8 kpc, which is again consistent with the distribution of OBAs (Lutovinov et al., 2013).

Nevertheless, significant differences emerge between the HMXB and OBA populations when comparing their physical locations within the Galaxy. The scale height of the HMXB population is larger than that of the OBA population: ∼ 90 pc and ∼ 30 pc, respectively (Lutovinov et al., 2013). On average, a HMXB is located 0.3 ± 0.1 kpc from the nearest OBA. Including this offset in the two-point cross-

correlation function increases the significance of the clustering between HMXBs and OBAs, which indicates that the HMXBs have moved away from their parent OBAs and from the Spiral Arms as well. Assuming typical HMXB ages, this corresponds to an average migration velocity of 100 ± 50 km s^{-1} (Bodaghee et al., 2012b). Coleiro and Chaty (2013), after computing the distance and absorption to 46 HMXBs by fitting the optical and infrared SED of the donor star, could associate them with their likely parent OBAs, deriving a clustering size between HMXB and OBA of 0.3 ± 0.05 kpc, with a characteristic inter-cluster distance of 1.7 ± 0.3 kpc. With these accurate HMXB distances, by taking into account the Galactic spiral arm rotation and assuming a regular value of kick velocity of 100 km s^{-1}, Coleiro and Chaty (2013) constrained age and maximum migration distance of 13 HMXBs: 9 BeXRBsand 4 sgHMXBs.

These velocities are higher than expected from recoil due to anisotropic mass loss from the primary to the secondary (Blaauw, 1961), or via dynamical ejection and outflows from the cluster (Poveda et al., 1967; Pflamm-Altenburg and Kroupa, 2010). Instead, the velocity range is consistent with values expected for a natal kick acquired during the formation of the NS, which can be significant in an asymmetrical supernova (e.g., Shklovskii, 1970). Empirical evidence of migration velocities in HMXBs can help determining the characteristic timescale between the formation of the NS and the X-ray emission phase, which is still poorly understood, as well as constraining models of type II supernovae. Unfortunately, there are only a handful of HMXBs whose proper motions are known well enough to enable the measurement of a kick velocity away from a specific OBA (e.g., Ankay et al., 2001; Ribó et al., 2002; Mirabel et al., 2004). Fortunately, the evolutionary history of massive binary stars is imprinted as an offset in the spatial distribution of HMXBs relative to their birthplaces, and this offset yields an average velocity for the population.

4.2. Luminosity Functions

A useful diagnostic of HMXB populations is the luminosity function $N(>L)$, which is the number distribution of sources with luminosities greater than L, plotted as a function of L, as shown in Fig. 20. The shape of the HMXB luminosity function depends on the recent star-formation rate of the host galaxy (e.g., Grimm et al., 2002), and on the relations governing the mass accretion rate and luminosity in wind-accreting systems (Postnov, 2003).

Luminosity functions are relatively easy to build for HMXBs in other galaxies since the entire population is located at the well-known distance of the host galaxy. Measuring the distances of HMXBs in the Milky Way, however, is more challenging given that the Galactic veil of dust and gas leads to optical extinction of the stellar companion, and photoelectric absorption of the soft X-rays. So not only are many of the distances unknown but also, for those objects whose distances are known, the sensitivity of the survey in each region of the Milky Way must also be considered.

Figure 20 presents the HMXB luminosity function with *INTEGRAL*-IBIS data (Lutovinov et al., 2013). A single power law does not adequately fit the luminosity function over the range of luminosities sampled (10^{34}–10^{37} erg s^{-1}), given that a break in the slope around 10^{36} erg s^{-1}and a flattening at lower luminosities are evident. That becomes even more clear if the spatial distribution of early type stars is taken into the account. This is illustrated by an independent reconstruction of the HMXB luminosity function using the same data-set by Doroshenko et al. (2014) and shown in Figure 20, where the impact of distance uncertainties to individual objects is minimized through Monte Carlo modeling under the assumption that the spatial distribution of HMXBs is roughly known.

These results could imply that the IBIS surveys may be missing a significant number of faint HMXBs. However, a flattening at the faint end was also observed in the luminosity function of HMXBs in the more uniform *Swift*-BAT survey (Voss and Ajello, 2010), as well as in the
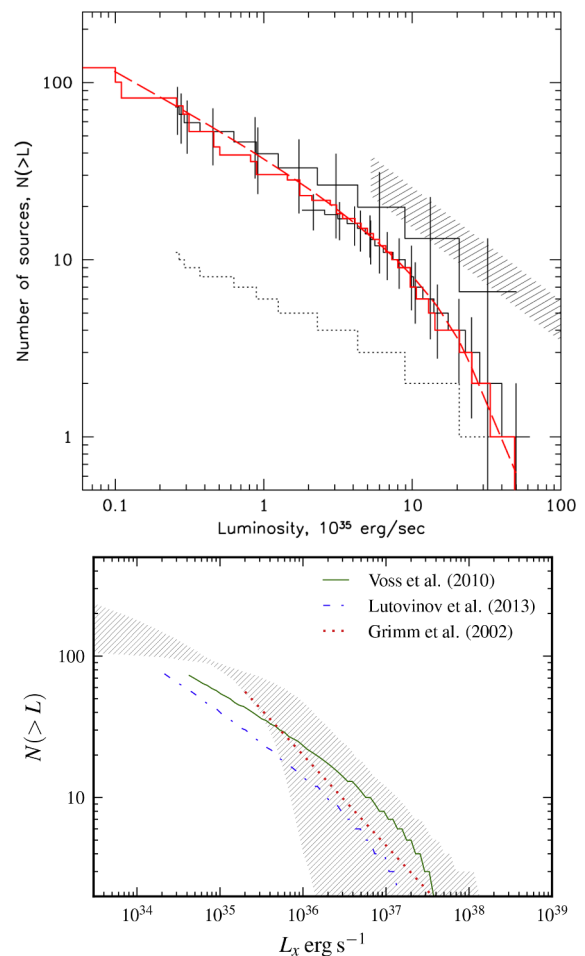

Fig. 20. Top panel: luminosity function for persistently-emitting HMXBs in the Milky Way (red histogram) fit with a broken power law (dashed curve) as presented in Lutovinov et al. (2013). Volume-limited samples are shown as black histograms. The shaded region corresponds to the luminosity function from *RXTE*-ASM data (Grimm et al., 2002). Bottom panel: the same luminosity function (shaded area) as reconstructed through Monte Carlo modeling by Doroshenko et al. (2014). For comparison, the results by Lutovinov et al. (2013) and Voss and Ajello (2010) are shown.

luminosity function of HMXBs in the Small Magellanic Cloud (Shtykovskiy and Gilfanov, 2005). Therefore, an adjustment may be necessary in the universal luminosity function which is expected to follow a single power law $dN/dL \propto L^{-\alpha}$ with $\alpha = 1.6 \pm 0.1$ for a wide range of luminosities (10^{35}–10^{40} erg s^{-1}). Surveys by *INTEGRAL*-IBIS and other facilities such as *eROSITA* will continue to probe the faint end of the luminosity function, helping to clarify the recent history of massive star formation and the relative contribution of HMXBs to the total X-ray luminosity of galaxies.

4.3. Cumulative Luminosity Distributions

A long-term systematic analysis of *INTEGRAL* data (fourteen year span) has been performed by Paizis and Sidoli (2014) and Sidoli and Paizis (2018) who investigated the hard X-ray properties of 58 HMXBs. The sample, about half of the total number of HMXBs known in our Galaxy, comprises persistent and transient systems, including BeXRBs, sgHMXBsand SFXTs hosting a NS or a BH. Light-curves of 2 ks time bins were used to derive hard X-ray (18–50 keV) cumulative luminosity distributions (CLD) for all the sources. This approach leads to a full quantitative characterization of the hard X-ray luminosity distributions of the single sources, displaying in a concise way the different
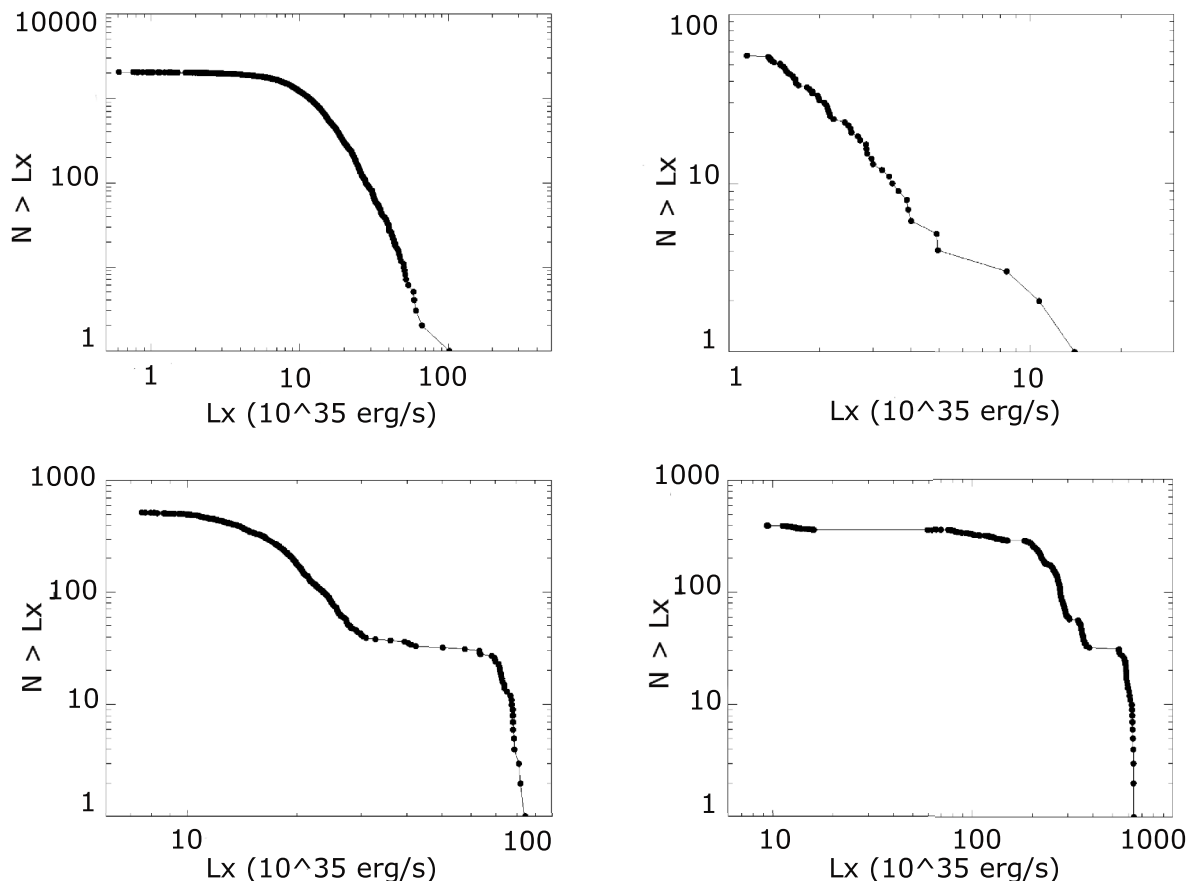
Fig. 21. Cumulative luminosity distributions (18–50 keV) of four representative sources considering fourteen years of *INTEGRAL* IBIS/ISGRI data. Each point refers to a source detection in a ~ 2 ks *INTEGRAL* pointing. The highest y-axis values indicate the duty cycles in the given band, while the range of variability can be seen on the x-axis. From left to right, top to bottom: Vela X - 1 (persistent sgHMXB), SAX J1818.6 - 1703 (SFXT) and the two BeXRB transients SAX J2103.5 + 4545 and EXO 0331 + 530 (the bimodal shape can be explained by the occurrence of normal and giant outbursts). Adapted from Sidoli and Paizis (2018).

phenomenologies and patterns at play, the sources' duty cycles, range of variability and the time spent in each luminosity state. Figure 21 shows the CLDs of four representative sources.

In Sidoli and Paizis (2018), the phenomenology observed with *INTEGRAL* is juxtaposed with other known source properties in order to obtain a quantitative overview of the main subclasses of accreting massive binaries as they tend to cluster in the different parameter spaces explored.

With respect to Lutovinov et al. (2013) who studied the luminosity and spatial properties of persistent HMXBs in our Galaxy with *INTEGRAL*, Sidoli and Paizis (2018), while considering transient sources as well, focused on the bright luminosity end. Indeed, the selection criteria chosen (source detection in a single 2 ks pointing) resulted in a flux-limited sample with a sensitivity of a few 10^{-10} erg s^{-1}cm^{-2}, about one order of magnitude worse than what considered by Lutovinov et al. (2013).

Motivated by the intriguing *INTEGRAL* results, the study of the HMXB cumulative luminosity distributions presented by Paizis and Sidoli (2014) was extended in the soft X-ray energy domain (2–10 keV) by Bozzo et al. (2015). These authors used Swift/XRT data collected during the long-term monitoring campaign of several classical sgHMXBs and SFXTs, which regularly span a significant fraction of the orbital phases of many revolutions of these systems (providing a few 100 ks of effective exposure per source), in order to provide an efficient
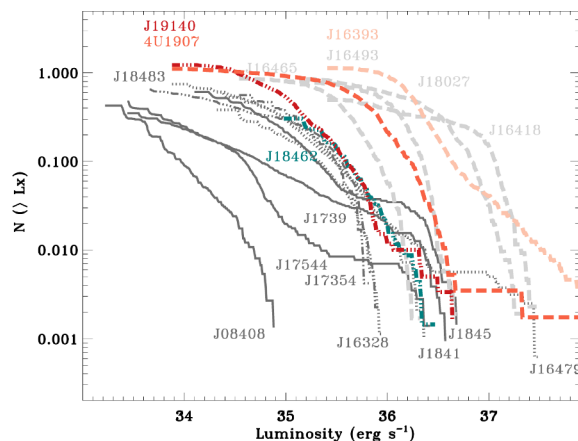

Fig. 22. Cumulative luminosity distributions (2–10 keV) of several SFXTs and classical sgHMXBs derived from the long term monitoring campaigns of these objects performed with Swift/XRT (Bozzo et al., 2015, Romano et al. 2020, in preparation). The figure is adapted from Bozzo et al. (2015) and includes both data previously published (gray lines) and newly obtained data (Romano et al. 2020, in preparation). Solid lines are used for SFXTs and dashed lines for classical sgHMXBs. The typical "step-like" shape of the SFXT cumulative luminosity distributions can be clearly seen in all cases.

probe of their different luminosity states. The advantage of the XRT data is that the instrument is endowed with a high sensitivity and can extend the cumulative luminosity functions down to fluxes as low as $\sim 10^{-13}$ erg s^{-1}cm^{-2}, complementing the *INTEGRAL* curves. We show in Fig. 22 an improved version of the fig. 5 of Bozzo et al. (2015), which includes the results of the most recent and partly still ongoing XRT observation campaigns (the gray curves are those already published previously, whereas the other ones will be reported with all details in Romano et al. 2020, in preparation). In agreement with the results found by *INTEGRAL*, the XRT observations revealed that the cumulative distributions of the SFXTs have a more complex shape, with multiple "steps" (as opposed to the single knee curve of the classical systems) marking the presence of different accretion states. These findings have been interpreted by Bozzo et al. (2015) in terms of the different accretion regimes introduced in Sect. 2.5.

5. Future perspective

INTEGRAL has now been confirmed to operate at least until end 2020, with a possible further extension up to the end of 2022. Other extensions will be decided following pending reviews of the mission status and operations, but are formally possible until 2029, when a planned maneuver will force the satellite to a controlled re-entry in the Earth atmosphere. As emphasized multiple times in this review, the unique combination of sensitivity, pointing strategy, and large field of view of the *INTEGRAL* instruments will surely lead in the years to come to the discovery of new transient HMXBs, including SFXTs. The most recent results in these fields, as summarized in this review, prove that each newly discovered IGR source offers new perspectives to understand the physics of HMXBs and often poses new theoretical/observational challenges. The community is thus certainly looking forward to more years of successful *INTEGRAL* operations.

Following the success of the *INTEGRAL* mission, a number of different high energy facilities, covering from the softer ($\lesssim 0.5$ keV) to the harder X-rays (up to the MeV range) are being planned or already in the timeline. These will certainly provide a dramatic step forward in our understanding of all classes of HMXBs.

The *Athena* mission (see, e.g., Nandra and (Athena Collaboration), 2013) is set to fly in the early 2030s and, especially thanks to the X-IFU instrument (Barret and (Athena X-IFU Collaboration), 2018), it will open the possibility of performing high resolution spectroscopy of HMXBs even at relatively low fluxes. These observations will be able to probe for the first time, among others, the physical processes occurring during the accretion of single clumps from the stellar winds onto the compact objects hosted in classical sgHMXBs and SFXTs (Bozzo and Athena SWG3. 3, 2015). This is something that today is only possible by exploiting the grating spectrometers on-board *Chandra* and *XMM-Newton* for the uniquely bright HMXB Cyg X-1 (Hirsch et al., 2019). High-resolution spectroscopy of wind-fed HMXBs with X-IFU (with a typical accuracy of a few eV, depending on the specific energy) will also permit us to investigate in unprecedented detail the physics of the interaction between the X-rays from the compact object and material in the stellar wind, finally providing a solid measure of the perturbed and unperturbed stellar wind. This is the key also to likely distinguish between the scenarios proposed to explain the different behaviours of classical sgHMXBs and SFXTs.

The eXTP mission (Zhang and (eXTP Collaboration), 2019) is planned to be at present the next X-ray facility harboring a large field-of-view instrument (WFM; Gálvez et al., 2019) that will cover the full sky every ~ 2 days looking for X-ray transient sources in the 2–50 keV energy band. The instrument is based on a similar coded-mask technique as *INTEGRAL*/IBIS, but will complement the *INTEGRAL* discoveries by monitoring the sky in the softer energy band. The eXTP/WFM will provide a good energy resolution of 300 eV on the entire band and a time resolution as accurate as a few μs. An on-board system will detect and broadcast to the ground impulsive events, as for

example the outbursts from SFXTs. The instrument will thus be capable to discover many more transient/flaring HMXBs[2], as well as flares/outbursts from already known sources, collecting for each of these events a uniquely rich amount of useful data that will be provided to the community a few hours after the detection. The eXTP/WFM will also provide daily monitoring data for hundreds of sources with good timing and spectral resolution, that can be used to verify the evolution of the spectral states, as well as the spin period and/or the timing state of the different HMXBs (including possible evolution over time of the cyclotron line features and orbital/super-orbital modulations). Furthermore, the suite of instruments on-board eXTP (Zhang and (eXTP Collaboration), 2019) will be able to provide an unprecedentedly high statistics, good energy resolution, and high timing accuracy data in a broad energy range (2–50 keV) to perform a combined timing-spectroscopy-polarimetry analysis of many bright HMXBs[3]. This will open new perspectives to resolve changes of the cyclotron line parameters as a function of the system physical conditions (geometry, luminosity, line of sight) and understand intimate details of the physics of accretion in wind- / disc-fed systems, as well as aspects of the microphysics of plasma penetration in the NS magnetosphere in a never accessed before way (in't Zand and (eXTP Collaboration), 2019; Santangelo et al., 2019).

Improvements over the already exciting results that will be provided by eXTP are expected from its successor STROBE-X (Ray and (STROBE-X Collaboration), 2019), which will provide yet more effective area to increase the statistics and optimize the background in a more extended energy range (0.5–50 keV). STROBE-X is a mission concept proposed for the NASA decadal survey[4].

Flares and outbursts from Galactic and extra-Galactic HMXBs are expected to be among the easiest targets for detection by the next generation of wide-field X-ray facilities using Lobster-eye telescopes (Angel, 1979), as those planned onboard the Einstein Probe (Yuan et al., 2018) and the THESEUS mission (Amati and (THESEUS Collaboration), 2018; Stratta and (THESEUS Collaboration), 2018). The former mission is led by China and is planned to be launched as early as 2021, while THESEUS is one of the three candidates competing for a launch opportunity in 2032 within the context of the ESA M5 call[5]. The advantage of Lobster-eye telescopes is to provide a large field of view (up to 60×60 deg in the currently planned configurations) and a low background, achieving a sensitivity able to discover sources as faint as $\sim 10^{-10}$ erg s^{-1} (0.3–6 keV) already in a few tens of seconds. This matches well the range of luminosity of the flares and outbursts observed from HMXBs. THESEUS will also be endowed with an infrared telescope (IRT) which will be automatically re-pointed toward the sources of interest, and could be used to identify the massive companions of HMXBs.

In the gamma-ray domain, the AMEGO[6] mission concept (McEnery and (AMEGO Collaboration), 2019) is expected in a farther future to provide new insights about the emissions from HMXBs in the MeV energy range, distinguishing between the possibilities that such emission is due to accretion phenomena or to the presence of jets (de Angelis and (E-Astrogram Collaboration), 2018).

At even higher energies, as summarized in Sect. 2.9, during the last decade an increasing number of HMXBs has been detected in the MeV–GeV energy range (HE), as well as in the TeV energy range (VHE).

---

[2] See, e.g., Bozzo et al. (2013). These authors estimated the number of SFXT outbursts for the WFM instrument on-board the LOFT mission (Feroci and (LOFT Collaboration), 2012), which has a similar design as the eXTP/WFM.

[3] Preliminary measurements of the X-ray polarimetry in HMXBs (Kallman et al., 2015) could be already expected thanks to the NASA mission IXPE (Soffitta, 2017), currently planned for a launch in 2021.

[4] See https://www.nrl.navy.mil/space/strobe-x-headed-decadal-survey

[5] See https://www.esa.int/Our_Activities/Space_Science/ESA_selects_three_new_mission_concepts_for_study.

[6] But see also the similar mission concept e-ASTROGAM (de Angelis and (E-Astrogam Collaboration), 2017).

This proved the existence of an emerging new population of "gamma-ray binaries" and/or "gamma-ray loud binaries" (Dubus, 2013; Chernyakova et al., 2019), which rapidly became subject of major interest. Similarly to these general classes, in principle SFXTs, as well as other flaring sgHMXBs, could be able to produce HE and VHE emission as well since they are characterized by the same ingredients in terms of a compact object and a massive early-type companion star. However, the detection of such emission is nontrivial for current generations of HE and VHE instruments, since it should likely be in the form of unpredictable flares having short duration, small duty cycle and relatively low flux. To date, only few hints have been reported in the literature on SFXTs as best candidate counterparts of unidentified transient HE sources, merely based on circumstantial evidences (Sguera et al., 2009; Sguera, 2009; Sguera et al., 2011). No detection of VHE emission from other sgHMXBshas been reported so far. Hopefully, this situation will change in the near future thanks to a new generation of ambitious facilities under constructions, e.g. the Cherenkov Telescope Array, which will offer an order of magnitude improvement in the VHE domain in terms of sensitivity and survey speed compared to existing facilities, hence holding the promise of performing well as a transient detection factory (Cherenkov Telescope Array Collaboration, 2019). We expect that future studies will likely shed new light by detection or not-detection SFXTs, as well as other sgHMXBs, as HE and VHE transient emitters. If confirmed, this would open the investigation to a completely unexplored energy window, allowing a deep study of the most extreme physical mechanisms at work, which could be tested on very short timescales, not usually investigated. All this could eventually add a further extreme characteristic to the class of SFXTs, as well as to other subclasses of HMXBs in general.

The *INTEGRAL*mission has provided an important impulse to the study of HMXBs: its large field of view together with its broad spectral range, sensitivity and angular resolution has allowed us to peer through the obscured as well as fast transient X-/gamma-ray sky. Our knowledge has grown broader and deeper in the ever-changing source population that traces the star-forming arms of our Galaxy. *INTEGRAL*plays an important role in connecting the soft X-rays to the very high-energy range of the electromagnetic spectrum (MeV to TeV), enriching our view of the physical processes involved. It serves as an important springboard for the missions and the knowledge to come.

Declaration of Competing Interest

None.

Acknowledgments

Appendix A. HMXBs discovered or identified with *INTEGRAL*

Table A.1
HMXB discovered or identified with *INTEGRAL*. Under System type, sgWF stands for wind-accreting sgHMXB, BeXRB for Be X-ray binary, SFXT for Supergiant Fast X-ray Transient and UXT for Unidentified X-ray Transient. Reference numbers are expanded below the table. Distance values are taken from Bailer-Jones et al. (2018) for many sources. For sources in the SMC we use the "canonical distance modulus" proposed by Graczyk et al. (2014), which is consistent, e.g., with de Grijs and Bono (2015). For sources in the LMC we use the recent value by Pietrzyński et al. (2019).

Source	R.A.	Decl.	P_s	P_b	distance	Companion	System	References
name	deg	deg	s	days	kpc	type	type	
IGR J00515 - 7328	13.003	- 73.490	–	–	60 ± 2	O8 V / B0 III	BeXRB	[5,6]
IGR J00569 - 7226	14.259	- 72.432	5.05	17.13	60 ± 2	B0.2 Ve	BeXRB	[7,8,9,10]
IGR J01054 - 7253	16.173	- 72.901	11.48	36.3	60 ± 2	O9.5-B0 IV-V	BeXRB	[11,12,13,14]
IGR J01217 - 7257	20.419	- 72.959	–	–	60 ± 2	B0-5 (II)e	BeXRB	[15,16]
IGR J01572 - 7259	29.318	- 72.976	11.58	35.6	60 ± 2	Be	BeXRB	[20,21]
IGR J05007 - 7047	75.203	- 70.775	–	30.77	49.6 ± 0.6	–	UXT	[25,26,27,28]
IGR J05305 - 6559	82.462	- 66.041	13.7	–	49.6 ± 0.6	B0.7Ve	BeXRB	[29,30]
IGR J05414 - 6858	85.377	- 69.008	4.42	19.9	49.6 ± 0.6	B0-1 IIIe	BeXRB	[31,32,33,34]
IGR J08262 - 3736	126.557	- 37.620			6.1	OB V	BeXRB	[41,42,43]
IGR J08408 - 4503	130.199	- 45.058	–	9.54	2.7	O8.5 Ib-II(f)p	SFXT	[38,39,40,4]
IGR J10100 - 5655	152.529	- 56.914	–	–	–	B0.5 Ve or B0 Ivpe	BeXRB	[44,45]
IGR J11215 - 5952	170.445	- 59.863	186.8	165	6. $5^{+1.4}_{-1.0}$	B0.5 Ia	SFXT	[46,47,48,4]
IGR J11305 - 6256	172.779	- 62.945	–	–	3	B0 IIIne	BeXRB	[49,50,4]
IGR J11435 - 6109	176.031	- 61.106	161.8	52.46	8 ± 2	B0.5 Ve	BeXRB	[51,45]
1ES 1210-646	183.312	- 64.879	–	6.71	2.8	B5 V	BeXRB	[52,42,53]
IGR J12341 - 6143	188.467	- 61.796	–	–	–	–	UXT	[54,55]
IGR J13020 - 6359	195.495	- 63.969	643	–	7 or 0.8–2.3	B0-6 Ve	BeXRB	[54,50,56,57]
IGR J13186 - 6257	199.652	- 62.946	–	19.99	0.7–5.4	B0-6 Ve	BeXRB	[58,59,57]
IGR J14059 - 6116	211.310	- 61.308	–	13.71	7.7	O6.5 III	BeXRB	[60,61]
IGR J14331 - 6112	218.273	- 61.221	–	–	~ 10	early B III or mid B V	BeXRB	[62,45]
IGR J14488 - 5942	222.180	- 59.705	–	49.63	–	Be	BeXRB	[41,63]
IGR J16195 - 4945	244.884	- 49.742	–	3.95	5	ON9.7 Iab	sgWF	[65,66,45,67]
IGR J16207 - 5129	245.193	- 51.502	–	9.73	1.8–4.1	B0 I / B1 Ia	sgWF	[65,68,69,70]
IGR J16283 - 4838	247.034	- 48.652	–	287.6 ± 1.7	18 ± 4	sgBe	sgWF	[71,72,73]
IGR J16318 - 4848	247.951	- 48.817	–	80	3.6 ± 2.6	B0-5 sgBe	sgWF	[74,75,76]

(continued on next page)

Table A.1 (*continued*)

Source	R.A.	Decl.	P_s	P_b	distance	Companion	System	References
name	deg	deg	s	days	kpc	type	type	
AX J1631.9 - 4752	248.007	- 47.875	1303	8.99	3.5	O8 I	sgWF	[77,78,79,80,81]
IGR J16328 - 4726	248.158	- 47.395	–	10.08	7.2 ± 0.3	O8 Iafpe	SFXT	[82,83,84,85]
IGR J16374 - 5043	249.306	- 50.725	–	–	3.1	–	SFXT	[87,55]
AX J1639.0 - 4642	249.772	- 46.704	912	3.69(4.24)	10.6	B IV-V(OB)†	sgWF	[77,88,89,90,91]
IGR J16418 - 4532	250.462	- 45.540	1246	3.74	13	O8.5 I	SFXT	[92,93,94,95,96]
IGR J16465 - 4507	251.647	- 45.118	228	30.32	9.5 ± 5.7	B0.5I/O9.5Ia	SFXT	[97,98,99,100]
IGR J16479 - 4514	252.027	- 45.202	–	3.32	~ 4.9/ ~ 4.5	O8.5Ib	SFXT	[101,94,102,103]
IGR J16493 - 4348	252.362	- 43.819	1093	6.78	16.0(> 6)	B0.5Ib	sgWF	[104,105,106,107]
AX J1700.2 - 4220	255.100	- 42.337	54.2	44.12	10	B2e	BeXRB	[77,68,108]
IGR J17200 - 3116	260.027	- 31.288	328.2	–	–	–	BeXRB	[65,109]
EXO 1722 - 363	261.297	- 36.283	413.7	9.72	5.3–8.7‡	O8.5I	sgWF	[110,111,65,112,113]
IGR J17354 - 3255	263.839	- 32.937	–	8.45	8.5	O8.5 Iab(f) or O9 Iab	SFXT	[114,115,116,45]
IGR J17375 - 3022	264.391	- 30.388	–	–	26*	–	SFXT	[117,118,55]
XTE J1739 - 302	264.775	- 30.358	–	12.87 or 51.47	2.7	O8Iab(f)	SFXT	119,120,121,122]
AX J1749.1 - 2733	267.287	- 27.554	132	185.5	14.5 ± 1.5	–	BeXRB	[123,124,125,126]
IGR J17503 - 2636	267.575	- 26.605	–	–	–	–	SFXT	[127]
IGR J17544 - 2619	268.560	- 26.317	11.58 or 71.49	4.93	3.6	O9Ib	SFXT	[128,130,131]
IGR J18027 - 2016	270.666	- 20.283	139.6	4.57(4.47)	12.4 ± 0.1	B1 Ib	sgWF	[132,76]
IGR J18179 - 1621	274.466	- 16.359	11.82	–	–	–	BeXRB	[133,134,135,136
SAX J1818.6 - 1703	274.662	- 17.052	–	30	2.1 ± 0.1	B0.5 Iab	SFXT	[137,138,139,140,141]
AX J1820.5 - 1434	275.125	- 14.573	152.3	54 or 111	4.7	O9.5-B0 Ve	UXT	[142,143,144,145]
IGR J18214 - 1318	275.332	- 13.311	–	–	8 ± 2	OB	sgWF	[54,146]
IGR J18219 - 1347	275.478	- 13.791	–	72.44	–	–	BeXRB?	[29,147,148]
IGR J18406 - 0539	280.196	- 5.681	–	–	1.1	B5 V	BeXRB	[149,50]
AX J1841.0 - 0536	280.252	- 5.596	–	6.45*	6.9	B0 I	SFXT	[150,151,152,153]
AX J1845.0 - 0433	281.259	- 4.565	–	5.72	6.4 ± 0.7	O9.5 I	SFXT	[154,155,156,157,45]
IGR J18462 - 0223	281.565	- 2.392	997	~ 2.13?	~ 11?	–	SFXT	[158,160]
IGR J18483 - 0311	282.075	- 3.183	21.05	18.55	2.8	B0.5-1Iab	SFXT	[161,162,156,76]

† In doubt as 91 found a Chandra position inconsistent with the proposed counterpart. ‡ Various existing distance estimates falling withing the quoted range 112.
* Tentative determination

References used in Table A.1

[1] den Hartog et al. (2004); [2] Reig et al. (2005); [3] in't Zand et al. (2007); [4] Hainich et al. (2020); [5] Coe et al. (2010a); [6] Masetti et al. (2013); [7] Coe et al. (2013); [8] Schmidtke and Cowley (2013); [9] Coe et al. (2015); [10] Evans et al. (2006); [11] Kahabka et al. (1999); [12] Bozzo et al. (2009a); [13] Coe et al. (2009); [14] Townsend et al. (2011b); [15] Coe et al. (2014); [16] Evans et al. (2004); [17] Grebenev et al. (2004b); [18] Corbet and Krimm (2010); [19] Tomsick et al. (2011); [20] Coe et al. (2008); [21] Segreto et al. (2013a); [22] Steiner et al. (2005); [23] Halpern and Tyagi (2005); [24] Kaur et al. (2008) [25] Sazonov et al. (2005); [26] Halpern (2005); [27] La Parola et al. (2010b); [28] Coe et al. (2010b); [29] Krivonos et al. (2010); [30] Grebenev et al. (2013); [31] Grebenev and Lutovinov (2010); [32] Lutovinov and Grebenev (2010); [33] Sturm et al. (2011); [34] Sturm et al. (2012); [35] Chenevez et al. (2004); [36] Tomsick et al. (2006b); [37] Reig and Zezas (2018); [38] Gotz et al. (2006); [39] Götz et al. (2007); [40] Ducci et al. (2019b); [41] Bird et al. (2010); [42] Masetti et al. (2010); [43] Bozzo et al. (2012b); [44] Kuiper et al. (2006); [45] Coleiro et al. (2013); [46] Lubiński et al. (2005); [47] Swank et al. (2007); Bosch-Ramon and Paredes, 2005Produit et al. (2004); [50] Masetti et al. (2006a); [51] Grebenev et al. (2004a); [52] Masetti et al. (2009); [53] Corbet and Mukai (2008); [54] Bird et al. (2006); [55] Sguera et al. (2020); [56] Krivonos et al. (2015); [57] Fortin et al. (2018); [58] Bird et al. (2007); [59] D'Aì et al. (2011); [60] Landi et al. (2017); [61] Corbet et al. (2019); [62] Masetti et al. (2008); [63] Corbet et al. (2010b); [64] Keek et al. (2006); [65] Walter et al. (2004); [66] Tomsick et al. (2006a); [67] Cusumano et al. (2016); [68] Masetti et al. (2006c); [69] Masetti et al. (2006b); [70] Nespoli et al. (2008); [71] Soldi et al. (2005); [72] Pellizza et al. (2011); [73] Cusumano et al. (2013); [74] Courvoisier et al. (2003); [75] Walter et al. (2003); [76] Jain et al. (2009b); [77] Sugizaki et al. (2001); [78] Rodriguez et al. (2003); [79] Corbet et al. (2005); [80] Lutovinov et al. (2005b); [81] Rodriguez et al. (2006); [82] Grupe et al. (2009); [83] Fiocchi et al. (2010); [84] Corbet et al. (2010a); [85] Persi et al. (2015); [86] Revnivtsev et al. (2003); [87] Pavan et al. (2010); [88] Bodaghee et al. (2006); [89] Thompson et al. (2006); [90] Corbet et al. (2010d); [91] Bodaghee et al. (2012a); [92] Tomsick et al. (2004); [93] Corbet et al. (2006a);[94] Chaty et al. (2008); [95] Sidoli et al. (2012); [96] Drave et al. (2013b); [97] Lutovinov et al. (2004); [98] Negueruela et al. (2005); [99] Romano et al. (2008); [100] Clark et al. (2010); [101] Molkov et al. (2003); [102] Rahoui et al. (2008); [103] Coley et al. (2015); [104] Grebenev et al. (2005); [105] Hill et al. (2008); [106] Corbet et al. (2010c); [107] Nespoli et al. (2010); [108] Markwardt et al. (2010); [109] Nichelli et al. (2011); [110] Warwick et al. (1988); [111] Tawara et al. (1989); [112] Thompson et al. (2007); [113] Mason et al. (2009); [114] Kuulkers et al. (2006); [115] D'Ai' et al. (2010); [116] Sguera et al. (2011); [117] Ricci et al. (2008); [118] Beckmann et al. (2008); [119] Smith (1997); [120] Sunyaev et al. (2003a); [121] Romano et al. (2009a); [122] Drave et al. (2010); [123] Sakano et al. (2002); [124] Grebenev and Sunyaev (2007); [125] Karasev et al. (2008); [126] Zurita Heras and Chaty (2008); [127] Ferrigno et al. (2019); [128] Sunyaev et al. (2003b); [129] Clark et al. (2009); [130] Drave et al. (2012); [131] Romano et al. (2015); [132] Revnivtsev et al. (2004); [133] Tuerler et al. (2012); [134] Halpern (2012b); [135] Bozzo et al. (2012a); [136] Li et al. (2012b); [137] in 't Zand et al. (1998); [138] Grebenev and Sunyaev (2005); [139] Sguera et al. (2005); [140] Bird et al. (2009); [141] Torrejón et al. (2010); [142] Kinugasa et al. (1998); [143] Kaur et al. (2010); [144] Segreto et al. (2013b); [145] Corbet et al. (2017); [146] Butler et al. (2009); [147] Karasev et al. (2012); [148] La Parola et al. (2013); [149] Molkov et al. (2004); [150] Bamba et al. (2001); [151] Rodriguez et al. (2004); [152] Sguera et al. (2009); [153] González-Galán (2014);

[154] Yamauchi et al. (1995); [155] Coe et al. (1996); [156] Sguera et al. (2007a); [157] Goossens et al. (2013); [158] Grebenev et al. (2007); [159] Grebenev and Sunyaev (2010) [160] Sguera et al. (2013); [161] Chernyakova et al. (2003); [162] Levine and Corbet (2006); [163] Sguera et al. (2007b); [164] Rodes-Roca et al. (2013); [165] Israel et al. (2016); [166] Sidoli et al. (2016a); [167] Sguera et al. (2017); [168] Hare et al. (2019); [169] Bozzo et al. (2011a) ; [170] Rodes-Roca et al. (2018); [171] Malacaria et al. (2020); [172] Morris et al. (2009); [173] Pradhan et al. (2013); [174] Reig and Zezas (2014a); [175] Reig and Zezas (2014b) [176] Krivonos et al. (2012); [177] Halpern (2012a); [178] Masetti et al. (2012); [179] Esposito et al. (2013);

References

Abdo, A.A., (Fermi LAT Collaboration), 2009. Fermi/LAT observations of LS 5039. ApJ 706 (1), L56–L61. https://doi.org/10.1088/0004-637X/706/1/L56.

Abdo, A.A., (Fermi LAT Collaboration), 2011. Discovery of High-energy Gamma-ray Emission from the Binary System PSR B1259-63/LS 2883 around Periastron with Fermi. ApJ 736, L11. https://doi.org/10.1088/2041-8205/736/1/L11.

Ackermann, M., (Fermi LAT Collaboration), 2013. Associating Long-term γ-Ray Variability with the Superorbital Period of LS I 61deg303. ApJ 773 (2), L35. https://doi.org/10.1088/2041-8205/773/2/L35.

Aftab, N., Islam, N., Paul, B., 2016. Variability study of the high-mass X-ray binary IGR J18027-2016 with Swift-XRT. MNRAS 463, 2032–2038. https://doi.org/10.1093/mnras/stw2037.

Ahnen, M.L., (MAGIC Collaboration), 2016. Super-orbital variability of LS I + 61 303 at TeV energies. A&A 591, A76. https://doi.org/10.1051/0004-6361/201527964.

Alfonso-Garzón, J., Domingo, A., Mas-Hesse, J.M., Giménez, A., 2012. The first INTEGRAL-OMC catalogue of optically variable sources. A&A 548, A79. https://doi.org/10.1051/0004-6361/201220095.

Aly, J.J., 1980. Electrodynamics of disk accretion onto magnetic neutron star. A&A 86, 192–197.

Amati, L., (THESEUS Collaboration), 2018. The THESEUS space mission concept: science case, design and expected performances. Advances in Space Research 62, 191–244. https://doi.org/10.1016/j.asr.2018.03.010.

Angel, J.R.P., 1979. Lobster eyes as X-ray telescopes. ApJ 233, 364–373. https://doi.org/10.1086/157397.

Ankay, A., Kaper, L., de Bruijne, J.H.J., Dewi, J., Hoogerwerf, R., Savonije, G.J., 2001. The origin of the runaway high-mass X-ray binary HD 153919/4U1700-37. A&A 370, 170–175. https://doi.org/10.1051/0004-6361:20010192.

Antoniou, V., Hatzidimitriou, D, Zezas, A., Reig, P., 2009. Optical Spectroscopy of 20 Be/X-ray Binaries in the Small Magellanic Cloud. ApJ 707, 1080–1097. https://doi.org/10.1088/0004-637X/707/2/1080.

Antoniou, V., Zezas, A., Hatzidimitriou, D., Kalogera, V., 2010. Star Formation History and X-ray Binary Populations: The Case of the Small Magellanic Cloud. ApJ 716 (2), L140–L145. https://doi.org/10.1088/2041-8205/716/2/L140.

Araya, R.A., Harding, A.K., 1999. Cyclotron Line Features from Near-critical Magnetic Fields: The Effect of Optical Depth and Plasma Geometry. ApJ 517 (1), 334–354. https://doi.org/10.1086/307157.

Arons, J., Lea, S.M., 1976. Accretion onto magnetized neutron stars - Structure and interchange instability of a model magnetosphere. ApJ 207, 914–936. https://doi.org/10.1086/154562.

Bachetti, M., Harrison, F.A., Walton, D.J., Grefenstette, B.W., Chakrabarty, D., Fürst, F., Barret, D., Beloborodov, A., Boggs, S.E., Christensen, F.E., Craig, W.W., Fabian, A.C., Hailey, C.J., Hornschemeier, A., Kaspi, V., Kulkarni, S.R., Maccarone, T., Miller, J.M., Rana, V., Stern, D., Tendulkar, S.P., Tomsick, J., Webb, N.A., Zhang, W.W., 2014. An ultraluminous X-ray source powered by an accreting neutron star. Nature 514 (7521), 202–204. https://doi.org/10.1038/nature13791.

Bailer-Jones, C.A.L., Rybizki, J., Fouesneau, M., Mantelet, G., Andrae, R., 2018. Estimating Distance from Parallaxes. IV. Distances to 1.33 Billion Stars in Gaia Data Release 2. AJ 156 (2), 58. https://doi.org/10.3847/1538-3881/aacb21.

Ballhausen, R., Lorenz, M., Fürst, F., Pottschmidt, K., et al., 2020. Dust and gas absorption in the high mass x-ray binary igr j16318 4848. A&A *accepted for publication*.

Balona, L.A., Ozuyar, D., 2020. TESS observations of Be stars: a new interpretation. MNRAS 493 (2), 2528–2544. https://doi.org/10.1093/mnras/staa389.

Bamba, A., Yokogawa, J., Ueno, M., Koyama, K., Yamauchi, S., 2001. Discovery of a Transient X-Ray Pulsar, AX J1841.0-0536, in the Scutum Arm Region with ASCA. PASJ 53 (6), 1179–1183. https://doi.org/10.1093/pasj/53.6.1179.

Barragan, L., Wilms, J., Kreykenbohm, I., Hanke, M., Fuerst, F., Pottschmidt, K., Rothschild, R.E., 2010. IGR J16318-4848: 7 years of INTEGRAL observations. Eighth Integral Workshop. The Restless Gamma-ray Universe (INTEGRAL 2010). pp. 135.

Barret, D., (Athena X-IFU Collaboration), 2018. The ATHENA X-ray Integral Field Unit (X-IFU). Proc. SPIE. Society of Photo-Optical Instrumentation Engineers (SPIE) Conference Series 10699. pp. 106991G. https://doi.org/10.1117/12.2312409. 1807.06092.

Barthelmy, S.D., Baumgartner, W., Cummings, J., Gehrels, N., Markwardt, C., Sakamoto, T., Godet, O., Evans, P., Osborne, J., Beardmore, A.P., Kennea, J., Falcone, A., Burrows, D., Campana, S., de Pasquale, M., 2008. Swift-BAT/-XRT refined analysis on trigger 324362 (LS I + 61 303). GRB Coordinates Network 8215.

Barthelmy, S.D., Gropp, J.D., Lien, A.Y., Palmer, D.M., Sbarufatti, B., 2019. Swift detection of LS I + 61 303. GRB Coordinates Network 23989, 1.

Basko, M.M., Sunyaev, R.A., 1976. The limiting luminosity of accreting neutron stars with magnetic fields. MNRAS 175, 395–417. https://doi.org/10.1093/mnras/175.2.395.

Becker, P.A., Klochkov, D., Schönherr, G., Nishimura, O., Ferrigno, C., Caballero, I., Kretschmar, P., Wolff, M.T., Wilms, J., Staubert, R., 2012. Spectral formation in accreting X-ray pulsars: bimodal variation of the cyclotron energy with luminosity. A&A 544, A123. https://doi.org/10.1051/0004-6361/201219065.

Becker, P.A., Wolff, M.T., 2007. Thermal and Bulk Comptonization in Accretion-powered X-Ray Pulsars. ApJ 654 (1), 435–457. https://doi.org/10.1086/509108.

Becker, P.A., Wolff, M.T., Wolfram, K.D., 2005. Bulk and Thermal Comptonization in Accretion Powered X-Ray Pulsars. American Astronomical Society Meeting Abstracts. 207. pp. 198.01.

Beckmann, V., Soldi, S., Bélanger, G., Brandt, S., Caballero-García, M.D., De Cesare, G., Gehrels, N., Grebenev, S., Vilhu, O., von Kienlin, A., Courvoisier, T.J.L., 2007. Cygnus X-3 transition from the ultrasoft to the hard state. A&A 473 (3), 903–905. https://doi.org/10.1051/0004-6361:20078160.

Beckmann, V., Soldi, S., Kennea, J.A., Rodriguez, J., 2008. IGR J17375-3022 detected and localised by Swift/XRT. The Astronomer's Telegram 1783, 1.

Belloni, T.M., 2010. States and Transitions in Black Hole Binaries. In: T. Belloni (Ed.), The Jet Paradigm: From Microquasars to Quasars, Lecture Notes in Physics, Berlin Springer Verlag. 794. pp. 53.

Bhalerao, V., Romano, P., Tomsick, J., Natalucci, L., Smith, D.M., Bellm, E., Boggs, S.E., Chakrabarty, D., Christensen, F.E., Craig, W.W., Fuerst, F., Hailey, C.J., Harrison, F.A., Krivonos, R.A., Lu, T.-N., Madsen, K., Stern, D., Younes, G., Zhang, W., 2015. NuSTAR detection of a cyclotron line in the supergiant fast X-ray transient IGR J17544-2619. MNRAS 447, 2274–2281. https://doi.org/10.1093/mnras/stu2495.

Bhattacharya, D., Wijers, R.A.M.J., Hartman, J.W., Verbunt, F., 1992. On the decay of the magnetic fields of single radio pulsars. A&A 254, 198–212.

Bird, A.J., Barlow, E.J., Bassani, L., Bazzano, A., Bélanger, G., Bodaghee, A., Capitanio, F., Dean, A.J., Fiocchi, M., Hill, A.B., Lebrun, F., Malizia, A., Mas-Hesse, J.M., Molina, M., Moran, L., Renaud, M., Sguera, V., Shaw, S.E., Stephen, J.B., Terrier, R., Ubertini, P., Walter, R., Willis, D.R., Winkler, C., 2006. The Second IBIS/ISGRI Soft Gamma-Ray Survey Catalog. ApJ 636 (2), 765–776. https://doi.org/10.1086/498090.

Bird, A.J., Bazzano, A., Bassani, L., Capitanio, F., Fiocchi, M., Hill, A.B., Malizia, A., McBride, V.A., Scaringi, S., Sguera, V., Stephen, J.B., Ubertini, P., Dean, A.J., Lebrun, F., Terrier, R., Renaud, M., Mattana, F., Götz, D., Rodriguez, J., Belanger, G., Walter, R., Winkler, C., 2010. The Fourth IBIS/ISGRI Soft Gamma-ray Survey Catalog. ApJS 186 (1), 1–9. https://doi.org/10.1088/0067-0049/186/1/1.

Bird, A.J., Bazzano, A., Hill, A.B., McBride, V.A., Sguera, V., Shaw, S.E., Watkins, H.J., 2009. Discovery of a 30-d period in the supergiant fast X-ray transient SAX J1818.6-1703. MNRAS 393, L11–L15. https://doi.org/10.1111/j.1745-3933.2008.00583.x.

Bird, A.J., Bazzano, A., Malizia, A., Fiocchi, M., Sguera, V., Bassani, L., Hill, A.B., Ubertini, P., Winkler, C., 2016. The IBIS Soft Gamma-Ray Sky after 1000 Integral Orbits. ApJS 223, 15. https://doi.org/10.3847/0067-0049/223/1/15.

Bird, A.J., Malizia, A., Bazzano, A., Barlow, E.J., Bassani, L., Hill, A.B., Bélanger, G., Capitanio, F., Clark, D.J., Dean, A.J., Fiocchi, M., Götz, D., Lebrun, F., Molina, M., Produit, N., Renaud, M., Sguera, V., Stephen, J.B., Terrier, R., Ubertini, P., Walter, R., Winkler, C., Zurita, J., 2007. The Third IBIS/ISGRI Soft Gamma-Ray Survey Catalog. ApJS 170 (1), 175–186. https://doi.org/10.1086/513148.

Blaauw, A., 1961. On the origin of the O- and B-type stars with high velocities (the "runaway" stars), and some related problems. Bull. Astron. Inst. Netherlands 15, 265.

Blondin, J., Kallman, T.R., Fryxell, B.A., Taam, R.E., 1990. Hydrodynamic Simulations of Stellar Wind Disruption by a Compact X-Ray Source. ApJ 356, 591. https://doi.org/10.1086/168865.

Bodaghee, A., Courvoisier, T.J.-L., Rodriguez, J., Beckmann, V., Produit, N., Hannikainen, D., Kuulkers, E., Willis, D.R., Wendt, G., 2007. A description of sources detected by INTEGRAL during the first 4 years of observations. A&A 467, 585–596. https://doi.org/10.1051/0004-6361:20077091.

Bodaghee, A., Rahoui, F., Tomsick, J.A., Rodriguez, J., 2012. Chandra Observations of Five INTEGRAL Sources: New X-Ray Positions for IGR J16393-4643 and IGR J17091-3624. ApJ 751 (2), 113. https://doi.org/10.1088/0004-637X/751/2/113.

Bodaghee, A., Tomsick, J.A., Rodriguez, J., Chaty, S., Pottschmidt, K., Walter, R., 2010. Broadband Suzaku Observations of IGR J16207-5129. ApJ 719, 451–458. https://doi.org/10.1088/0004-637X/719/1/451.

Bodaghee, A., Tomsick, J.A., Rodriguez, J., James, J.B., 2012. Clustering between High-mass X-Ray Binaries and OB Associations in the Milky Way. ApJ 744, 108. https://doi.org/10.1088/0004-637X/744/2/108.

Bodaghee, A., Walter, R., Zurita Heras, J.A., Bird, A.J., Courvoisier, T.J.-L., Malizia, A., Terrier, R., Ubertini, P., 2006. IGR J16393-4643: a new heavily-obscured X-ray pulsar. A&A 447, 1027–1034. https://doi.org/10.1051/0004-6361:20053809.

Boggess, A., Carr, F.A., Evans, D.C., Fischel, D., Freeman, H.R., Fuechsel, C.F., Klinglesmith, D.A., Krueger, V.L., Longanecker, G.W., Moore, J.V., 1978. The IUE spacecraft and instrumentation. Nature 275 (5679), 372–377. https://doi.org/10.1038/275372a0.

Boldin, P.A., Tsygankov, S.S., Lutovinov, A.A., 2013. On timing and spectral characteristics of the X-ray pulsar 4U 0115+63: Evolution of the pulsation period and the cyclotron line energy. Astronomy Letters 39 (6), 375–388. https://doi.org/10.1134/S1063773713060029.

Bonning, E.W., Falanga, M., 2005. INTEGRAL high energy observations of 2S 0114+65. A&A 436 (2), L31–L34. https://doi.org/10.1051/0004-6361:200500117.

Boon, C.M., Bird, A.J., Hill, A.B., Sidoli, L., Sguera, V., Goossens, M.E., Fiocchi, M.,

McBride, V.A., Drave, S.P., 2016. Spectral variation in the supergiant fast X-ray transient SAX J1818.6-1703 observed by XMM-Newton and INTEGRAL. MNRAS 456, 4111–4120. https://doi.org/10.1093/mnras/stv2975.

Bosch-Ramon, V., Paredes, J.M., 2005. High-energy γ-ray Emission from Microquasars: LS 5039 and LS I +61 303. Chinese Journal of Astronomy and Astrophysics Supplement 5, 133–138.

Bozzo, E., Ascenzi, S., Ducci, L., Papitto, A., Burderi, L., Stella, L., 2018. Magnetospheric radius of an inclined rotator in the magnetically threaded disk model. A&A 617, A126. https://doi.org/10.1051/0004-6361/201732004.

Bozzo, E., Athena SWG3. 3, 2015. End Points of Stellar Evolution. In: Ehle, M. (Ed.), Exploring the Hot and Energetic Universe: The first scientific conference dedicated to the Athena X-ray observatory, pp. 39.

Bozzo, E., Bernardini, F., Ferrigno, C., Falanga, M., Romano, P., Oskinova, L., 2017. The accretion environment of supergiant fast X-ray transients probed with XMM-Newton. A&A 608, A128. https://doi.org/10.1051/0004-6361/201730398.

Bozzo, E., Bernardini, F., Ferrigno, C., Falanga, M., Romano, P., Oskinova, L., 2017. The accretion environment of supergiant fast X-ray transients probed with XMM-Newton. A&A 608, A128. https://doi.org/10.1051/0004-6361/201730398.

Bozzo, E., Bhalerao, V., Pradhan, P., Tomsick, J., Romano, P., Ferrigno, C., Chaty, S., Oskinova, L., Manousakis, A., Walter, R., Falanga, M., Campana, S., Stella, L., Ramolla, M., Chini, R., 2016. Multi-wavelength observations of IGR J17544-2619 from quiescence to outburst. A&A 596, A16. https://doi.org/10.1051/0004-6361/201629311.

Bozzo, E., Coe, M.J., den Hartog, P., Birdd, A.J., Lubiński, P., Maccarone, T., Beckmann, V., Ubertini, P., Watanabe, K., 2009. IGR J01054-7253: a new INTEGRAL source discovered in the SMC. The Astronomer's Telegram 2079, 1.

Bozzo, E., Falanga, M., Stella, L., 2008. Are There Magnetars in High-Mass X-Ray Binaries? The Case of Supergiant Fast X-Ray Transients. ApJ 683, 1031–1044. https://doi.org/10.1086/589990.

Bozzo, E., Falanga, M., Stella, L., 2008. Hunting for Magnetars in High Mass X-Ray Binaries. The Case of SuperGiant Fast X-Ray Transients. arXiv e-prints.

Bozzo, E., Ferrigno, C., Falanga, M., Walter, R., 2011. INTEGRAL and Swift observations of IGR J19294+1816 in outburst. A&A 531, A65. https://doi.org/10.1051/0004-6361/201116729.

Bozzo, E., Ferrigno, C., Türler, M., Manousakis, A., Falanga, M., 2012. IGR J18179-1621: an obscured X-ray pulsar discovered by INTEGRAL. A&A 545, A83. https://doi.org/10.1051/0004-6361/201219344.

Bozzo, E., Giunta, A., Cusumano, G., Ferrigno, C., Walter, R., Campana, S., Falanga, M., Israel, G., Stella, L., 2011. XMM-Newton observations of IGR J18410-0535: the ingestion of a clump by a supergiant fast X-ray transient. A&A 531, A130. https://doi.org/10.1051/0004-6361/201116726.

Bozzo, E., Oskinova, L., Feldmeier, A., Falanga, M., 2016. Clumpy wind accretion in supergiant neutron star high mass X-ray binaries. A&A 589, A102. https://doi.org/10.1051/0004-6361/201628341.

Bozzo, E., Pavan, L., Ferrigno, C., Falanga, M., Campana, S., Paltani, S., Stella, L., Walter, R., 2012. XMM-Newton observations of four high mass X-ray binaries and IGR J17348-2045. A&A 544, A118. https://doi.org/10.1051/0004-6361/201218900.

Bozzo, E., Romano, P., Ducci, L., Bernardini, F., Falanga, M., 2015. Supergiant fast X-ray transients as an under-luminous class of supergiant X-ray binaries. Advances in Space Research 55, 1255–1263. https://doi.org/10.1016/j.asr.2014.11.012.

Bozzo, E., Romano, P., Ferrigno, C., Esposito, P., Mangano, V., 2013. Observations of supergiant fast X-ray transients with LOFT. Advances in Space Research 51, 1593–1599. https://doi.org/10.1016/j.asr.2012.12.001.

Bozzo, E., Stella, L., Ferrigno, C., Giunta, A., Falanga, M., Campana, S., Israel, G., Leyder, J.C., 2010. The supergiant fast X-ray transients XTE J1739-302 and IGR J08408-4503 in quiescence with XMM-Newton. A&A 519, A6. https://doi.org/10.1051/0004-6361/201014095.

Bozzo, E., Stella, L., Vietri, M., Ghosh, P., 2009. Can disk-magnetosphere interaction models and beat frequency models for quasi-periodic oscillation in accreting X-ray pulsars be reconciled? A&A 493, 809–818. https://doi.org/10.1051/0004-6361/200810658.

Burnard, D.J., Arons, J., Lea, S.M., 1983. Accretion onto magnetized neutron stars - X-ray pulsars with intermediate rotation rates. ApJ 266, 175–187. https://doi.org/10.1086/160768.

Burrows, D.N., Chester, M.M., D'Elia, V., Palmer, D.M., Romano, P., Saxton, C.J., Sonbas, E., Stamatikos, M., Stratta, G., 2012. Swift detection of a burst from LS I +61 303. GRB Coordinates Network 12914, 1.

Butler, S.C., Tomsick, J.A., Chaty, S., Heras, J.A.Z., Rodriguez, J., Walter, R., Kaaret, P., Kalemci, E., Özbey, M., 2009. Identifications of Five INTEGRAL Sources via Optical Spectroscopy. ApJ 698 (1), 502–508. https://doi.org/10.1088/0004-637X/698/1/502.

Şahiner, Ş., Inam, S.Ç., Baykal, A., 2012. A comprehensive study of RXTE and INTEGRAL observations of the X-ray pulsar 4U 1907+09. MNRAS 421, 2079–2087. https://doi.org/10.1111/j.1365-2966.2012.20455.x.

Caballero, I., Kretschmar, P., Santangelo, A., Staubert, R., Klochkov, D., Camero, A., Ferrigno, C., Finger, M.H., Kreykenbohm, I., McBride, V.A., Pottschmidt, K., Rothschild, R.E., Schönherr, G., Segreto, A., Suchy, S., Wilms, J., Wilson, C.A., 2007. A 0535+26 in the August/September 2005 outburst observed by RXTE and INTEGRAL. A&A 465, L21–L24. https://doi.org/10.1051/0004-6361/20067032.

Cabanac, C., Roques, J.-P., Jourdain, E., 2011. Fast Timing Analysis of Cygnus X-1 Using the SPectrometer on the International Gamma-Ray Astrophysics Laboratory. ApJ 739, 58. https://doi.org/10.1088/0004-637X/739/2/58.

Caliandro, G.A., Cheung, C.C., Li, J., Scargle, J.D., Torres, D.F., Wood, K.S., Chernyakova, M., 2015. Gamma-Ray Flare Activity from PSR B1259-63 during 2014 Periastron Passage and Comparison to Its 2010 Passage. ApJ 811 (1), 68. https://doi.org/10.1088/0004-637X/811/1/68.

Camero-Arranz, A., Wilson, C.A., Connell, P., Martínez Núñez, S., Blay, P., Beckmann, V., Reglero, V., 2005. INTEGRAL observations of the Be/X-ray binary EXO 2030+375 during outburst. A&A 441, 261–269. https://doi.org/10.1051/0004-6361/20053335.

Cangemi, F., Beuchert, T., Siegert, T., Grinberg, V., Wilms, J., Rodriguez, J., Kreykenbohm, I., Laurent, P., Pottschmidt, K., 2019. Long-term spectral study of the black hole Cygnus X-1 using INTEGRAL. arXiv e-prints. arXiv:1904.09112

Canuto, V., Lodenquai, J., Ruderman, M., 1971. Thomson Scattering in a Strong Magnetic Field. Phys. Rev. D 3 (10), 2303–2308. https://doi.org/10.1103/PhysRevD.3.2303.

Castor, J.I., Abbott, D.C., Klein, R.I., 1975. Radiation-driven winds in of stars. ApJ 195, 157–174.

Chang, Z., Zhang, S., Ji, L., Chen, Y.P., Kretschmar, P., Kuulkers, E., Collmar, W., Liu, C.Z., 2016. Investigation of the energy dependence of the orbital light curve in LS 5039. MNRAS 463, 495–501. https://doi.org/10.1093/mnras/stw2009.

Chaty, S., LeReun, A., Negueruela, I., Coleiro, A., Castro, N., Simón-Díaz, S., Zurita Heras, J.A., Goldoni, P., Goldwurm, A., 2016. Multiwavelength study of the fast rotating supergiant high-mass X-ray binary IGR J16465-4507. A&A 591, A87. https://doi.org/10.1051/0004-6361/201628110.

Chaty, S., Rahoui, F., 2012. Broadband ESO/VISIR-Spitzer Infrared Spectroscopy of the Obscured Supergiant X-Ray Binary IGR J16318-4848. ApJ 751, 150. https://doi.org/10.1088/0004-637X/751/2/150.

Chaty, S., Rahoui, F., Foellmi, C., Tomsick, J.A., Rodriguez, J., Walter, R., 2008. Multi-wavelength observations of Galactic hard X-ray sources discovered by INTEGRAL. I. The nature of the companion star. A&A 484, 783–800. https://doi.org/10.1051/0004-6361/20078768.

Chenevez, J., Budtz-Jorgensen, C., Lund, N., Westergaard, N.J., Kretschmar, P., Rodriguez, J., Orr, A., Hermsen, W., 2004. IGR J06074+2205 a new X-ray source discovered by INTEGRAL. The Astronomer's Telegram 223, 1.

Cherenkov Telescope Array Collaboration, 2019. Science with the Cherenkov Telescope Array. World Scientific Publishinghttps://doi.org/10.1142/10986.

Cherepashchuk, A., Postnov, K., Molkov, S., Antokhina, E., Belinski, A., 2019. SS433: a massive X-ray binary at advanced evolutionary stage. arXiv e-prints. arXiv:1905.02938

Chernyakova, M., Lutovinov, A., Capitanio, F., Lund, N., Gehrels, N., 2003. IGR J18483-0311. The Astronomer's Telegram 157, 1.

Chernyakova, M., Lutovinov, A., Rodríguez, J., Revnivtsev, M., 2005. Discovery and study of the accreting pulsar 2RXP J130159.6-635806. MNRAS 364, 455–461. https://doi.org/10.1111/j.1365-2966.2005.09548.x.

Chernyakova, M., Malyshev, D., Paizis, A., La Palombara, N., Balbo, M., Walter, R., Hnatyk, B., van Soelen, B., Romano, P., Munar-Adrover, P., Vovk, I., Piano, G., Capitanio, F., Falceta-Gonçalves, D., Landoni, M., Luque-Escamilla, P.L., Martí, J., Paredes, J.M., Ribó, M., Safi-Harb, S., Saha, L., Sidoli, L., Vercellone, S., 2019. Overview of non-transient γ-ray binaries and prospects for the Cherenkov Telescope Array. A&A 631, A177. https://doi.org/10.1051/0004-6361/201936501.

Chernyakova, M., Neronov, A., Molkov, S., Malyshev, D., Lutovinov, A., Pooley, G., 2012. Superorbital Modulation of X-Ray Emission from Gamma-Ray Binary LSI +61° 303. ApJ 747, L29. https://doi.org/10.1088/2041-8205/747/2/L29.

Chernyakova, M., Neronov, A., van Soelen, B., Callanan, P., O'Shaughnessy, L., Babyk, I., Tsygankov, S., Vovk, I., Krivonos, R., Tomsick, J.A., Malyshev, D., Li, J., Wood, K., Torres, D., Zhang, S., Kretschmar, P., McSwain, M.V., Buckley, D.A.H., Koen, C., 2015. Multi-wavelength observations of the binary system PSR B1259-63/LS 2883 around the 2014 periastron passage. MNRAS 454, 1358–1370. https://doi.org/10.1093/mnras/stv1988.

Chernyakova, M., Neronov, A., Walter, R., 2006. INTEGRAL and XMM-Newton observations of LSI +61° 303. MNRAS 372, 1585–1592. https://doi.org/10.1111/j.1365-2966.2006.10946.x.

Chodil, G., Mark, H., Rodrigues, R., Seward, F.D., Swift, C.D., 1967. X-ray intensities and spectra from several cosmic sources. ApJ 150, 57–65.

Chou, Y., Grindlay, J.E., 2001. Binary and Long-Term (Triple?) Modulations of 4U 1820-30 in NGC 6624. ApJ 563 (2), 934–940. https://doi.org/10.1086/324038.

Clark, D.J., Hill, A.B., Bird, A.J., McBride, V.A., Scaringi, S., Dean, A.J., 2009. Discovery of the orbital period in the supergiant fast X-ray transient IGR J17544-2619. MNRAS 399, L113–L117. https://doi.org/10.1111/j.1745-3933.2009.00737.x.

Clark, D.J., Sguera, V., Bird, A.J., McBride, V.A., Hill, A.B., Scaringi, S., Drave, S., Bazzano, A., Dean, A.J., 2010. The orbital period in the supergiant fast X-ray transient IGR J16465-4507. MNRAS 406, L75–L79. https://doi.org/10.1111/j.1745-3933.2010.00885.x.

Coburn, W., Heindl, W.A., Gruber, D.E., Rothschild, R.E., Staubert, R., Wilms, J., Kreykenbohm, I., 2001. Discovery of a Cyclotron Resonant Scattering Feature in the Rossi X-Ray Timing Explorer Spectrum of 4U 0352+309 (X Persei). ApJ 552 (2), 738–747. https://doi.org/10.1086/320565.

Coburn, W., Heindl, W.A., Rothschild, R.E., Gruber, D.E., Kreykenbohm, I., Wilms, J., Kretschmar, P., Staubert, R., 2002. Magnetic Fields of Accreting X-Ray Pulsars with the Rossi X-Ray Timing Explorer. ApJ 580, 394–412. https://doi.org/10.1086/343033.

Coe, M., Bird, A.J., McBride, V.A., Townsend, L.J., Corbet, R.H.D., Udalski, A., 2009. Optical counterpart and a probable pulse period in IGR J01054-7253. The Astronomer's Telegram 2088, 1.

Coe, M.J., Bartlett, E.S., Bird, A.J., Haberl, F., Kennea, J.A., McBride, V.A., Townsend, L.J., Udalski, A., 2015. SXP 5.05 = IGR J00569-7226: using X-rays to explore the structure of a Be star's circumstellar disc. MNRAS 447 (3), 2387–2403. https://doi.org/10.1093/mnras/stu2568.

Coe, M.J., Bird, A.J., Buckley, D.A.H., Corbet, R.H.D., Dean, A.J., Finger, M., Galache, J.L., Haberl, F., McBride, V.A., Negueruela, I., Schurch, M., Townsend, L.J., Udalski, A., Wilms, J., Zezas, A., 2010. INTEGRAL deep observations of the Small Magellanic Cloud. MNRAS 406 (4), 2533–2539. https://doi.org/10.1111/j.1365-2966.2010.16844.x.

Coe, M.J., Bird, A.J., McBride, V., Bartlett, E.S., Haberl, F., 2013. Detection of a new, bright X-ray source in the Small Magellanic Cloud. The Astronomer's Telegram 5547, 1.

Coe, M.J., Bird, A.J., McBride, V.A., Bartlett, E.S., Townsend, L.J., Haberl, F., Kennea, J., Udalski, A., 2014. Detection of an X-ray outburst by INTEGRAL from a previously unknown SMC source IGR J01217-7257. The Astronomer's Telegram 5806, 1.

Coe, M.J., Edge, W.R.T., Galache, J.L., McBride, V.A., 2005. Optical properties of Small Magellanic Cloud X-ray binaries. MNRAS 356 (2), 502–514. https://doi.org/10.1111/j.1365-2966.2004.08467.x.

Coe, M.J., Fabregat, J., Negueruela, I., Roche, P., Steele, I.A., 1996. Discovery of the optical counterpart to the ASCA transient AX 1845.0-0433. MNRAS 281 (1), 333–338. https://doi.org/10.1093/mnras/281.1.333.

Coe, M.J., Kirk, J., 2015. Catalogue of Be/X-ray binary systems in the Small Magellanic Cloud: X-ray, optical and IR properties. MNRAS 452, 969–977. https://doi.org/10.1093/mnras/stv1283.

Coe, M.J., McBride, V.A., Bird, A.J., Corbet, R.H.D., 2008. Discovery of a new HMXB in the Magellanic Bridge. The Astronomer's Telegram 1882, 1.

Coe, M.J., Townsend, L.J., Udalski, A., 2010. Confirmation of the optical identification and binary period in IGR J05007-7047. The Astronomer's Telegram 2597, 1.

Coleiro, A., Chaty, S., 2013. Distribution of High-mass X-Ray Binaries in the Milky Way. ApJ 764, 185. https://doi.org/10.1088/0004-637X/764/2/185.

Coleiro, A., Chaty, S., Zurita Heras, J.A., Rahoui, F., Tomsick, J.A., 2013. Infrared identification of high-mass X-ray binaries discovered by INTEGRAL. A&A 560, A108. https://doi.org/10.1051/0004-6361/201322382.

Coley, J.B., Corbet, R.H.D., Fürst, F., Huxtable, G., Krimm, H.A., Pearlman, A.B., Pottschmidt, K., 2019. A Study of the 20 day Superorbital Modulation in the High-mass X-Ray Binary IGR J16493-4348. ApJ 879 (1), 34. https://doi.org/10.3847/1538-4357/ab223c.

Coley, J.B., Corbet, R.H.D., Krimm, H.A., 2015. Probing the Masses and Radii of Donor Stars in Eclipsing X-Ray Binaries with the Swift Burst Alert Telescope. ApJ 808 (2), 140. https://doi.org/10.1088/0004-637X/808/2/140.

Corbet, R., Barbier, L., Barthelmy, S., Cummings, J., Fenimore, E., Gehrels, N., Hullinger, D., Krimm, H., Markwardt, C., Palmer, D., Parsons, A., Sakamoto, T., Sato, G., Tueller, J., Remillard, R., 2006. Swift/BAT and RXTE/ASM Discovery of the Orbital Period of IGR J16418-4532. The Astronomer's Telegram 779, 1.

Corbet, R., Barbier, L., Barthelmy, S., Cummings, J., Fenimore, E., Gehrels, N., Hullinger, D., Krimm, H., Markwardt, C., Palmer, D., Parsons, A., Sakamoto, T., Sato, G., Tueller, J., Swift-Survey Team, 2005. Swift/BAT Discovery of the Orbital Period of IGR J16320-4751. The Astronomer's Telegram 649, 1.

Corbet, R.H.D., 1986. The three types of high-mass x-ray pulsator. MNRAS 220, 1047–1056.

Corbet, R.H.D., Barthelmy, S.D., Baumgartner, W.H., Krimm, H.A., Markwardt, C.B., Skinner, G.K., Tueller, J., 2010. A 10 Day Period in IGR J16328-4726 from Swift/BAT Observations. The Astronomer's Telegram 2588, 1.

Corbet, R.H.D., Barthelmy, S.D., Baumgartner, W.H., Krimm, H.A., Markwardt, C.B., Skinner, G.K., Tueller, J., 2010. A 49 Day Period in IGR J14488-5942/Swift J1448.4-5945 from Swift/BAT Observations. The Astronomer's Telegram 2598, 1.

Corbet, R.H.D., Barthelmy, S.D., Baumgartner, W.H., Krimm, H.A., Markwardt, C.B., Skinner, G.K., Tueller, J., 2010. A 6.8 Day Period in IGR J16493-4348 from Swift/BAT and RXTE/PCA Observations. The Astronomer's Telegram 2599, 1.

Corbet, R.H.D., Chomiuk, L., Coe, M.J., Coley, J.B., Dubus, G., Edwards, P.G., Martin, P., McBride, V.A., Stevens, J., Strader, J., Townsend, L.J., 2019. Discovery of the Galactic High-mass Gamma-Ray Binary 4FGL J1405.1-6119. ApJ 884 (1), 93. https://doi.org/10.3847/1538-4357/ab3e32.

Corbet, R.H.D., Chomiuk, L., Coe, M.J., Coley, J.B., Dubus, G., Edwards, P.G., Martin, P., McBride, V.A., Stevens, J., Strader, J., Townsend, L.J., Udalski, A., 2016. A Luminous Gamma-ray Binary in the Large Magellanic Cloud. ApJ 829, 105. https://doi.org/10.3847/0004-637X/829/2/105.

Corbet, R.H.D., Coley, J.B., Krimm, H.A., 2017. Diverse Long-term Variability of Five Candidate High-mass X-Ray Binaries from Swift Burst Alert Telescope Observations. ApJ 846 (2), 161. https://doi.org/10.3847/1538-4357/aa8638.

Corbet, R.H.D., Coley, J.B., Krimm, H.A., Pottschmidt, K., 2018. Apparent Superorbital Modulation in 4U 1538-52 at Four Times the Orbital Period. The Astronomer's Telegram 11918, 1.

Corbet, R.H.D., Krimm, H.A., 2010. A 160 day Period in the Be star X-ray Binary IGR J01363+6610 from Swift BAT Observations. The Astronomer's Telegram 3079, 1.

Corbet, R.H.D., Krimm, H.A., 2013. Superorbital Periodic Modulation in Wind-accretion High-mass X-Ray Binaries from Swift Burst Alert Telescope Observations. ApJ 778, 45. https://doi.org/10.1088/0004-637X/778/1/45.

Corbet, R.H.D., Krimm, H.A., Barthelmy, S.D., Baumgartner, W.H., Markwardt, C.B., Skinner, G.K., Tueller, J., 2010. A 4.2 Day Period in the X-ray Pulsar IGR J16393-4643 from Swift/BAT and RXTE/PCA Observations. The Astronomer's Telegram 2570.

Corbet, R.H.D., Markwardt, C., Barbier, L., Barthelmy, S., Cummings, J., Gehrels, N., Krimm, H., Palmer, D., Sakamoto, T., Sato, G., Tueller, J., on behalf of the Swift/BAT Survey team, 2006. Periodicities In X-ray Binaries From Swift/BAT Observations. Bulletin of the American Astronomical Society. Bulletin of the American Astronomical Society 38. pp. 335.

Corbet, R.H.D., Mukai, K., 2008. The Orbital Period of 4U 1210-64. The Astronomer's Telegram 1861, 1.

Courvoisier, T.J.L., Walter, R., Rodriguez, J., Bouchet, L., Lutovinov, A.A., 2003. IGR J16318-4848. IAU Circ. 8063, 3.

Cranmer, S.R., Owocki, S.P., 1996. Hydrodynamical Simulations of Corotating Interaction Regions and Discrete Absorption Components in Rotating O-Star Winds. ApJ 462, 469.

Cusumano, G., La Parola, V., Segreto, A., D'Aì, A., 2016. Swift reveals the eclipsing nature of the high-mass X-ray binary IGR J16195-4945. MNRAS 456 (3), 2717–2721. https://doi.org/10.1093/mnras/stv2851.

Cusumano, G., Segreto, A., La Parola, V., D'Aì, A., Masetti, N., Tagliaferri, G., 2013. Swift Observations of the High-mass X-Ray Binary IGR J16283-4838 Unveil a 288 Day Orbital Period. ApJ 775 (1), L25. https://doi.org/10.1088/2041-8205/775/1/L25.

Dage, K.C., Clarkson, W.I., Charles, P.A., Laycock, S.G.T., Shih, I.C., 2019. Long-term properties of accretion discs in X-ray binaries - III. A search for spin-superorbital correlation in SMC X-1. MNRAS 482 (1), 337–350. https://doi.org/10.1093/mnras/sty2572.

D'Aì, A., Cusumano, G., La Parola, V., Segreto, A., 2010. Discovery of the orbital period in the Swift/Bat data of the highly absorbed HMXB IGR J17354-3255. The Astronomer's Telegram 2596, 1.

D'Aì, A., La Parola, V., Cusumano, G., Segreto, A., Romano, P., Vercellone, S., Robba, N.R., 2011. The Swift-BAT survey reveals the orbital period of three high-mass X-ray binaries. A&A 529, A30. https://doi.org/10.1051/0004-6361/201016401.

Daugherty, J.K., Harding, A.K., 1986. Compton Scattering in Strong Magnetic Fields. ApJ 309, 362. https://doi.org/10.1086/164608.

Davidson, K., Ostriker, J.P., 1973. Neutron-star accretion in a stellar wind: Model for a pulsed x-ray source. ApJ 179, 585–598.

Davies, R.E., Fabian, A.C., Pringle, J.E., 1979. Spindown of neutron stars in close binary systems. MNRAS 186, 779–782. https://doi.org/10.1093/mnras/186.4.779.

Davies, R.E., Pringle, J.E., 1981. Spindown of neutron stars in close binary systems. II. MNRAS 196, 209–224. https://doi.org/10.1093/mnras/196.2.209.

de Angelis, A., (E-Astrogam Collaboration), 2017. The e-ASTROGAM mission. Exploring the extreme Universe with gamma rays in the MeV - GeV range. Experimental Astronomy 44 (1), 25–82. https://doi.org/10.1007/s10686-017-9533-6.

de Angelis, A., (E-Astrogam Collaboration), 2018. Science with e-ASTROGAM. A space mission for MeV-GeV gamma-ray astrophysics. Journal of High Energy Astrophysics 19, 1–106. https://doi.org/10.1016/j.jheap.2018.07.001.

de Grijs, R., Bono, G., 2015. Clustering of Local Group Distances: Publication Bias or Correlated Measurements? III. The Small Magellanic Cloud. AJ 149 (6), 179. https://doi.org/10.1088/0004-6256/149/6/179.

Dean, A.J., Bazzano, A., Hill, A.B., Stephen, J.B., Bassani, L., Barlow, E.J., Bird, A.J., Lebrun, F., Sguera, V., Shaw, S.E., Ubertini, P., Walter, R., Willis, D.R., 2005. Global characteristics of the first IBIS/ISGRI catalogue sources: unveiling a murky episode of binary star evolution. A&A 443, 485–494. https://doi.org/10.1051/0004-6361:20053513.

den Hartog, P.R., Kuiper, L.M., Corbet, R.H.D., in't Zand, J.J.M., Hermsen, W., Vink, J., Remillard, R., van der Klis, M., 2004. IGR J00370+6122 - A new high-mass X-ray binary. The Astronomer's Telegram 281, 1.

Di Salvo, T., Burderi, L., Robba, N.R., Guainazzi, M., 1998. The Two-Component X-Ray Broadband Spectrum of X Persei Observed by BeppoSAX. ApJ 509 (2), 897–903. https://doi.org/10.1086/306525.

Domingo, A., Gutiérrez-Sánchez, R., Rísquez, D., Caballero-García, M.D., Mas-Hesse, J.M., Solano, E., 2010. The INTEGRAL-OMC Scientific Archive. Astrophysics and Space Science Proceedings 14, 493. https://doi.org/10.1007/978-3-642-11250-8_143.

Doroshenko, V., Ducci, L., Santangelo, A., Sasaki, M., 2014. Population of the Galactic X-ray binaries and eRosita. A&A 567, A7. https://doi.org/10.1051/0004-6361/201423766.

Doroshenko, V., Santangelo, A., Ducci, L., Klochkov, D., 2012. Supergiant, fast, but not so transient 4U 1907+09. A&A 548, A19. https://doi.org/10.1051/0004-6361/201220085.

Doroshenko, V., Santangelo, A., Kreykenbohm, I., Doroshenko, R., 2012. The hard X-ray emission of X Persei. A&A 540, L1. https://doi.org/10.1051/0004-6361/201218878.

Drave, S.P., Bird, A.J., Goossens, M.E., Sidoli, L., Sguera, V., Fiocchi, M., Bazzano, A., 2013. Confirmation of the superorbital modulation of the high mass X-ray binaries 4U 1909+07, IGR J16479-4514 and IGR J16418-4532 with INTEGRAL/IBIS. The Astronomer's Telegram 5131, 1.

Drave, S.P., Bird, A.J., Sidoli, L., Sguera, V., Bazzano, A., Hill, A.B., Goossens, M.E., 2014. New insights on accretion in supergiant fast X-ray transients from XMM-Newton and INTEGRAL observations of IGR J17544-2619. MNRAS 439, 2175–2185. https://doi.org/10.1093/mnras/stu110.

Drave, S.P., Bird, A.J., Sidoli, L., Sguera, V., McBride, V.A., Hill, A.B., Bazzano, A., Goossens, M.E., 2013. INTEGRAL and XMM-Newton observations of IGR J16418-4532: evidence of accretion regime transitions in a supergiant fast X-ray transient. MNRAS 433 (1), 528–542. https://doi.org/10.1093/mnras/stt754.

Drave, S.P., Bird, A.J., Townsend, L.J., Hill, A.B., McBride, V.A., Sguera, V., Bazzano, A., Clark, D.J., 2012. X-ray pulsations from the region of the supergiant fast X-ray transient IGR J17544-2619. A&A 539, A21. https://doi.org/10.1051/0004-6361/201117947.

Drave, S.P., Clark, D.J., Bird, A.J., McBride, V.A., Hill, A.B., Sguera, V., Scaringi, S., Bazzano, A., 2010. Discovery of the 51.47-d orbital period in the supergiant fast X-ray transient XTE J1739-302 with INTEGRAL. MNRAS 409, 1220–1226. https://doi.org/10.1111/j.1365-2966.2010.17383.x.

Dubus, G., 2006. Gamma-ray binaries: pulsars in disguise? A&A 456 (3), 801–817. https://doi.org/10.1051/0004-6361:20054779.

Dubus, G., 2013. Gamma-ray binaries and related systems. A&A Rev. 21, 64. https://doi.org/10.1007/s00159-013-0064-5.

Ducci, L., Doroshenko, V., Sasaki, M., Santangelo, A., Esposito, P., Romano, P., Vercellone, S., 2013. Spectral and temporal properties of the supergiant fast X-ray transient IGR J18483-0311 observed by INTEGRAL. A&A 559, A135. https://doi.org/10.1051/0004-6361/201322299.

Ducci, L., Malacaria, C., Romano, P., Ji, L., Bozzo, E., Saathoff, I., Santangelo, A., Udalski, A., 2019. X-ray and optical monitoring of the December 2017 outburst of the Be/X-ray binary AXJ0049.4-7323. A&A 621, A94. https://doi.org/10.1051/0004-6361/201834432.

Ducci, L., Romano, P., Ji, L., Santangelo, A., 2019. Accretion disc by Roche lobe overflow in the supergiant fast X-ray transient IGR J08408-4503. A&A 631, A135. https://doi.org/10.1051/0004-6361/201936544.

Ducci, L., Sidoli, L., Paizis, A., 2010. INTEGRAL results on Supergiant Fast X-ray Transients and accretion mechanism interpretation: ionization effect and formation of transient accretion disks. ArXiv e-prints1006.3256.

Eger, P., Laffon, H., Bordas, P., de Oña Whilhelmi, E., Hinton, J., Pühlhofer, G., 2016. Discovery of a variable X-ray counterpart to HESS J1832-093: a new gamma-ray binary? MNRAS 457, 1753–1758. https://doi.org/10.1093/mnras/stw125.

El Mellah, I., Sander, A.A.C., Sundqvist, J.O., Keppens, R., 2019. Formation of wind-captured disks in supergiant X-ray binaries. Consequences for Vela X-1 and Cygnus X-1. A&A 622, A189. https://doi.org/10.1051/0004-6361/201834498.

El Mellah, I., Sundqvist, J.O., Keppens, R., 2018. Accretion from a clumpy massive-star wind in supergiant X-ray binaries. MNRAS 475 (3), 3240–3252. https://doi.org/10.1093/mnras/stx3211.

Elsner, R.F., Lamb, F.K., 1977. Accretion by magnetic neutron stars. I - Magnetospheric structure and stability. ApJ 215, 897–913. https://doi.org/10.1086/155427.

Elsner, R.F., Lamb, F.K., 1984. Accretion by magnetic neutron stars. II - Plasma entry into the magnetosphere via diffusion, polar cusps, and magnetic field reconnection. ApJ 278, 326–344. https://doi.org/10.1086/161797.

Esposito, P., Israel, G.L., Milisavljevic, D., Mapelli, M., Zampieri, L., Sidoli, L., Fabbiano, G., Rodríguez Castillo, G.A., 2015. Periodic signals from the Circinus region: two new cataclysmic variables and the ultraluminous X-ray source candidate GC X-1. MNRAS 452 (2), 1112–1127. https://doi.org/10.1093/mnras/stv1379.

Esposito, P., Israel, G.L., Sidoli, L., Mason, E., Rodríguez Castillo, G.A., Halpern, J.P., Moretti, A., Götz, D., 2013. Discovery of 47-s pulsations in the X-ray source 1RXS J225352.8+624354. MNRAS 433 (3), 2028–2035. https://doi.org/10.1093/mnras/stt870.

Evans, C.J., Howarth, I.D., Irwin, M.J., Burnley, A.W., Harries, T.J., 2004. A 2dF survey of the Small Magellanic Cloud. MNRAS 353 (2), 601–623. https://doi.org/10.1111/j.1365-2966.2004.08096.x.

Evans, C.J., Lennon, D.J., Smartt, S.J., Trundle, C., 2006. The VLT-FLAMES survey of massive stars: observations centered on the Magellanic Cloud clusters NGC 330, NGC 346, NGC 2004, and the N11 region. A&A 456 (2), 623–638. https://doi.org/10.1051/0004-6361:20064988.

Falanga, M., Bozzo, E., Lutovinov, A., Bonnet-Bidaud, J.M., Fetisova, Y., Puls, J., 2015. Ephemeris, orbital decay, and masses of ten eclipsing high-mass X-ray binaries. A&A 577, A130. https://doi.org/10.1051/0004-6361/201425191.

Falkner, S., 2018. Modeling X-ray pulsars in curved space-time. University of Erlangen-Nuremberg Dissertation.

Farinelli, R., Ferrigno, C., Bozzo, E., Becker, P.A., 2016. A new model for the X-ray continuum of the magnetized accreting pulsars. A&A 591, A29. https://doi.org/10.1051/0004-6361/201527257.

Fender, R.P., Belloni, T.M., Gallo, E., 2004. Towards a unified model for black hole X-ray binary jets. MNRAS 355, 1105–1118. https://doi.org/10.1111/j.1365-2966.2004.08384.x.

Fermi LAT Collaboration, 2012. Periodic Emission from the Gamma-Ray Binary 1FGL J1018.6-5856. Science 335, 189. https://doi.org/10.1126/science.1213974.

Feroci, M., (LOFT Collaboration), 2012. The Large Observatory for X-ray Timing (LOFT). Experimental Astronomy 34, 415–444. https://doi.org/10.1007/s10686-011-9237-2.

Ferrigno, C., Becker, P.A., Segreto, A., Mineo, T., Santangelo, A., 2009. Study of the accreting pulsar 4U 0115+63 using a bulk and thermal Comptonization model. A&A 498 (3), 825–836. https://doi.org/10.1051/0004-6361/200809373.

Ferrigno, C., Bozzo, E., Sanna, A., Jaisawal, G.K., Girard, J.M., Di Salvo, T., Burderi, L., 2019. IGR J17503-2636: a candidate supergiant fast X-ray transient. A&A 624, A142. https://doi.org/10.1051/0004-6361/201935185.

Ferrigno, C., Ducci, L., Bozzo, E., Kretschmar, P., Kühnel, M., Malacaria, C., Pottschmidt, K., Santangelo, A., Savchenko, V., Wilms, J., 2016. Two giant outbursts of V0332+53 observed with INTEGRAL. A&A 595, A17. https://doi.org/10.1051/0004-6361/201628865.

Filippova, E.V., Mereminskiy, I.A., Lutovinov, A.A., Molkov, S.V., Tsygankov, S.S., 2017. Radius of the neutron star magnetosphere during disk accretion. Astronomy Letters 43, 706–729. https://doi.org/10.1134/S1063773717110020.

Filippova, E.V., Tsygankov, S.S., Lutovinov, A.A., Sunyaev, A.A., 2007. Spectral Analysis of X-Ray Pulsars with the INTEGRAL Observatory. The Obscured Universe. Proceedings of the VI INTEGRAL Workshop. ESA Special Publication 622. pp. 449. astro-ph/0610782.

Filippova, E.V., Tsygankov, S.S., Lutovinov, A.A., Sunyaev, R.A., 2005. Hard Spectra of X-ray Pulsars from INTEGRAL Data. Astronomy Letters 31 (11), 729–747. https://doi.org/10.1134/1.2123288.

Filliatre, P., Chaty, S., 2004. The Optical/Near-Infrared Counterpart of the INTEGRAL Obscured Source IGR J16318-4848: An sgB[e] in a High-Mass X-Ray Binary? ApJ 616, 469–484. https://doi.org/10.1086/424869.

Fiocchi, M., Sguera, V., Bazzano, A., Bassani, L., Bird, A.J., Natalucci, L., Ubertini, P., 2010. IGR J16328-4726: A New Candidate Supergiant Fast X-ray Transient. ApJ 725 (1), L68–L72. https://doi.org/10.1088/2041-8205/725/1/L68.

Forman, W., Jones, C., Tananbaum, H., Gursky, H., Kellogg, E., Giacconi, R., 1973. Uhuru observations of the binary x-ray source 2u 0900–40. ApJ 182, L103–L107.

Fornasini, F.M., 2016. The Faint, the Poor, and the Steady: studies of low-luminosity, metal-poor, and non-pulsating populations of high-mass X-ray binaries. University of California, Berkeley.

Fornasini, F.M., Tomsick, J.A., Bodaghee, A., Krivonos, R.A., An, H., Rahoui, F., Gotthelf, E.V., Bauer, F.E., Stern, D., 2014. The Norma Arm Region Chandra Survey Catalog: X-Ray Populations in the Spiral Arms. ApJ 796 (2), 105. https://doi.org/10.1088/0004-637X/796/2/105.

Fornasini, F.M., Tomsick, J.A., Hong, J., Gotthelf, E.V., Bauer, F., Rahoui, F., Stern, D.,

Bodaghee, A., Chiu, J.-L., Clavel, M., Corral-Santana, J., Hailey, C.J., Krivonos, R.A., Mori, K., Alexander, D.M., Barret, D., Boggs, S.E., Christensen, F.E., Craig, W.W., Forster, K., Giommi, P., Grefenstette, B.W., Harrison, F.A., Hornstrup, A., Kitaguchi, T., Koglin, J.E., Madsen, K.K., Mao, P.H., Miyasaka, H., Perri, M., Pivovaroff, M.J., Puccetti, S., Rana, V., Westergaard, N.J., Zhang, W.W., 2017. The NuSTAR Hard X-Ray Survey of the Norma Arm Region. ApJS 229 (2), 33. https://doi.org/10.3847/1538-4365/aa61fc.

Fortin, F., Chaty, S., Coleiro, A., Tomsick, J.A., Nitschelm, C.H.R., 2018. Spectroscopic identification of INTEGRAL high-energy sources with VLT/ISAAC. A&A 618, A150. https://doi.org/10.1051/0004-6361/201731265.

Fortin, F., Chaty, S., Sander, A., 2020. Optical and Infrared Study of the Obscured B[e] Supergiant High-mass X-Ray Binary IGR J16318-4848. ApJ 894 (2), 86. https://doi.org/10.3847/1538-4357/ab881c.

Fransson, C., Fabian, A.C., 1980. X-ray induced shocks in stellar winds. A&A 87, 102–108.

Fritz, S., Kreykenbohm, I., Wilms, J., Staubert, R., Bayazit, F., Pottschmidt, K., Rodriguez, J., Santangelo, A., 2006. A torque reversal of 4U 1907+09. A&A 458 (3), 885–893. https://doi.org/10.1051/0004-6361:20065557.

Fürst, F., Falkner, S., Marcu-Cheatham, D., Grefenstette, B., Tomsick, J., Pottschmidt, K., Walton, D.J., Natalucci, L., Kretschmar, P., 2018. Multiple cyclotron line-forming regions in GX 301-2. A&A 620, A153. https://doi.org/10.1051/0004-6361/201732102.

Fürst, F., Grefenstette, B.W., Staubert, R., Tomsick, J.A., Bachetti, M., Barret, D., Bellm, E.C., Boggs, S.E., Chenevez, J., Christensen, F.E., Craig, W.W., Hailey, C.J., Harrison, F., Klochkov, D., Madsen, K.K., Pottschmidt, K., Stern, D., Walton, D.J., Wilms, J., Zhang, W., 2013. The Smooth Cyclotron Line in Her X-1 as Seen with Nuclear Spectroscopic Telescope Array. ApJ 779 (1), 69. https://doi.org/10.1088/0004-637X/779/1/69.

Fürst, F., Kreykenbohm, I., Pottschmidt, K., Wilms, J., Hanke, M., Rothschild, R.E., Kretschmar, P., Schulz, N.S., Huenemoerder, D.P., Klochkov, D., Staubert, R., 2010. X-ray variation statistics and wind clumping in Vela X-1. A&A 519, A37+. https://doi.org/10.1051/0004-6361/200913981.

Gaia Collaboration, 2018. Gaia Data Release 2. Summary of the contents and survey properties. A&A 616, A1. https://doi.org/10.1051/0004-6361/201833051.

Galache, J.L., Corbet, R.H.D., Coe, M.J., Laycock, S., Schurch, M.P.E., Markwardt, C., Marshall, F.E., Lochner, J., 2008. A Long Look at the Be/X-Ray Binaries of the Small Magellanic Cloud. ApJS 177 (1), 189–215. https://doi.org/10.1086/587743.

Gálvez, J.L., Hernanz, M., Mansanet, C., LOFT-WFM Collaboration, 2019. A Wide Field Monitor (WFM) for the new generation X-ray missions eXTP (China) and STROBE-X (NASA). Highlights on Spanish Astrophysics X. pp. 560–567.

Gamen, R., Barbà, R.H., Walborn, N.R., Morrell, N.I., Arias, J.I., Maíz Apellániz, J., Sota, A., Alfaro, E.J., 2015. The eccentric short-period orbit of the supergiant fast X-ray transient HD 74194 (=LM Vel). A&A 583, L4. https://doi.org/10.1051/0004-6361/201527140.

García, F., Fogantini, F.A., Chaty, S., Combi, J.A., 2018. Spectral evolution of the supergiant HMXB IGR J16320-4751 along its orbit using XMM-Newton. A&A 618, A61. https://doi.org/10.1051/0004-6361/201833365.

Ghosh, P., Lamb, F.K., 1979. Accretion by rotating magnetic neutron stars. II - Radial and vertical structure of the transition zone in disk accretion. ApJ 232, 259–276. https://doi.org/10.1086/157285.

Ghosh, P., Lamb, F.K., 1979. Accretion by rotating magnetic neutron stars. III - Accretion torques and period changes in pulsating X-ray sources. ApJ 234, 296–316. https://doi.org/10.1086/157498.

Giacconi, R., Gursky, H., Paolini, F.R., Rossi, B.B., 1962. Evidence for x Rays From Sources Outside the Solar System. Phys. Rev. Lett. 9 (11), 439–443. https://doi.org/10.1103/PhysRevLett.9.439.

Giménez-García, A., Shenar, T., Torrejón, J.M., Oskinova, L., Martínez-Núñez, S., Hamann, W.-R., Rodes-Roca, J.J., González-Galán, A., Alonso-Santiago, J., González-Fernández, C., Bernabeu, G., Sander, A., 2016. Measuring the stellar wind parameters in IGR J17544-2619 and Vela X-1 constrains the accretion physics in supergiant fast X-ray transient and classical supergiant X-ray binaries. A&A 591, A26. https://doi.org/10.1051/0004-6361/201527551.

Giménez-García, A., Torrejón, J.M., Eikmann, W., Martínez-Núñez, S., Oskinova, L.M., Rodes-Roca, J.J., Bernabéu, G., 2015. An XMM-Newton view of FeKα in HMXBs. A&A 576, A108. https://doi.org/10.1051/0004-6361/201425004.

González-Galán, A., 2014. Fundamental properties of High-Mass X-ray Binaries. Universidad de Alicante.

González-Riestra, R., Oosterbroek, T., Kuulkers, E., Orr, A., Parmar, A.N., 2004. XMM-Newton observations of the INTEGRAL X-ray transient IGR J17544-2619. A&A 420, 589–594. https://doi.org/10.1051/0004-6361:20035940.

Goossens, M.E., Bird, A.J., Drave, S.P., Bazzano, A., Hill, A.B., McBride, V.A., Sguera, V., Sidoli, L., 2013. Discovering a 5.72-d period in the supergiant fast X-ray transient AX J1845.0-0433. MNRAS 434, 2182–2187. https://doi.org/10.1093/mnras/stt1166.

Götz, D., Falanga, M., Senziani, F., De Luca, A., Schanne, S., von Kienlin, A., 2007. IGR J08408-4503: A New Recurrent Supergiant Fast X-Ray Transient. ApJ 655, L101–L104. https://doi.org/10.1086/511818.

Gotz, D., Schanne, S., Rodriguez, J., Leyder, J.C., von Kienlin, A., Mowlavi, N., Mereghetti, S., 2006. Outburst of a new source IGR J08408-4503 detected by INTEGRAL. The Astronomer's Telegram 813, 1.

Graczyk, D., Pietrzyński, G., Thompson, I.B., Gieren, W., Pilecki, B., Konorski, P., Udalski, A., Soszyński, I., Villanova, S., Górski, M., Suchomska, K., Karczmarek, P., Kudritzki, R.-P., Bresolin, F., Gallenne, A., 2014. The Araucaria Project. The Distance to the Small Magellanic Cloud from Late-type Eclipsing Binaries. ApJ 780 (1), 59. https://doi.org/10.1088/0004-637X/780/1/59.

Grebenev, S., 2009. Supergiant Fast X-ray Transients observed by INTEGRAL. The Extreme Sky: Sampling the Universe above 10 keV. pp. 60.

Grebenev, S.A., 2017. The nature of the bimodal luminosity distribution of ultraluminous

X-ray pulsars. Astronomy Letters 43 (7), 464–471. https://doi.org/10.1134/S1063773717050012.

Grebenev, S.A., Bird, A.J., Molkov, S.V., Soldi, S., Kretschmar, P., Diehl, R., Budz-Joergensen, C., McBreen, B., 2005. IGR J16493-4348 - a radiopulsar or a new X-ray binary. The Astronomer's Telegram 457, 1.

Grebenev, S.A., Lutovinov, A.A., 2010. New X-ray source IGR J05414-6858 discovered with INTEGRAL. The Astronomer's Telegram 2695, 1.

Grebenev, S.A., Lutovinov, A.A., Sunyaev, R.A., 2003. New outburst of IGR J17544-2619. The Astronomer's Telegram 192, 1.

Grebenev, S.A., Lutovinov, A.A., Tsygankov, S.S., Mereminskiy, I.A., 2013. Deep hard X-ray survey of the Large Magellanic Cloud. MNRAS 428 (1), 50–57. https://doi.org/10.1093/mnras/sts008.

Grebenev, S.A., Revnivtsev, M.G., Sunyaev, R.A., 2007. Discovery of the new fast X-ray transient IGRJ18462-0223 with INTEGRAL. The Astronomer's Telegram 1319, 1.

Grebenev, S.A., Sunyaev, R.A., 2005. Outburst of the X-ray transient SAX J1818.6-1703 detected by the INTEGRAL observatory in September 2003. Astronomy Letters 31, 672–680. https://doi.org/10.1134/1.2075310.

Grebenev, S.A., Sunyaev, R.A., 2007. The first observation of AX J1749.1-2733 in a bright X-ray state—-Another fast transient revealed by INTEGRAL. Astronomy Letters 33, 149–158. https://doi.org/10.1134/S1063773707030024.

Grebenev, S.A., Sunyaev, R.A., 2010. New fast X-ray transient IGR J18462-0223 discovered by the INTEGRAL observatory. Astronomy Letters 36, 533–539. https://doi.org/10.1134/S1063773710080013.

Grebenev, S.A., Ubertini, P., Chenevez, J., Mowlavi, N., Roques, J.P., Gehrels, N., Kuulkers, E., 2004. New X-ray transient IGR J11435-6109 discovered with INTEGRAL. The Astronomer's Telegram 350, 1.

Grebenev, S.A., Ubertini, P., Chenevez, J., Orr, A., Sunyaev, R.A., 2004. New X-ray transient IGR J01363+6610 discovered by INTEGRAL. The Astronomer's Telegram 275, 1.

Grimm, H.-J., Gilfanov, M., Sunyaev, R., 2002. The Milky Way in X-rays for an outside observer. Log(N)-Log(S) and luminosity function of X-ray binaries from RXTE/ASM data. A&A 391, 923–944. https://doi.org/10.1051/0004-6361:20020826.

Grinberg, V., Hell, N., El Mellah, I., Neilsen, J., Sander, A.A.C., Leutenegger, M., Fürst, F., Huenemoerder, D.P., Kretschmar, P., Kühnel, M., Martínez-Núñez, S., Niu, S., Pottschmidt, K., Schulz, N.S., Wilms, J., Nowak, M.A., 2017. The clumpy absorber in the high-mass X-ray binary Vela X-1. A&A 608, A143. https://doi.org/10.1051/0004-6361/201731843.

Grinberg, V., Hell, N., Pottschmidt, K., Böck, M., Nowak, M.A., Rodriguez, J., Bodaghee, A., Cadolle Bel, M., Case, G.L., Hanke, M., Kühnel, M., Markoff, S.B., Pooley, G.G., Rothschild, R.E., Tomsick, J.A., Wilson-Hodge, C.A., Wilms, J., 2013. Long term variability of Cygnus X-1. V. State definitions with all sky monitors. A&A 554, A88. https://doi.org/10.1051/0004-6361/201321128.

Grundstrom, E.D., Gies, D.R., 2006. Estimating Be Star Disk Radii using Hα Emission Equivalent Widths. ApJ 651, L53–L56. https://doi.org/10.1086/509635.

Grupe, D., Kennea, J., Evans, P., Romano, P., Markwardt, C., Chester, M., 2009. Swift detection of a flare from IGR J16328-4726. The Astronomer's Telegram 2075, 1.

Gutiérrez, R., Solano, E., Domingo, A., García, J., 2004. The Optical Monitoring Camera Data Server: Contents and Functionalities. In: Ochsenbein, F., Allen, M.G., Egret, D. (Eds.), Astronomical Data Analysis Software and Systems (ADASS) XIII. Astronomical Society of the Pacific Conference Series 314. pp. 153.

Haberl, F., Sturm, R., 2016. High-mass X-ray binaries in the Small Magellanic Cloud. A&A 586, A81. https://doi.org/10.1051/0004-6361/201527326.

Hainich, R., Oskinova, L.M., Torrejón, J.M., Fuerst, F., Bodaghee, A., Shenar, T., Sand er, A.A.C., Todt, H., Spetzer, K., Hamann, W.R., 2020. The stellar and wind parameters of six prototypical HMXBs and their evolutionary status. A&A 634, A49. https://doi.org/10.1051/0004-6361/201935498.

Halonen, R.J., Mackay, F.E., Jones, C.E., 2013. Computing the Continuum Polarization from Thomson Scattering in Gaseous Circumstellar Disks. ApJS 204, 11. https://doi.org/10.1088/0067-0049/204/1/11.

Halpern, J.P., 2005. Chandra and Optical Identification of INTEGRAL Sources. The Astronomer's Telegram 572, 1.

Halpern, J.P., 2012. Discovery of 46.6 s X-ray Pulsations from the Candidate for IGR J22534+6243. The Astronomer's Telegram 4240, 1.

Halpern, J.P., 2012. Swift Detection of 11.82 s Pulsations from IGR J18179-1621. The Astronomer's Telegram 3949, 1.

Halpern, J.P., Tyagi, S., 2005. Be Star Counterpart of X-ray Transient IGR J01583+6713. The Astronomer's Telegram 681, 1.

Hannikainen, D.C., Rawlings, M.G., Muhli, P., Vilhu, O., Schultz, J., Rodriguez, J., 2007. The nature of the infrared counterpart of IGR J19140+0951. MNRAS 380, 665–668. https://doi.org/10.1111/j.1365-2966.2007.12092.x.

Hanson, M.M., Conti, P.S., Rieke, M.J., 1996. A Spectral Atlas of Hot, Luminous Stars at 2 Microns. ApJS 107, 281. https://doi.org/10.1086/192366.

Hanson, M.M., Kudritzki, R.-P., Kenworthy, M.A., Puls, J., Tokunaga, A.T., 2005. A Medium Resolution Near-Infrared Spectral Atlas of O and Early-B Stars. ApJS 161, 154–170. https://doi.org/10.1086/444363.

Hanson, M.M., Rieke, G.H., Luhman, K.L., 1998. Near-Infrared H-Band Features in Late O and B Stars. AJ 116, 1915–1921. https://doi.org/10.1086/300556.

Hanuschik, R.W., 1995. Shell lines in disks around Be stars. 1: Simple approximations for Keplerian disks. A&A 295, 423–434.

Harding, A.K., Daugherty, J.K., 1991. Cyclotron Resonant Scattering and Absorption. ApJ 374, 687. https://doi.org/10.1086/170153.

Hare, J., Halpern, J.P., Clavel, M., Grindlay, J.E., Rahoui, F., Tomsick, J.A., 2019. Chandra, MDM, Swift, and NuSTAR Observations Confirming the SFXT Nature of AX J1949.8+2534. ApJ 878 (1), 15. https://doi.org/10.3847/1538-4357/ab1cbe.

Haubois, X., Mota, B.C., Carciofi, A.C., Draper, Z.H., Wisniewski, J.P., Bednarski, D., Rivinius, T., 2014. Dynamical Evolution of Viscous Disks around Be Stars. II.

Polarimetry. ApJ 785, 12. https://doi.org/10.1088/0004-637X/785/1/12.

Heemskerk, M.H.M., van Paradijs, J., 1989. Analysis of the optical light curve of the massive X-ray binary LMC X-4. A&A 223, 154–164.

Heida, M., Lau, R.M., Davies, B., Brightman, M., Fürst, F., Grefenstette, B.W., Kennea, J.A., Tramper, F., Walton, D.J., Harrison, F.A., 2019. Discovery of a Red Supergiant Donor Star in SN2010da/NGC 300 ULX-1. ApJ 883 (2), L34. https://doi.org/10.3847/2041-8213/ab4139.

Hill, A.B., Dean, A.J., Landi, R., McBride, V.A., de Rosa, A., Bird, A.J., Bazzano, A., Sguera, V., 2008. Probing the nature of IGR J16493-4348: spectral and temporal analysis of the 1-100 keV emission. MNRAS 385 (1), 423–429. https://doi.org/10.1111/j.1365-2966.2008.12849.x.

Hirsch, M., Hell, N., Grinberg, V., Ballhausen, R., Nowak, M.A., Pottschmidt, K., Schulz, N.S., Dauser, T., Hanke, M., Kallman, T.R., Brown, G.V., Wilms, J., 2019. Chandra X-ray spectroscopy of the focused wind in the Cygnus X-1 system. III. Dipping in the low/hard state. A&A 626, A64. https://doi.org/10.1051/0004-6361/201935074.

Hoffmann, A.D., Klochkov, D., Santangelo, A., Horns, D., Segreto, A., Staubert, R., Pühlhofer, G., 2009. INTEGRAL observation of hard X-ray variability of the TeV binary LS 5039/RX J1826.2-1450. A&A 494, L37–L40. https://doi.org/10.1051/0004-6361:200811397.

Hu, C.-P., Chou, Y., Ng, C.Y., Lin, L.C.-C., Yen, D.C.-C., 2017. Evolution of Spin, Orbital, and Superorbital Modulations of 4U 0114+650. ApJ 844 (1), 16. https://doi.org/10.3847/1538-4357/aa79a3.

Hubrig, S., Sidoli, L., Postnov, K., Schöller, M., Kholtygin, A.F., Järvinen, S.P., Steinbrunner, P., 2018. A search for the presence of magnetic fields in the two supergiant fast X-ray transients, IGR J08408-4503 and IGR J11215-5952. MNRAS 474, L27–L31. https://doi.org/10.1093/mnrasl/slx187.

Hummel, W., 1994. Line formation in Be star envelopes. 1: Inhomogeneous density distributions. A&A 289, 458–468.

Hutchings, J.B., Crampton, D., Cowley, A.P., Osmer, P.S., 1977. The spectroscopic orbit and masses of SK 160/SMC X-1. ApJ 217, 186–196. https://doi.org/10.1086/155569.

Illarionov, A.F., Sunyaev, R.A., 1975. Why the Number of Galactic X-ray Stars Is so Small? A&A 39, 185.

in 't Zand, J., Heise, J., Smith, M., Muller, J.M., Ubertini, P., Bazzano, A., 1998. SAX J1818.6-1703 and KS 1741-293. IAU Circ. 6840, 2.

Inoue, H., 1975. X-ray emission from a neutron star with a strong magnetic dipole field. PASJ 27 (2), 311–323.

in't Zand, J.J.M., 2005. Chandra observation of the fast X-ray transient IGR J17544-2619: evidence for a neutron star? A&A 441, L1–L4. https://doi.org/10.1051/0004-6361:200500162.

in't Zand, J.J.M., (eXTP Collaboration), 2019. Observatory science with eXTP. Science China Physics, Mechanics, and Astronomy 62, 29506. https://doi.org/10.1007/s11433-017-9186-1.

in't Zand, J.J.M., Jonker, P.G., Nelemans, G., Steeghs, D., O'Brien, K., 2006. Optical identification of IGR J19140+0951. A&A 448, 1101–1106. https://doi.org/10.1051/0004-6361:20053411.

in't Zand, J.J.M., Kuiper, L., den Hartog, P.R., Hermsen, W., Corbet, R.H.D., 2007. A probable accretion-powered X-ray pulsar in IGR J00370+6122. A&A 469 (3), 1063–1068. https://doi.org/10.1051/0004-6361:20077189.

Isenberg, M., Lamb, D.Q., Wang, J.C.L., 1998. Effects of the Geometry of the Line-forming Region on the Properties of Cyclotron Resonant Scattering Lines. ApJ 505 (2), 688–714. https://doi.org/10.1086/306171.

Israel, G.L., Esposito, P., D'Elia, V., Sidoli, L., 2013. A new transient X-ray pulsar in the Small Magellanic Cloud. The Astronomer's Telegram 5552, 1.

Israel, G.L., Esposito, P., Rodríguez Castillo, G.A., Sidoli, L., 2016. The Chandra ACIS Timing Survey Project: glimpsing a sample of faint X-ray pulsators. MNRAS 462 (4), 4371–4385. https://doi.org/10.1093/mnras/stw1897.

Jain, C., Paul, B., Dutta, A., 2009. Discovery of a short orbital period in the Supergiant Fast X-ray Transient IGR J16479-4514. MNRAS 397, L11–L15. https://doi.org/10.1111/j.1745-3933.2009.00668.x.

Jain, C., Paul, B., Dutta, A., 2009. Orbital X-ray modulation study of three supergiant HMXBs. Research in Astronomy and Astrophysics 9 (12), 1303–1316. https://doi.org/10.1088/1674-4527/9/12/002.

Jenke, P., Wilson-Hodge, C.A., 2017. Fermi GBM detects pulsations from Swift J0243.6+6124. The Astronomer's Telegram 10812, 1.

Jenke, P.A., Finger, M.H., Wilson-Hodge, C.A., Camero-Arranz, A., 2012. Orbital Decay and Evidence of Disk Formation in the X-Ray Binary Pulsar OAO 1657-415. ApJ 759 (2), 124. https://doi.org/10.1088/0004-637X/759/2/124.

Johnson, T.J., Wood, K.S., Kerr, M., Corbet, R.H.D., Cheung, C.C., Ray, P.S., Omodei, N., 2018. A Luminous and Highly Variable Gamma-Ray Flare Following the 2017 Periastron of PSR B1259-63/LS 2883. ApJ 863, 27. https://doi.org/10.3847/1538-4357/aad185.

Jourdain, E., Roques, J.P., Chauvin, M., Clark, D.J., 2012. Separation of Two Contributions to the High Energy Emission of Cygnus X-1: Polarization Measurements with INTEGRAL SPI. ApJ 761, 27. https://doi.org/10.1088/0004-637X/761/1/27.

Kaaret, P., Feng, H., Roberts, T.P., 2017. Ultraluminous X-Ray Sources. ARA&A 55 (1), 303–341. https://doi.org/10.1146/annurev-astro-091916-055259.

Kahabka, P., Pietsch, W., Filipović, M.D., Haberl, F., 1999. A ROSAT PSPC X-ray survey of the Small Magellanic Cloud. A&AS 136, 81–94. https://doi.org/10.1051/aas:1999199.

Kallman, T., Dorodnitsyn, A., Blondin, J., 2015. X-Ray Polarization from High-mass X-Ray Binaries. ApJ 815 (1), 53. https://doi.org/10.1088/0004-637X/815/1/53.

Karasev, D.I., Lutovinov, A.A., Revnivtsev, M.G., Krivonos, R.A., 2012. Accurate localization and identification of six hard X-ray sources from Chandra and XMM-Newton data. Astronomy Letters 38 (10), 629–637. https://doi.org/10.1134/S1063773712100039.

Karasev, D.I., Tsygankov, S.S., Lutovinov, A.A., 2008. Discovery of X-ray pulsations from the HMXB source AXJ1749.1-2733. MNRAS 386 (1), L10–L14. https://doi.org/10.1111/j.1745-3933.2008.00449.x.

Karino, S., Nakamura, K., Taani, A., 2019. Stellar wind accretion and accretion disk formation: Applications to neutron star high-mass X-ray binaries. PASJ 71 (3), 58. https://doi.org/10.1093/pasj/psz034.

Kaur, R., Paul, B., Kumar, B., Sagar, R., 2008. Multiwavelength study of the transient X-ray binary IGR J01583+6713. MNRAS 386 (4), 2253–2261. https://doi.org/10.1111/j.1365-2966.2008.13233.x.

Kaur, R., Wijnands, R., Paul, B., Patruno, A., Degenaar, N., 2010. Near-infrared/optical identification of five low-luminosity X-ray pulsators. MNRAS 402 (4), 2388–2396. https://doi.org/10.1111/j.1365-2966.2009.15919.x.

Keek, S., Kuiper, L., Hermsen, W., 2006. The discovery of five new hard X-ray sources in the Circinus region by INTEGRAL. The Astronomer's Telegram 810, 1.

Kennea, J.A., Lien, A.Y., Krimm, H.A., Cenko, S.B., Siegel, M.H., 2017. Swift J0243.6+6124: Swift discovery of an accreting NS transient. The Astronomer's Telegram 10809, 1.

Kennea, J.A., Palmer, D., Burrows, D., Gehrels, N., 2005. Swift/XRT observations of XTE J1727-476/IGR J17269-4737. The Astronomer's Telegram 626.

Kinugasa, K., Torii, K., Hashimoto, Y., Tsunemi, H., Hayashida, K., Kitamoto, S., Kamata, Y., Dotani, T., Nagase, F., Sugizaki, M., Ueda, Y., Kawai, N., Makishima, K., Yamauchi, S., 1998. Discovery of the Faint X-Ray Pulsar AX J1820.5-1434 with ASCA. ApJ 495 (1), 435–439. https://doi.org/10.1086/305291.

Klochkov, D., Doroshenko, V., Santangelo, A., Staubert, R., Ferrigno, C., Kretschmar, P., Caballero, I., Wilms, J., Kreykenbohm, I., Pottschmidt, K., 2012. Outburst of GX 304-1 monitored with INTEGRAL: positive correlation between the cyclotron line energy and flux. A&A 542, L28. https://doi.org/10.1051/0004-6361/201219385.

Klochkov, D., Horns, D., Santangelo, A., Staubert, R., Segreto, A., Ferrigno, C., Kretschmar, P., Kreykenbohm, I., La Barbera, A., Masetti, N., McCollough, M., Pottschmidt, K., Schönherr, G., Wilms, J., 2007. INTEGRAL and Swift observations of EXO 2030+375 during a giant outburst. A&A 464 (3), L45–L48. https://doi.org/10.1051/0004-6361:20066801.

Klochkov, D., Santangelo, A., Staubert, R., Ferrigno, C., 2008. Giant outburst of EXO 2030+375: pulse-phase resolved analysis of INTEGRAL data. A&A 491 (3), 833–840. https://doi.org/10.1051/0004-6361:200810673.

Klochkov, D., Staubert, R., Postnov, K., Shakura, N., Santangelo, A., 2009. Continuous monitoring of pulse period variations in Hercules X-1 using Swift/BAT. A&A 506, 1261–1267. https://doi.org/10.1051/0004-6361/200912791.

Klochkov, D., Staubert, R., Santangelo, A., Rothschild, R.E., Ferrigno, C., 2011. Pulse-amplitude-resolved spectroscopy of bright accreting pulsars: indication of two accretion regimes. A&A 532, A126. https://doi.org/10.1051/0004-6361/201116800.

Kluźniak, W., Rappaport, S., 2007. Magnetically Torqued Thin Accretion Disks. ApJ 671, 1990–2005. https://doi.org/10.1086/522954.

Koenigsberger, G., Georgiev, L., Moreno, E., Richer, M.G., Toledano, O., Canalizo, G., Arrieta, A., 2006. The X-ray binary 2S0114+650=LSI+65 010. A slow pulsar or tidally-induced pulsations? A&A 458 (2), 513–522. https://doi.org/10.1051/0004-6361:20065305.

Kotze, M.M., Charles, P.A., 2012. Characterizing X-ray binary long-term variability. MNRAS 420 (2), 1575–1589. https://doi.org/10.1111/j.1365-2966.2011.20146.x.

Kretschmar, P., Kreykenbohm, I., Pottschmidt, K., Wilms, J., Coburn, W., Boggs, S., Staubert, R., Santangelo, A., Kendziorra, E., Segreto, A., Orlandini, M., Bildsten, L., Araya-Gochez, R., 2005. Integral observes possible cyclotron line at 47 keV for 1A 0535+262. The Astronomer's Telegram 601.

Kretschmar, P., Martínez-Núñez, S., Fürst, F., Grinberg, V., Lomaeva, M., El Mellah, I., Manousakis, A., Sander, A.A.C., Degenaar, N., van den Eijnden, J., 2019. Vela X-1 as a laboratory for accretion in High-Mass X-ray Binaries. arXiv e-prints. arXiv:1905.08578

Kreykenbohm, I., Mowlavi, N., Produit, N., Soldi, S., Walter, R., Dubath, P., Lubiński, P., Türler, M., Coburn, W., Santangelo, A., Rothschild, R.E., Staubert, R., 2005. INTEGRAL observation of V 0332+53 in outburst. A&A 433, L45–L48. https://doi.org/10.1051/0004-6361:200500023.

Kreykenbohm, I., Wilms, J., Kretschmar, P., Torrejón, J.M., Pottschmidt, K., Hanke, M., Santangelo, A., Ferrigno, C., Staubert, R., 2008. High variability in Vela X-1: giant flares and off states. A&A 492 (2), 511–525. https://doi.org/10.1051/0004-6361:200809956.

Krivonos, R., Tsygankov, S., Lutovinov, A., Revnivtsev, M., Churazov, E., Sunyaev, R., 2012. INTEGRAL/IBIS nine-year Galactic hard X-ray survey. A&A 545, A27. https://doi.org/10.1051/0004-6361/201219617.

Krivonos, R., Tsygankov, S., Revnivtsev, M., Grebenev, S., Churazov, E., Sunyaev, R., 2010. INTEGRAL/IBIS 7-year All-Sky Hard X-Ray Survey. II. Catalog of sources. A&A 523, A61. https://doi.org/10.1051/0004-6361/201014935.

Krivonos, R.A., Tsygankov, S.S., Lutovinov, A.e.A., Tomsick, J.A., Chakrabarty, D., Bachetti, M., Boggs, S.E., Chernyakova, M., Christensen, F.E., Craig, W.W., Fürst, F., Hailey, C.J., Harrison, F.A., Lansbury, G.B., Rahoui, F., Stern, D., Zhang, W.W., 2015. NuSTAR Discovery of an Unusually Steady Long-term Spin-up of the Be Binary 2RXP J130159.6-635806. ApJ 809 (2), 140. https://doi.org/10.1088/0004-637X/809/2/140.

Krivonos, R.A., Tsygankov, S.S., Mereminskiy, I.A., Lutovinov, A.A., Sazonov, S.Y., Sunyaev, R.A., 2017. New hard X-ray sources discovered in the ongoing INTEGRAL Galactic plane survey after 14 yr of observations. MNRAS 470, 512–516. https://doi.org/10.1093/mnras/stx1276.

Krtička, J., Kubát, J., Krtičková, I., 2018. Wind inhibition by X-ray irradiation in HMXBs: the influence of clumping and the final X-ray luminosity. A&A 620, A150. https://doi.org/10.1051/0004-6361/201833419.

Kudritzki, R.P., 2002. Line-driven Winds, Ionizing Fluxes, and Ultraviolet Spectra of Hot Stars at Extremely Low Metallicity. I. Very Massive O Stars. ApJ 577, 389–408.

https://doi.org/10.1086/342178.

Kudritzki, R.-P., Puls, J., 2000. Winds from hot stars. Annual Review of Astronomy and Astrophysics 38 (1), 613–666. https://doi.org/10.1146/annurev.astro.38.1.613.

Kuiper, L., Keek, S., Hermsen, W., Jonker, P.G., Steeghs, D., 2006. Discovery of four new hard X-ray sources in the Circinus and Carina region by INTEGRAL. The Astronomer's Telegram 684, 1.

Kulkarni, A.K., Romanova, M.M., 2008. Accretion to magnetized stars through the Rayleigh-Taylor instability: global 3D simulations. MNRAS 386, 673–687. https://doi.org/10.1111/j.1365-2966.2008.13094.x.

Kuulkers, E., 2005. An absorbed view of a new class of INTEGRAL sources. In: Burderi, L., Antonelli, L.A., D'Antona, F., di Salvo, T., Israel, G.L., Piersanti, L., Tornambè, A., Straniero, O. (Eds.), Interacting Binaries: Accretion, Evolution, and Outcomes. American Institute of Physics Conference Series 797. pp. 402–409. https://doi.org/10.1063/1.2130260. astro-ph/0504625.

Kuulkers, E., Shaw, S., Paizis, A., Gros, A., Chenevez, J., Sanchez-Fernandez, C., Brandt, S., Courvoisier, T.J.L., Garau, A.D., Ebisawa, K., Kretschmar, P., Markwardt, C., Mowlavi, N., Oosterbroek, T., Orr, A., Oneca, D.R., Wijnand s, J., 2006. New INTEGRAL source, IGR J17354-3255, and continuation of the INTEGRAL Galactic Bulge monitoring program. The Astronomer's Telegram 874, 1.

La Palombara, N., Mereghetti, S., 2006. XMM-Newton observation of the Be/neutron star system RX J0146.9+6121: a soft X-ray excess in a low luminosity accreting pulsar. A&A 455, 283–289. https://doi.org/10.1051/0004-6361:20065107.

La Parola, V., Cusumano, G., Romano, P., Segreto, A., Vercellone, S., Chincarini, G., 2010. Detection of an orbital period in the supergiant high-mass X-ray binary IGR J16465-4507 with Swift-BAT. MNRAS 405, L66–L70. https://doi.org/10.1111/j.1745-3933.2010.00860.x.

La Parola, V., Cusumano, G., Segreto, A., D'Aì, A., Masetti, N., D'Elia, V., 2013. Swift-BAT Hard X-Ray Sky Monitoring Unveils the Orbital Period of the HMXB IGR J18219-1347. ApJ 775 (1), L24. https://doi.org/10.1088/2041-8205/775/1/L24.

La Parola, V., Cusumano, G., Segreto, A., Romano, P., Vercellone, S., D'Ai', A., 2010. Discovery of a 30.77-day orbital period in the HMXB IGR J05007-7047. The Astronomer's Telegram 2594, 1.

Lai, D., 2014. Theory of Disk Accretion onto Magnetic Stars. European Physical Journal Web of Conferences. European Physical Journal Web of Conferences 64. pp. 01001. https://doi.org/10.1051/epjconf/20136401001. 1402.1903.

Lamb, F.K., Pethick, C.J., Pines, D., 1973. A Model for Compact X-Ray Sources: Accretion by Rotating Magnetic Stars. ApJ 184, 271–290. https://doi.org/10.1086/152325.

Landi, R., Bassani, L., Bazzano, A., Bird, A.J., Fiocchi, M., Malizia, A., Panessa, F., Sguera, V., Ubertini, P., 2017. Investigating the X-ray counterparts to unidentified sources in the 1000-orbit INTEGRAL/IBIS catalogue. MNRAS 470 (1), 1107–1120. https://doi.org/10.1093/mnras/stx908.

Lattimer, J.M., Prakash, M., 2001. Neutron Star Structure and the Equation of State. ApJ 550, 426–442. https://doi.org/10.1086/319702.

Laurent, P., Rodriguez, J., Wilms, J., Cadolle Bel, M., Pottschmidt, K., Grinberg, V., 2011. Polarized Gamma-Ray Emission from the Galactic Black Hole Cygnus X-1. Science 332, 438. https://doi.org/10.1126/science.1200848.

Laycock, S., Cappallo, R., Oram, K., Balchunas, A., 2014. A Transient Supergiant X-Ray Binary in IC 10: An Extragalactic SFXT? ApJ 789, 64. https://doi.org/10.1088/0004-637X/789/1/64.

Leahy, D.A., Li, L., 1995. Including the effect of gravitational light bending in X-ray profile modelling. MNRAS 277 (3), 1177–1184. https://doi.org/10.1093/mnras/277.3.1177.

Levine, A.M., Corbet, R., 2006. Detection of Additional Periodicities in RXTE ASM Light Curves. The Astronomer's Telegram 940, 1.

Li, J., Torres, D.F., Chen, Y., Götz, D., Rea, N., Zhang, S., Caliandro, G.A., Wang, J., 2011. INTEGRAL Observations of the γ-Ray Binary 1FGL J1018.6-5856. ApJ 738, L31. https://doi.org/10.1088/2041-8205/738/2/L31.

Li, J., Torres, D.F., Zhang, S., 2014. Spectral Analysis in Orbital/Superorbital Phase Space and Hints of Superorbital Variability in the Hard X-Rays of LS I +61° 303. ApJ 785, L19. https://doi.org/10.1088/2041-8205/785/1/L19.

Li, J., Torres, D.F., Zhang, S., Chen, Y., Hadasch, D., Ray, P.S., Kretschmar, P., Rea, N., Wang, J., 2011. Long-term X-Ray Monitoring of LS I +61deg303: Analysis of Spectral Variability and Flares. ApJ 733, 89. https://doi.org/10.1088/0004-637X/733/2/89.

Li, J., Torres, D.F., Zhang, S., Hadasch, D., Rea, N., Caliandro, G.A., Chen, Y., Wang, J., 2012. Unveiling the Super-orbital Modulation of LS I +61deg303 in X-Rays. ApJ 744, L13. https://doi.org/10.1088/2041-8205/744/1/L13.

Li, J., Zhang, S., Torres, D.F., Papitto, A., Chen, Y.P., Wang, J.M., 2012. INTEGRAL and Swift/XRT observations of IGR J18179-1621. MNRAS 426, L16–L20. https://doi.org/10.1111/j.1745-3933.2012.01313.x.

Lii, P.S., Romanova, M.M., Ustyugova, G.V., Koldoba, A.V., Lovelace, R.V.E., 2014. Propeller-driven outflows from an MRI disc. MNRAS 441, 86–100. https://doi.org/10.1093/mnras/stu495.

Lobel, A., Blomme, R., 2008. Modeling Ultraviolet Wind Line Variability in Massive Hot Stars. ApJ 678 (1), 408–430. https://doi.org/10.1086/529129.

Lovelace, R.V.E., Romanova, M.M., Bisnovatyi-Kogan, G.S., 1995. Spin-up/spin-down of magnetized stars with accretion discs and outflows. MNRAS 275, 244–254. https://doi.org/10.1093/mnras/275.2.244.

Lubiński, P., Cadolle Bel, M., von Kienlin, A., Budtz-Jorgensen, C., McBreen, B., Kretschmar, P., Hermsen, W., Shtykovsky, P., 2005. IGR J11215-5952 discovered in INTEGRAL Galactic Plane Scans. The Astronomer's Telegram 469, 1.

Lucy, L.B., Solomon, P.M., 1970. Mass Loss by Hot Stars. ApJ 159, 879. https://doi.org/10.1086/150365.

Lucy, L.B., White, R.L., 1980. X-ray emission from the winds of hot stars. ApJ 241, 300–305. https://doi.org/10.1086/158342.

Lutovinov, A., Grebenev, S., 2010. Swift follow-up observations of a new transient source IGRJ05414-6858. The Astronomer's Telegram 2696, 1.

Lutovinov, A., Revnivtsev, M., Gilfanov, M., Shtykovskiy, P., Molkov, S., Sunyaev, R., 2005. INTEGRAL insight into the inner parts of the Galaxy. High mass X-ray binaries. A&A 444, 821–829. https://doi.org/10.1051/0004-6361:20042392.

Lutovinov, A., Rodrigues, J., Budtz-Jorgensen, C., Grebenev, S., Winkler, C., 2004. NTEGRAL discovered a new transient source IGRJ16465-4507. The Astronomer's Telegram 329, 1.

Lutovinov, A., Rodriguez, J., Revnivtsev, M., Shtykovskiy, P., 2005. Discovery of X-ray pulsations from IGR J16320-4751 = AX J1631.9-4752. A&A 433 (2), L41–L44. https://doi.org/10.1051/0004-6361:200500092.

Lutovinov, A., Tsyganov, S., Chernyakova, M., 2012. Strong outburst activity of the X-ray pulsar X Persei during 2001-2011. MNRAS 423 (2), 1978–1984. https://doi.org/10.1111/j.1365-2966.2012.21036.x.

Lutovinov, A.A., Revnivtsev, M.G., Tsyganov, S.S., Krivonos, R.A., 2013. Population of persistent high-mass X-ray binaries in the Milky Way. MNRAS 431, 327–341. https://doi.org/10.1093/mnras/stt168.

Lutovinov, A.A., Tsyganov, S.S., 2009. Timing characteristics of the hard X-ray emission from bright X-ray pulsars based on INTEGRAL data. Astronomy Letters 35 (7), 433–456. https://doi.org/10.1134/S1063773709070019.

Lutovinov, A.A., Tsyganov, S.S., Krivonos, R.A., Molkov, S.V., Poutanen, J., 2017. Propeller Effect in the Transient X-Ray Pulsar SMC X-2. ApJ 834, 209. https://doi.org/10.3847/1538-4357/834/2/209.

Maccarone, T.J., Girard, T.M., Casetti-Dinescu, D.I., 2014. High proper motion X-ray binaries from the Yale Southern Proper Motion Survey. MNRAS 440, 1626–1633. https://doi.org/10.1093/mnras/stu320.

Malacaria, C., Jenke, P., Roberts, O.J., Wilson-Hodge, C.A., Cleveland, W.H., Mailyan, B., GBM Accreting Pulsars Program Team, 2020. The Ups and Downs of Accreting X-Ray Pulsars: Decade-long Observations with the Fermi Gamma-Ray Burst Monitor. ApJ 896 (1), 90. https://doi.org/10.3847/1538-4357/ab855c.

Manousakis, A., 2011. Accretion in High Mass X-ray Binaries. Université de Genève Dissertation.

Manousakis, A., Walter, R., 2015. Origin of the X-ray off-states in Vela X-1. A&A 575, A58. https://doi.org/10.1051/0004-6361/201321414.

Manousakis, A., Walter, R., 2015. The stellar wind velocity field of HD 77581. A&A 584, A25. https://doi.org/10.1051/0004-6361/201526893.

Maraschi, L., Treves, A., van den Heuvel, E.P.J., 1976. B-emission Stars and X-ray sources. Nature 259, 292. https://doi.org/10.1038/259292a0.

Marcu, D.M., Fürst, F., Pottschmidt, K., Grinberg, V., Müller, S., Wilms, J., Postnov, K.A., Corbet, R.H.D., Markwardt, C.B., Cadolle Bel, M., 2011. The 5 hr Pulse Period and Broadband Spectrum of the Symbiotic X-Ray Binary 3A 1954 + 319. ApJ 742, L11. https://doi.org/10.1088/2041-8205/742/1/L11.

Markwardt, C.B., Baumgartner, W.H., Skinner, G.K., Corbet, R.H.D., 2010. AX J1700.2-4220 is a 54 second X-ray pulsar. The Astronomer's Telegram 2564, 1.

Martí-Devesa, G., Reimer, O., 2020. X-ray and γ-ray orbital variability from the γ-ray binary HESS J1832-093. A&A 637, A23. https://doi.org/10.1051/0004-6361/202037442.

Martin, R.G., Nixon, C., Armitage, P.J., Lubow, S.H., Price, D.J., 2014. Giant Outbursts in Be/X-Ray Binaries. ApJ 790, L34. https://doi.org/10.1088/2041-8205/790/2/L34.

Martin, R.G., Pringle, J.E., Tout, C.A., Lubow, S.H., 2011. Tidal warping and precession of Be star decretion discs. MNRAS 416, 2827–2839. https://doi.org/10.1111/j.1365-2966.2011.19231.x.

Martínez-Núñez, S., Kretschmar, P., Bozzo, E., Oskinova, L.M., Puls, J., Sidoli, L., Sundqvist, J.O., Blay, P., Falanga, M., Fürst, F., Gímenez-García, A., Kreykenbohm, I., Kühnel, M., Sander, A., Torrejón, J.M., Wilms, J., 2017. Towards a Unified View of Inhomogeneous Stellar Winds in Isolated Supergiant Stars and Supergiant High Mass X-Ray Binaries. Space Sci. Rev. 212, 59–150. https://doi.org/10.1007/s11214-017-0340-1.

Mas-Hesse, J.M., (INTEGRAL OMC Consortium), 2003. OMC: An Optical Monitoring Camera for INTEGRAL. Instrument description and performance. A&A 411, L261–L268. https://doi.org/10.1051/0004-6361:20031418.

Masetti, N., Jimenez-Bailon, E., Chavushyan, V., Parisi, P., Bazzano, A., Landi, R., Bird, A.J., 2012. Optical spectroscopy of X-ray source IGR J22534 + 6243. The Astronomer's Telegram 4248, 1.

Masetti, N., Mason, E., Bassani, L., Bird, A.J., Maiorano, E., Malizia, A., Palazzi, E., Stephen, J.B., Bazzano, A., Dean, A.J., Ubertini, P., Walter, R., 2006. Unveiling the nature of INTEGRAL objects through optical spectroscopy. II. The nature of four unidentified sources. A&A 448, 547–556. https://doi.org/10.1051/0004-6361:20054086.

Masetti, N., Mason, E., Morelli, L., Cellone, S.A., McBride, V.A., Palazzi, E., Bassani, L., Bazzano, A., Bird, A.J., Charles, P.A., Dean, A.J., Galaz, G., Gehrels, N., Landi, R., Malizia, A., Minniti, D., Panessa, F., Romero, G.E., Stephen, J.B., Ubertini, P., Walter, R., 2008. Unveiling the nature of INTEGRAL objects through optical spectroscopy. VI. A multi-observatory identification campaign. A&A 482, 113–132. https://doi.org/10.1051/0004-6361:20079332.

Masetti, N., Morelli, L., Palazzi, E., Galaz, G., Bassani, L., Bazzano, A., Bird, A.J., Dean, A.J., Israel, G.L., Landi, R., Malizia, A., Minniti, D., Schiavone, F., Stephen, J.B., Ubertini, P., Walter, R., 2006. Unveiling the nature of INTEGRAL objects through optical spectroscopy. V. Identification and properties of 21 southern hard X-ray sources. A&A 459 (1), 21–30. https://doi.org/10.1051/0004-6361:20066055.

Masetti, N., Morelli, L., Palazzi, E., Stephen, J., Bazzano, A., Dean, A.J., Walter, R., Minniti, D., 2006. Optical classification of 8 INTEGRAL sources. The Astronomer's Telegram 783, 1.

Masetti, N., Parisi, P., Palazzi, E., Jiménez-Bailón, E., Chavushyan, V., Bassani, L., Bazzano, A., Bird, A.J., Dean, A.J., Charles, P.A., Galaz, G., Landi, R., Malizia, A., Mason, E., McBride, V.A., Minniti, D., Morelli, L., Schiavone, F., Stephen, J.B., Ubertini, P., 2010. Unveiling the nature of INTEGRAL objects through optical spectroscopy. VIII. Identification of 44 newly detected hard X-ray sources. A&A 519, A96.

https://doi.org/10.1051/0004-6361/201014852.

Masetti, N., Parisi, P., Palazzi, E., Jiménez-Bailón, E., Chavushyan, V., McBride, V., Rojas, A.F., Steward, L., Bassani, L., Bazzano, A., Bird, A.J., Charles, P.A., Galaz, G., Landi, R., Malizia, A., Mason, E., Minniti, D., Morelli, L., Schiavone, F., Stephen, J.B., Ubertini, P., 2013. Unveiling the nature of INTEGRAL objects through optical spectroscopy. X. A new multi-year, multi-observatory campaign. A&A 556, A120. https://doi.org/10.1051/0004-6361/201322026.

Masetti, N., Parisi, P., Palazzi, E., Jiménez-Bailón, E., Morelli, L., Chavushyan, V., Mason, E., McBride, V.A., Bassani, L., Bazzano, A., Bird, A.J., Dean, A.J., Galaz, G., Gehrels, N., Landi, R., Malizia, A., Minniti, D., Schiavone, F., Stephen, J.B., Ubertini, P., 2009. Unveiling the nature of INTEGRAL objects through optical spectroscopy. VII. Identification of 20 Galactic and extragalactic hard X-ray sources. A&A 495 (1), 121–135. https://doi.org/10.1051/0004-6361:200811322.

Mason, A.B., Clark, J.S., Norton, A.J., Negueruela, I., Roche, P., 2009. Spectral classification of the mass donors in the high-mass X-ray binaries EXO 1722-363 and OAO 1657-415. A&A 505 (1), 281–286. https://doi.org/10.1051/0004-6361/200912480.

Massa, D., Oskinova, L., Fullerton, A.W., Prinja, R.K., Bohlender, D.A., Morrison, N.D., Blake, M., Pych, W., 2014. CIR modulation of the X-ray flux from the O7.5 III(n)((f)) star ξ Persei. MNRAS 441, 2173–2180. https://doi.org/10.1093/mnras/stu565.

Massi, M., Migliari, S., Chernyakova, M., 2017. The black hole candidate LS I +61° 0303. MNRAS 468, 3689–3693. https://doi.org/10.1093/mnras/stx778.

Massi, M., Torricelli-Ciamponi, G., 2016. Origin of the long-term modulation of radio emission in LS I +61° 303. A&A 585, A123. https://doi.org/10.1051/0004-6361/201526938.

Matt, G., Guainazzi, M., 2003. The properties of the absorbing and line-emitting material in IGR J16318 - 4848. MNRAS 341, L13–L17. https://doi.org/10.1046/j.1365-8711.2003.06658.x.

McBride, V.A., Coe, M.J., Bird, A.J., Dean, A.J., Hill, A.B., McGowan, K.E., Schurch, M.P.E., Udalski, A., Soszynski, I., Finger, M., Wilson, C.A., Corbet, R.H.D., Negueruela, I., 2007. INTEGRAL observations of the Small Magellanic Cloud. MNRAS 382 (2), 743–749. https://doi.org/10.1111/j.1365-2966.2007.12423.x.

McBride, V.A., Coe, M.J., Negueruela, I., Schurch, M.P.E., McGowan, K.E., 2008. Spectral distribution of Be/X-ray binaries in the Small Magellanic Cloud. MNRAS 388 (3), 1198–1204. https://doi.org/10.1111/j.1365-2966.2008.13410.x.

McClintock, J.E., Remillard, R.A., 2006. Black hole binaries. 39. Cambridge University Press, pp. 157–213.

McEnery, J., (AMEGO Collaboration), 2019. All-sky Medium Energy Gamma-ray Observatory: Exploring the Extreme Multimessenger Universe. arXiv e-prints. arXiv:1907.07558

Meszaros, P., Nagel, W., 1985. X-ray pulsar models. I. Angle-dependent cyclotron line formation and comptonization. ApJ 298, 147–160. https://doi.org/10.1086/163594.

Meszaros, P., Nagel, W., 1985. X-ray pulsar models. II. Comptonized spectra and pulse shapes. ApJ 299, 138–153. https://doi.org/10.1086/163687.

Meszaros, P., Riffert, H., 1988. Gravitational Light Bending near Neutron Stars. II. Accreting Pulsar Spectra as a Function of Phase. ApJ 327, 712. https://doi.org/10.1086/166227.

Mihara, T., Makishima, K., Nagase, F., 1998. Cyclotron line variability. Advances in Space Research 22 (7), 987–996. https://doi.org/10.1016/S0273-1177(98)00128-8.

Mihara, T., Makishima, K., Nagase, F., 2004. Luminosity-related Changes in the Cyclotron Resonance Structure of the Binary X-Ray Pulsar 4U 0115 + 63. ApJ 610 (1), 390–401. https://doi.org/10.1086/421543.

Mirabel, I.F., Rodrigues, I., Liu, Q.Z., 2004. A microquasar shot out from its birth place. A&A 422, L29–L32. https://doi.org/10.1051/0004-6361:200400016.

Mirzoyan, R., Mukherjee, R., 2017. TeV gamma-ray emission from PSR J2032 + 4127/MT91 213 at periastron. The Astronomer's Telegram 10971.

Molkov, S., Mowlavi, N., Goldwurm, A., Strong, A., Lund, N., Paul, J., Oosterbroek, T., 2003. IGR J16479-4514. The Astronomer's Telegram 176, 1.

Molkov, S.V., Cherepashchuk, A.M., Lutovinov, A.A., Revnivtsev, M.G., Postnov, K.A., Sunyaev, R.A., 2004. A Hard X-ray Survey of the Sagittarius Arm Tangent with the IBIS Telescope of the INTEGRAL Observatory: A Catalog of Sources. Astronomy Letters 30, 534–539. https://doi.org/10.1134/1.1784495.

Monageng, I.M., McBride, V.A., Coe, M.J., Steele, I.A., Reig, P., 2017. On the relationship between circumstellar disc size and X-ray outbursts in Be/X-ray binaries. MNRAS 464 (1), 572–585. https://doi.org/10.1093/mnras/stw2354.

Moritani, Y., Nogami, D., Okazaki, A.T., Imada, A., Kambe, E., Honda, S., Hashimoto, O., Ichikawa, K., 2011. Drastic Spectroscopic Variability of the Be/X-Ray Binary Ariel 0535 + 262/V725 Tau during and after the 2009 Giant Outburst. PASJ 63, 25–29. https://doi.org/10.1093/pasj/63.4.L25.

Moritani, Y., Nogami, D., Okazaki, A.T., Imada, A., Kambe, E., Honda, S., Hashimoto, O., Mizoguchi, S., Kanda, Y., Sadakane, K., Ichikawa, K., 2013. Precessing Warped Be Disk Triggering the Giant Outbursts in 2009 and 2011 in A0535 + 262/V725Tau. PASJ 65, 83. https://doi.org/10.1093/pasj/65.4.83.

Morris, D.C., Smith, R.K., Markwardt, C.B., Mushotzky, R.F., Tueller, J., Kallman, T.R., Dhuga, K.S., 2009. Suzaku Observations of Four Heavily Absorbed HMXBs. ApJ 699 (1), 892–901. https://doi.org/10.1088/0004-637X/699/1/892.

Motch, C., Pakull, M.W., Grisé, F., Soria, R., 2011. The supergiant optical counterpart of ULX P13 in NGC 7793. Astronomische Nachrichten 332 (4), 367. https://doi.org/10.1002/asna.201011501.

Mowlavi, N., Kreykenbohm, I., Shaw, S.E., Pottschmidt, K., Wilms, J., Rodriguez, J., Produit, N., Soldi, S., Larsson, S., Dubath, P., 2006. INTEGRAL observation of the high-mass X-ray transient V 0332 + 53 during the 2005 outburst decline. A&A 451 (1), 187–194. https://doi.org/10.1051/0004-6361:20054235.

Mullan, D.J., 1984. Corotating interaction regions in stellar winds. ApJ 283, 303–312. https://doi.org/10.1086/162307.

Müller, S., Ferrigno, C., Kühnel, M., Schönherr, G., Becker, P.A., Wolff, M.T., Hertel, D., Schwarm, F.W., Grinberg, V., Obst, M., 2013. No anticorrelation between cyclotron

line energy and X-ray flux in 4U 0115 + 634. A&A 551, A6. https://doi.org/10.1051/0004-6361/201220359.

Mushtukov, A.A., Suleimanov, V.F., Tsygankov, S.S., Poutanen, J., 2015. The critical accretion luminosity for magnetized neutron stars. MNRAS 447 (2), 1847–1856. https://doi.org/10.1093/mnras/stu2484.

Mushtukov, A.A., Tsygankov, S.S., Serber, A.e.V., Suleimanov, V.F., Poutanen, J., 2015. Positive correlation between the cyclotron line energy and luminosity in sub-critical X-ray pulsars: Doppler effect in the accretion channel. MNRAS 454 (3), 2714–2721. https://doi.org/10.1093/mnras/stv2182.

Mushtukov, A.A., Verhagen, P.A., Tsygankov, S.S., van der Klis, M., Lutovinov, A.A., Larchenkova, T.I., 2018. On the radiation beaming of bright X-ray pulsars and constraints on neutron star mass-radius relation. MNRAS 474 (4), 5425–5436. https://doi.org/10.1093/mnras/stx2905.

Nabizadeh, A., Mönkkönen, J., Tsygankov, S.S., Doroshenko, V., Molkov, S.V., Poutanen, J., 2019. NuSTAR observations of wind-fed X-ray pulsar GX 301-2 during unusual spin-up event. A&A 629, A101. https://doi.org/10.1051/0004-6361/201936045.

Nakajima, M., Mihara, T., Makishima, K., Niko, H., 2006. Study of the luminosity-dependent cyclotron resonance energies of the binary X-ray pulsar 4U 0115 + 63 with RXTE. Advances in Space Research 38 (12), 2756–2758. https://doi.org/10.1016/j.asr.2005.09.049.

Nandra, K., (Athena Collaboration), 2013. The Hot and Energetic Universe: A White Paper presenting the science theme motivating the Athena + mission. arXiv e-prints. arXiv:1306.2307

Nazé, Y., Oskinova, L.M., Gosset, E., 2013. A Detailed X-Ray Investigation of ζ Puppis. II. The Variability on Short and Long Timescales. ApJ 763, 143. https://doi.org/10.1088/0004-637X/763/2/143.

Negueruela, I., Okazaki, A.T., Fabregat, J., Coe, M.J., Munari, U., Tomov, T., 2001. The Be/X-ray transient 4U 0115 + 63/V635 Cassiopeiae. II. Outburst mechanisms. A&A 369, 117–131. https://doi.org/10.1051/0004-6361:20010077.

Negueruela, I., Schurch, M.P.E., 2007. A search for counterparts to massive X-ray binaries using photometric catalogues. A&A 461, 631–639. https://doi.org/10.1051/0004-6361:20066054.

Negueruela, I., Smith, D.M., Chaty, S., 2005. Optical counterpart to IGR J16465-4507. The Astronomer's Telegram 429, 1.

Negueruela, I., Smith, D.M., Harrison, T.E., Torrejón, J.M., 2006. The Optical Counterpart to the Peculiar X-Ray Transient XTE J1739-302. ApJ 638, 982–986.

Negueruela, I., Smith, D.M., Reig, P., Chaty, S., Torrejón, J.M., 2006. Supergiant Fast X-ray Transients: a new class of high mass X-ray binaries unveiled by INTEGRAL. In: Wilson, A. (Ed.), ESA Special Publication. 604. pp. 165–170.

Nespoli, E., Fabregat, J., Mennickent, R.E., 2008. Unveiling the nature of six HMXBs through IR spectroscopy. A&A 486, 911–917. https://doi.org/10.1051/0004-6361:200809645.

Nespoli, E., Fabregat, J., Mennickent, R.E., 2010. Unveiling the nature of IGR J16493-4348 with IR spectroscopy. A&A 516, A106. https://doi.org/10.1051/0004-6361/201014348.

Nichelli, E., Israel, G.L., Moretti, A., Campana, S., Göz, D., Stella, L., 2011. Swift discovery of 328s coherent pulsations from the HMXB IGR J17200-3116. The Astronomer's Telegram 3205, 1.

Nishimura, O., 2008. Formation Mechanism for Broad and Shallow Profiles of Cyclotron Lines in Accreting X-Ray Pulsars. ApJ 672, 1127–1136. https://doi.org/10.1086/523782.

Nösel, S., Sharma, R., Massi, M., Cimò, G., Chernyakova, M., 2018. Hour time-scale QPOs in the X-ray and radio emission of LS I +61 303. MNRAS 476 (2), 2516–2521. https://doi.org/10.1093/mnras/sty417.

Nowak, M.A., Hanke, M., Trowbridge, S.N., Markoff, S.B., Wilms, J., Pottschmidt, K., Coppi, P., Maitra, D., Davis, J.E., Tramper, F., 2011. Corona, Jet, and Relativistic Line Models for Suzaku/RXTE/Chandra-HETG Observations of the Cygnus X-1 Hard State. ApJ 728, 13. https://doi.org/10.1088/0004-637X/728/1/13.

Nowak, M.A., Paizis, A., Rodriguez, J., Chaty, S., Del Santo, M., Grinberg, V., Wilms, J., Ubertini, P., Chini, R., 2012. X-Ray and Near-infrared Observations of the Obscured Accreting Pulsar IGR J18179-1621. ApJ 757, 143. https://doi.org/10.1088/0004-637X/757/2/143.

Ögelman, H., Beuermann, K.P., Kanbach, G., Mayer-Hasselwander, H.A., Capozzi, D., Fiordilino, E., Molteni, D., 1977. Increase in the pulsational period of 3U 0900-40. A&A 58, 385–388.

Ogilvie, G.I., Dubus, G., 2001. Precessing warped accretion discs in X-ray binaries. MNRAS 320 (4), 485–503. https://doi.org/10.1046/j.1365-8711.2001.04011.x.

Okazaki, A.T., Bate, M.R., Ogilvie, G.I., Pringle, J.E., 2002. Viscous effects on the interaction between the coplanar decretion disc and the neutron star in Be/X-ray binaries. MNRAS 337, 967–980. https://doi.org/10.1046/j.1365-8711.2002.05960.x.

Okazaki, A.T., Hayasaki, K., Moritani, Y., 2013. Origin of Two Types of X-ray Outbursts in Be/X-Ray Binaries. I. Accretion Scenarios. PASJ 65, 41. https://doi.org/10.1093/pasj/65.2.41.

Okazaki, A.T., Negueruela, I., 2001. A natural explanation for periodic X-ray outbursts in Be/X-ray binaries. A&A 377, 161–174. https://doi.org/10.1051/0004-6361:20011083.

Oskinova, L.M., Clarke, D., Pollock, A.M.T., 2001. Rotationally modulated X-ray emission from the single O star ζ Ophiuchi. A&A 378, L21–L24. https://doi.org/10.1051/0004-6361:20011222.

Owocki, S.P., Castor, J.I., Rybicki, G.B., 1988. Time-dependent models of radiatively driven stellar winds. I - Nonlinear evolution of instabilities for a pure absorption model. ApJ 335, 914–930. https://doi.org/10.1086/166977.

Owocki, S.P., Rybicki, G.B., 1984. Instabilities in line-driven stellar winds. I. Dependence on perturbation wavelength. ApJ 284, 337–350. https://doi.org/10.1086/162412.

Paizis, A., Nowak, M.A., Wilms, J., Chaty, S., Corbel, S., Rodriguez, J., Del Santo, M., Ubertini, P., Chini, R., 2011. Unveiling the Nature of IGR J17177-3656 with X-Ray, Near-infrared, and Radio Observations. ApJ 738, 183. https://doi.org/10.1088/0004-637X/738/2/183.

Paizis, A., Sidoli, L., 2014. Cumulative luminosity distributions of supergiant fast X-ray transients in hard X-rays. MNRAS 439, 3439–3452. https://doi.org/10.1093/mnras/stu191.

Papitto, A., Torres, D.F., Rea, N., 2012. Possible Changes of State and Relevant Timescales for a Neutron Star in LS I + 61 303. ApJ 756 (2), 188. https://doi.org/10.1088/0004-637X/756/2/188.

Paredes, J.M., Ribó, M., Bosch-Ramon, V., West, J.R., Butt, Y.M., Torres, D.F., Martí, J., 2007. Chandra Observations of the Gamma-Ray Binary LS I + 61 303: Extended X-Ray Structure? ApJ 664 (1), L39–L42. https://doi.org/10.1086/520674.

Paredes-Fortuny, X., Ribó, M., Bosch-Ramon, V., Casares, J., Fors, O., Núñez, J., 2015. Evidence of coupling between the thermal and nonthermal emission in the gamma-ray binary LS I +61° 303. A&A 575, L6. https://doi.org/10.1051/0004-6361/201425361.

Patel, S.K., Kouveliotou, C., Tennant, A., Woods, P.M., King, A., Finger, M.H., Ubertini, P., Winkler, C., Courvoisier, T.J.-L., van der Klis, M., Wachter, S., Gaensler, B.M., Phillips, C.J., 2004. The Peculiar X-Ray Transient IGR J16358-4726. ApJ 602, L45–L48. https://doi.org/10.1086/382210.

Paul, B., Naik, S., 2011. Transient High Mass X-ray Binaries. Bulletin of the Astronomical Society of India 39, 429–449.

Pavan, L., Bozzo, E., Ferrigno, C., Ricci, C., Manousakis, A., Walter, R., Stella, L., 2011. AX J1910.7 + 0917 and three newly discovered INTEGRAL sources. A&A 526, A122. https://doi.org/10.1051/0004-6361/201015561.

Pavan, L., Terrier, R., Ferrigno, C., Bozzo, E., Mereghetti, S., Paizis, A., Ducci, L., Gotz, D., Bazzano, A., Fiocchi, M., De Rosa, A., Tarana, A., Del Santo, M., Natalucci, L., Panessa, F., Capitanio, F., Sguera, V., Bianchin, V., Watanabe, K., Kuiper, L., Barragan, L., Chenevez, J., Caballero, I., Shrader, C., Bird, A., Puehlhofer, G., Sanchez-Fernand ez, C., Skinner, G., den Hartog, P.R., Pottschmidt, K., Negueruela, I., Prat, L., 2010. INTEGRAL discovery of a new transient source: IGR J16374-5043. The Astronomer's Telegram 2809, 1.

Pellizza, L.J., Chaty, S., Chisari, N.E., 2011. Unveiling the nature of IGR J16283-4838. A&A 526, A15. https://doi.org/10.1051/0004-6361/201014954.

Pellizza, L.J., Chaty, S., Negueruela, I., 2006. IGR J17544-2619: a new supergiant fast X-ray transient revealed by optical/infrared observations. A&A 455, 653–658.

Persi, P., Fiocchi, M., Tapia, M., Roth, M., Bazzano, A., Ubertini, P., Parisi, P., 2015. On the Near-infrared Identification of the INTEGRAL Source IGR J16328-4726. AJ 150 (1), 21. https://doi.org/10.1088/0004-6256/150/1/21.

Pflamm-Altenburg, J., Kroupa, P., 2010. The two-step ejection of massive stars and the issue of their formation in isolation. MNRAS 404, 1564–1568. https://doi.org/10.1111/j.1365-2966.2010.16376.x.

Pietrzyński, G., Graczyk, D., Gallenne, A., Gieren, W., Thompson, I.B., Pilecki, B., Karczmarek, P., Górski, M., Suchomska, K., Taormina, M., Zgirski, B., Wielgórski, P., Kołaczkowski, Z., Konorski, P., Villanova, S., Nardetto, N., Kervella, P., Bresolin, F., Kudritzki, R.P., Storm, J., Smolec, R., Narloch, W., 2019. A distance to the Large Magellanic Cloud that is precise to one per cent. Nature 567 (7747), 200–203. https://doi.org/10.1038/s41586-019-0999-4.

Poeckert, R., Bastien, P., Landstreet, J.D., 1979. Intrinsic polarization of Be stars. AJ 84, 812–830. https://doi.org/10.1086/112484.

Porter, J.M., 1998. On the warping of Be star discs. A&A 336, 966–971.

Postnov, K., Kuranov, A., Yungelson, L., 2018. X-ray binaries with neutron stars at different accretion stages. arXiv e-prints.

Postnov, K., Oskinova, L., Torrejón, J.M., 2017. A propelling neutron star in the enigmatic Be-star γ Cassiopeia. MNRAS 465, L119–L123. https://doi.org/10.1093/mnrasl/slw223.

Postnov, K., Oskinova, L., Torrejón, J.M., 2017. Low-luminosity stellar wind accretion onto neutron stars in HMXBs. arXiv e-prints.

Postnov, K.A., 2003. The Universal Luminosity Function of Binary X-ray Sources in Galaxies. Astronomy Letters 29, 372–373. https://doi.org/10.1134/1.1579783.

Poutanen, J., Mushtukov, A.A., Suleimanov, V.F., Tsygankov, S.S., Nagirner, D.I., Doroshenko, V., Lutovinov, A.e.A., 2013. A Reflection Model for the Cyclotron Lines in the Spectra of X-Ray Pulsars. ApJ 777 (2), 115. https://doi.org/10.1088/0004-637X/777/2/115.

Poveda, A., Ruiz, J., Allen, C., 1967. Run-away Stars as the Result of the Gravitational Collapse of Proto-stellar Clusters. Boletin de los Observatorios Tonantzintla y Tacubaya 4, 86–90.

Pradhan, P., Bozzo, E., Paul, B., 2018. Supergiant fast X-ray transients versus classical supergiant high mass X-ray binaries: Does the difference lie in the companion wind? A&A 610, A50. https://doi.org/10.1051/0004-6361/201731487.

Pradhan, P., Bozzo, E., Paul, B., Manousakis, A., Ferrigno, C., 2019. Probing clumpy wind accretion in IGR J18027-2016 with XMM-Newton. arXiv e-prints.

Pradhan, P., Maitra, C., Paul, B., Paul, B.C., 2013. Revisiting SW J2000.6 + 3210: a persistent Be X-ray pulsar? MNRAS 436 (2), 945–952. https://doi.org/10.1093/mnras/stt1504.

Pringle, J.E., 1996. Self-induced warping of accretion discs. MNRAS 281 (1), 357–361. https://doi.org/10.1093/mnras/281.1.357.

Pringle, J.E., Rees, M.J., 1972. Accretion disk models for compact x-ray sources. A&A 21, 1–9.

Produit, N., Ballet, J., Mowlavi, N., 2004. New gamma-ray transient, IGR J11305-6256 discovered by INTEGRAL. The Astronomer's Telegram 278, 1.

Puls, J., Vink, J.S., Najarro, F., 2008. Mass loss from hot massive stars. A&A Rev. 16 (3-4), 209–325. https://doi.org/10.1007/s00159-008-0015-8.

Quast, M., Langer, N., Tauris, T.M., 2019. Mass transfer on a nuclear timescale in models of supergiant and ultra-luminous X-ray binaries. A&A 628, A19. https://doi.org/10.1051/0004-6361/201935453.

Quirrenbach, A., Bjorkman, K.S., Bjorkman, J.E., Hummel, C.A., Buscher, D.F.,

Armstrong, J.T., Mozurkewich, D., Elias, N.M.I., Babler, B.L., 1997. Constraints on the Geometry of Circumstellar Envelopes: Optical Interferometric and Spectropolarimetric Observations of Seven Be Stars. ApJ 479 (1), 477–496. https://doi.org/10.1086/303854.

Rahoui, F., Chaty, S., Lagage, P.O., Pantin, E., 2008. Multi-wavelength observations of Galactic hard X-ray sources discovered by INTEGRAL. II. The environment of the companion star. A&A 484 (3), 801–813. https://doi.org/10.1051/0004-6361/20078774.

Rampy, R.A., Smith, D.M., Negueruela, I., 2009. IGR J17544—2619 in Depth With Suzaku: Direct Evidence for Clumpy Winds in a Supergiant Fast X-ray Transient. ApJ 707, 243–249. https://doi.org/10.1088/0004-637X/707/1/243.

Rappaport, S.A., Joss, P.C., 1983. X-ray pulsars in massive binary systems. In: Lewin, W.H.G., van den Heuvel, E.P.J. (Eds.), Accretion-Driven Stellar X-ray Sources, pp. 1–39.

Ray, P.S., (STROBE-X Collaboration), 2019. STROBE-X: X-ray Timing and Spectroscopy on Dynamical Timescales from Microseconds to Years. arXiv e-prints.

Rea, N., Torres, D.F., van der Klis, M., Jonker, P.G., Méndez, M., Sierpowska-Bartosik, A., 2010. Deep Chandra observations of TeV binaries - I. LSI+61˚303. MNRAS 405 (4), 2206–2214. https://doi.org/10.1111/j.1365-2966.2010.16642.x.

Reig, P., 2007. On the neutron star-disc interaction in Be/X-ray binaries. MNRAS 377, 867–873. https://doi.org/10.1111/j.1365-2966.2007.11657.x.

Reig, P., 2011. Be/X-ray binaries. Ap&SS 332, 1–29. https://doi.org/10.1007/s10509-010-0575-8.

Reig, P., Blinov, D., 2018. Warped disks during type II outbursts in Be/X-ray binaries: evidence from optical polarimetry. A&A 619, A19. https://doi.org/10.1051/0004-6361/201833649.

Reig, P., Fabregat, J., Coe, M.J., 1997. A new correlation for Be/X-ray binaries: the orbital period-Hα equivalent width diagram. A&A 322, 193–196.

Reig, P., Larionov, V., Negueruela, I., Arkharov, A.A., Kudryavtseva, N.A., 2007. The Be/X-ray transient 4U 0115+63/V635 Cassiopeiae. III. Quasi-cyclic variability. A&A 462, 1081–1089. https://doi.org/10.1051/0004-6361/20066217.

Reig, P., Negueruela, I., Papamastorakis, G., Manousakis, A., Kougentakis, T., 2005. Identification of the optical counterparts of high-mass X-ray binaries through optical photometry and spectroscopy. A&A 440 (2), 637–646. https://doi.org/10.1051/0004-6361:20052684.

Reig, P., Nersesian, A., Zezas, A., Gkouvelis, L., Coe, M.J., 2016. Long-term optical variability of high-mass X-ray binaries. II. Spectroscopy. A&A 590, A122. https://doi.org/10.1051/0004-6361/201628271.

Reig, P., Roche, P., 1999. Discovery of two new persistent Be/X-ray pulsar systems. MNRAS 306 (1), 100–106. https://doi.org/10.1046/j.1365-8711.1999.02473.x.

Reig, P., Zezas, A., 2014. Disc-loss episode in the Be shell optical counterpart to the high-mass X-ray binary IGR J21343+4738. A&A 561, A137. https://doi.org/10.1051/0004-6361/201321408.

Reig, P., Zezas, A., 2014. Discovery of X-ray pulsations in the Be/X-ray binary IGR J21343+4738. MNRAS 442 (1), 472–478. https://doi.org/10.1093/mnras/stu898.

Reig, P., Zezas, A., 2018. Discovery of X-ray pulsations in the Be/X-ray binary IGR J06074+2205. A&A 613, A52. https://doi.org/10.1051/0004-6361/201732533.

Revnivtsev, M., Churazov, E., Postnov, K., Tsygankov, S., 2009. Quenching of the strong aperiodic accretion disk variability at the magnetospheric boundary. A&A 507, 1211–1215. https://doi.org/10.1051/0004-6361/200912317.

Revnivtsev, M., Tuerler, M., Del Santo, M., Westergaard, N.J., Gehrels, N., Winkler, C., 2003. IGR J16358-4726. IAU Circ. 8097, 2.

Revnivtsev, M.G., Sunyaev, R.A., Varshalovich, D.A., Zheleznyakov, V.V., Cherepashchuk, A.M., Lutovinov, A.A., Churazov, E.M., Grebenev, S.A., Gilfanov, M.R., 2004. A Hard X-ray Survey of the Galactic-Center Region with the IBIS Telescope of the INTEGRAL Observatory: A Catalog of Sources. Astronomy Letters 30, 382–389. https://doi.org/10.1134/1.1764884.

Ribó, M., Paredes, J.M., Romero, G.E., Benaglia, P., Martí, J., Fors, O., García-Sánchez, J., 2002. <ASTROBJ>LS 5039</ASTROBJ>: A runaway microquasar ejected from the galactic plane. A&A 384, 954–964. https://doi.org/10.1051/0004-6361:20020093.

Ricci, C., Soldi, S., Beckmann, V., Miller, J.M., Caballero-Garcia, M.D., Kuulkers, E., 2008. IGR J17375-3022: a new hard X-ray transient detected by INTEGRAL. The Astronomer's Telegram 1781, 1.

Riffert, H., Klingler, M., Ruder, H., 1999. Bremsstrahlung Emissivity of a Proton-Electron Plasma in a Strong Magnetic Field. Phys. Rev. Lett. 82 (17), 3432–3435. https://doi.org/10.1103/PhysRevLett.82.3432.

Riffert, H., Meszaros, P., 1988. Gravitational Light Bending near Neutron Stars. I. Emission from Columns and Hot Spots. ApJ 325, 207. https://doi.org/10.1086/165996.

Rodes-Roca, J.J., Bernabeu, G., Magazzù, A., Torrejón, J.M., Solano, E., 2018. IGR J19294+1816: a new Be-X-ray binary revealed through infrared spectroscopy. MNRAS 476, 2110–2116. https://doi.org/10.1093/mnras/sty333.

Rodes-Roca, J.J., Torrejón, J.M., Martínez-Núñez, S., Bernabéu, G., Magazzú, A., 2013. Infrared identification of 2XMM J191043.4+091629.4. A&A 555, A115. https://doi.org/10.1051/0004-6361/201321923.

Rodriguez, J., Bodaghee, A., Kaaret, P., Tomsick, J.A., Kuulkers, E., Malaguti, G., Petrucci, P.-O., Cabanac, C., Chernyakova, M., Corbel, S., Deluit, S., Di Cocco, G., Ebisawa, K., Goldwurm, A., Henri, G., Lebrun, F., Paizis, A., Walter, R., Foschini, L., 2006. INTEGRAL and XMM-Newton observations of the X-ray pulsar IGR J16320-4751/AX J1631.9-4752. MNRAS 366, 274–282. https://doi.org/10.1111/j.1365-2966.2005.09855.x.

Rodriguez, J., Garau, A.D., Grebenev, S., Parmard, A., Roques, J.P., Schonfelder, V., Ubertini, P., Walter, R., Westergaard, N.J., 2004. INTEGRAL discovery of a possible new source IGR J18410-0535. The Astronomer's Telegram 340, 1.

Rodriguez, J., Grinberg, V., Laurent, P., Cadolle Bel, M., Pottschmidt, K., Pooley, G.,

Bodaghee, A., Wilms, J., Gouiffès, C., 2015. Spectral State Dependence of the 0.4-2 MeV Polarized Emission in Cygnus X-1 Seen with INTEGRAL/IBIS, and Links with the AMI Radio Data. ApJ 807, 17. https://doi.org/10.1088/0004-637X/807/1/17.

Rodriguez, J., Paizis, A., 2005. Possible infra-red counterpart to IGR J16283-4838. The Astronomer's Telegram 460.

Rodriguez, J., Tomsick, J.A., Chaty, S., 2009. Swift follow-up observations of 17 INTEGRAL sources of uncertain or unknown nature. A&A 494, 417–428. https://doi.org/10.1051/0004-6361:200810773.

Rodriguez, J., Tomsick, J.A., Foschini, L., Walter, R., Goldwurm, A., Corbel, S., Kaaret, P., 2003. An XMM-Newton observation of IGR J16320-4751 = AX J1631.9-4752. A&A 407, L41–L45. https://doi.org/10.1051/0004-6361:20031093.

Romano, P., 2015. Seven years with the Swift Supergiant Fast X-ray Transients project. Journal of High Energy Astrophysics 7, 126–136. https://doi.org/10.1016/j.jheap.2015.04.008.

Romano, P., Bozzo, E., Esposito, P., Sbarufatti, B., Haberl, F., Ponti, G., D'Avanzo, P., Ducci, L., Segreto, A., Jin, C., Masetti, N., Del Santo, M., Campana, S., Mangano, V., 2016. Searching for supergiant fast X-ray transients with Swift. A&A 593, A96. https://doi.org/10.1051/0004-6361/201628808.

Romano, P., Bozzo, E., Mangano, V., Esposito, P., Israel, G., Tiengo, A., Campana, S., Ducci, L., Ferrigno, C., Kennea, J.A., 2015. Giant outburst from the supergiant fast X-ray transient IGR J17544-2619: accretion from a transient disc? A&A 576, L4. https://doi.org/10.1051/0004-6361/201525749.

Romano, P., Ducci, L., Mangano, V., Esposito, P., Bozzo, E., Vercellone, S., 2014. Soft X-ray characterisation of the long-term properties of supergiant fast X-ray transients. A&A 568, A55. https://doi.org/10.1051/0004-6361/201423867.

Romano, P., Krimm, H.A., Palmer, D.M., Ducci, L., Esposito, P., Vercellone, S., Evans, P.A., Guidorzi, C., Mangano, V., Kennea, J.A., Barthelmy, S.D., Burrows, D.N., Gehrels, N., 2014. The 100-month Swift catalogue of supergiant fast X-ray transients. I. BAT on-board and transient monitor flares. A&A 562, A2. https://doi.org/10.1051/0004-6361/201322516.

Romano, P., Sidoli, L., Cusumano, G., La Parola, V., Vercellone, S., Pagani, C., Ducci, L., Mangano, V., Cummings, J., Krimm, H.A., Guidorzi, C., Kennea, J.A., Hoversten, E.A., Burrows, D.N., Gehrels, N., 2009. Monitoring supergiant fast X-ray transients with Swift: results from the first year. MNRAS 399 (4), 2021–2032. https://doi.org/10.1111/j.1365-2966.2009.15356.x.

Romano, P., Sidoli, L., Cusumano, G., Vercellone, S., Mangano, V., Krimm, H.A., 2009. Disentangling the System Geometry of the Supergiant Fast X-Ray Transient IGR J11215—-5952 with Swift. ApJ 696, 2068–2074. https://doi.org/10.1088/0004-637X/696/2/2068.

Romano, P., Sidoli, L., Mangano, V., Mereghetti, S., Cusumano, G., 2007. Swift/XRT observes the fifth outburst of the periodic supergiant fast X-ray transient IGR J11215-5952. A&A 469, L5–L8. https://doi.org/10.1051/0004-6361:20077383.

Romano, P., Sidoli, L., Mangano, V., Vercellone, S., Kennea, J.A., Cusumano, G., Krimm, H.A., Burrows, D.N., Gehrels, N., 2008. Monitoring Supergiant Fast X-Ray Transients with Swift. II. Rise to the Outburst in IGR J16479-4514. ApJ 680, L137. https://doi.org/10.1086/590082.

Russeil, D., 2003. Star-forming complexes and the spiral structure of our Galaxy. A&A 397, 133–146. https://doi.org/10.1051/0004-6361:20021504.

Saha, L., Chitnis, V.R., Shukla, A., Rao, A.R., Acharya, B.S., 2016. The Multi-wavelength Characteristics of the TeV Binary LS I +61 303. ApJ 823, 134. https://doi.org/10.3847/0004-637X/823/2/134.

Sakano, M., Koyama, K., Murakami, H., Maeda, Y., Yamauchi, S., 2002. ASCA X-Ray Source Catalog in the Galactic Center Region. ApJS 138 (1), 19–34. https://doi.org/10.1086/324020.

Sander, A.A.C., Fürst, F., Kretschmar, P., Oskinova, L.M., Todt, H., Hainich, R., Shenar, T., Hamann, W.R., 2018. Coupling hydrodynamics with comoving frame radiative transfer. II. Stellar wind stratification in the high-mass X-ray binary Vela X-1. A&A 610, A60. https://doi.org/10.1051/0004-6361/201731575.

Sanjurjo-Ferrín, G., Torrejón, J.M., Postnov, K., Oskinova, L., Rodes-Roca, J.J., Bernabeu, G., 2017. XMM-Newton spectroscopy of the accreting magnetar candidate 4U0114+65. A&A 606, A145. https://doi.org/10.1051/0004-6361/201630119.

Santangelo, A., Zane, S., Feng, H., Xu, R., Doroshenko, V., Bozzo, E., Caiazzo, I., Zelati, F.C., Esposito, P., González-Caniulef, D., Heyl, J., Huppenkothen, D., Israel, G., Li, Z., Lin, L., Mignani, R., Rea, N., Orlandini, M., Taverna, R., Tong, H., Turolla, R., Baglio, C., Bernardini, F., Bucciantini, N., Feroci, M., Fürst, F., Göğüş, E., Güngör, C., Ji, L., Lu, F., Manousakis, A., Mereghetti, S., Mikusincova, R., Paul, B., Prescod-Weinstein, C., Younes, G., Tiengo, A., Xu, Y., Watts, A., Zhang, S., Zhan, S.-N., 2019. Physics and astrophysics of strong magnetic field systems with eXTP. Science China Physics, Mechanics, and Astronomy 62, 29505. https://doi.org/10.1007/s11433-018-9234-3.

Savonije, G.J., 1978. Roche-lobe overflow in x-ray binaries. A&A 62, 317–338.

Savonije, J., 1983. Evolution and mass transfer in X-ray binaries. In: Lewin, W.H.G., van den Heuvel, E.P.J. (Eds.), Accretion-Driven Stellar X-ray Sources, pp. 343–366.

Sazonov, S., Churazov, E., Revnivtsev, M., Vikhlinin, A., Sunyaev, R., 2005. Identification of 8 INTEGRAL hard X-ray sources with Chandra. A&A 444 (2), L37–L40. https://doi.org/10.1051/0004-6361:200500205.

Sazonov, S., Paizis, A., Bazzano, A., Chelovekov, I., Khabibullin, I., Postnov, K., Mereminskiy, I., Fiocchi, M., Bélanger, G., Bird, A.J., Bozzo, E., Chenevez, J., Del Santo, M., Falanga, M., Farinelli, R., Ferrigno, C., Grebenev, S., Krivonos, R., Kuulkers, E., Lund, N., Sanchez-Fernand ez, C., Tarana, A., Ubertini, P., Wilms, J., 2020. The Galactic LMXB Population and the Galactic Centre Region. arXiv e-prints. arXiv:2006.05063

Sazonov, S.Y., Lutovinov, A.A., Krivonos, R.A., 2014. Cutoff in the hard X-ray spectra of the ultraluminous X-ray sources HolX X-1 and M82 X-1. Astronomy Letters 40 (2-3), 65–74. https://doi.org/10.1134/S1063773714030062.

Schaller, G., Schaerer, D., Meynet, G., Maeder, A., 1992. New grids of stellar models from 0.8 to 120 solar masses at Z = 0.020 and Z = 0.001. A&AS 96, 269–331.

Schmidtke, P.C., Cowley, A.P., 2013. Discovery of Optical Periods for IGR J00569-7226. The Astronomer's Telegram 5557, 1.

Schönherr, G., Wilms, J., Kretschmar, P., Kreykenbohm, I., Santangelo, A., Rothschild, R.E., Coburn, W., Staubert, R., 2007. A model for cyclotron resonance scattering features. A&A 472 (2), 353–365. https://doi.org/10.1051/0004-6361:20077218.

Schreier, E., Levinson, R., Gursky, H., Kellogg, E., Tananbaum, H., Giacconi, R., 1972. Evidence for the binary nature of centaurus x-3 from uhuru x-ray observations. ApJ 172, L79–L89.

Schwarm, F.W., Ballhausen, R., Falkner, S., Schönherr, G., Pottschmidt, K., Wolff, M.T., Becker, P.A., Fürst, F., Marcu-Cheatham, D.M., Hemphill, P.B., Sokolova-Lapa, E., Dauser, T., Klochkov, D., Ferrigno, C., Wilms, J., 2017. Cyclotron resonant scattering feature simulations. II. Description of the CRSF simulation process. A&A 601, A99. https://doi.org/10.1051/0004-6361/201630250.

Schwarm, F.W., Schönherr, G., Falkner, S., Pottschmidt, K., Wolff, M.T., Becker, P.A., Sokolova-Lapa, E., Klochkov, D., Ferrigno, C., Fürst, F., Hemphill, P.B., Marcu-Cheatham, D.M., Dauser, T., Wilms, J., 2017. Cyclotron resonant scattering feature simulations. I. Thermally averaged cyclotron scattering cross sections, mean free photon-path tables, and electron momentum sampling. A&A 597, A3. https://doi.org/10.1051/0004-6361/201629352.

Segreto, A., Cusumano, G., La Parola, V., D'Aì, A., Masetti, N., D'Avanzo, P., 2013. Swift discovery of the orbital period of the high mass X-ray binary IGR J015712-7259 in the Small Magellanic Cloud. A&A 557, A113. https://doi.org/10.1051/0004-6361/201321897.

Segreto, A., La Parola, V., Cusumano, G., D'Aì, A., Masetti, N., Campana, S., 2013. The 54-day orbital period of AX J1820.5-1434 unveiled by Swift. A&A 558, A99. https://doi.org/10.1051/0004-6361/201321892.

Sguera, V., 2009. Hard fast X-ray transients as possible counterparts of unidentified MeV/TeV sources. arXiv e-prints.

Sguera, V., Barlow, E.J., Bird, A.J., Clark, D.J., Dean, A.J., Hill, A.B., Moran, L., Shaw, S.E., Willis, D.R., Bazzano, A., Ubertini, P., Malizia, A., 2005. INTEGRAL observations of recurrent fast X-ray transient sources. A&A 444, 221–231. https://doi.org/10.1051/0004-6361:20053103.

Sguera, V., Bazzano, A., Bird, A.J., Dean, A.J., Ubertini, P., Barlow, E.J., Bassani, L., Clark, D.J., Hill, A.B., Malizia, A., Molina, M., Stephen, J.B., 2006. Unveiling Supergiant Fast X-Ray Transient Sources with INTEGRAL. ApJ 646, 452–463. https://doi.org/10.1086/504827.

Sguera, V., Bird, A.J., Dean, A.J., Ubertini, P., Landi, R., Malizia, A., Barlow, E.J., Clark, D.J., Hill, A.B., Molina, M., 2007. INTEGRAL and Swift observations of the supergiant fast X-ray transient AX J1845.0-0433 = IGR J18450-0435. A&A 462 (2), 695–698. https://doi.org/10.1051/0004-6361:20066210.

Sguera, V., Drave, S.P., Bird, A.J., Bazzano, A., Landi, R., Ubertini, P., 2011. IGR J17354-3255 as a candidate intermediate supergiant fast X-ray transient possibly associated with the transient MeV AGL J1734-3310. MNRAS 417, 573–579. https://doi.org/10.1111/j.1365-2966.2011.19298.x.

Sguera, V., Drave, S.P., Sidoli, L., Masetti, N., Landi, R., Bird, A.J., Bazzano, A., 2013. X-ray, optical, and infrared investigation of the candidate supergiant fast X-ray transient IGR J18462 - 0223. A&A 556, A27. https://doi.org/10.1051/0004-6361/201220785.

Sguera, V., Ducci, L., Sidoli, L., Bazzano, A., Bassani, L., 2010. XMM-Newton and INTEGRAL study of the SFXT IGR J18483-0311 in quiescence: hint of a cyclotron emission feature? MNRAS 402, L49–L53. https://doi.org/10.1111/j.1745-3933.2009.00798.x.

Sguera, V., Hill, A.B., Bird, A.J., Dean, A.J., Bazzano, A., Ubertini, P., Masetti, N., Landi, R., Malizia, A., Clark, D.J., Molina, M., 2007. IGR J18483-0311: an accreting X-ray pulsar observed by INTEGRAL. A&A 467, 249–257. https://doi.org/10.1051/0004-6361:20066762.

Sguera, V., Romero, G.E., Bazzano, A., Masetti, N., Bird, A.J., Bassani, L., 2009. Dissecting the Region of 3EG J1837-0423 and HESS J1841-055 with INTEGRAL. ApJ 697, 1194–1205. https://doi.org/10.1088/0004-637X/697/2/1194.

Sguera, V., Sidoli, L., Bird, A.J., Paizis, A., Bazzano, A., 2020. Chasing candidate Supergiant Fast X-ray Transients in the 1000 orbits INTEGRAL/IBIS catalogue. MNRAS 491 (3), 4543–4553. https://doi.org/10.1093/mnras/stz3330.

Sguera, V., Sidoli, L., Paizis, A., Masetti, N., Bird, A.J., Bazzano, A., 2017. First hard X-ray detection and broad-band X-ray study of the unidentified transient AX J1949.8 + 2534. MNRAS 469, 3901–3908. https://doi.org/10.1093/mnras/stx1111.

Shakura, N., Postnov, K., Hjalmarsdotter, L., 2013. On the nature of 'off' states in slowly rotating low-luminosity X-ray pulsars. MNRAS 428, 670–677. https://doi.org/10.1093/mnras/sts062.

Shakura, N., Postnov, K., Kochetkova, A., Hjalmarsdotter, L., 2012. Theory of quasi-spherical accretion in X-ray pulsars. MNRAS 420, 216–236. https://doi.org/10.1111/j.1365-2966.2011.20026.x.

Shakura, N., Postnov, K., Kochetkova, A., Hjalmarsdotter, L., 2018. Quasi-Spherical Subsonic Accretion onto Magnetized Neutron Stars. In: Shakura, N. (Ed.), Astrophysics and Space Science. Astrophysics and Space Science Library 454. pp. 331. https://doi.org/10.1007/978-3-319-93009-1_7.

Shakura, N., Postnov, K., Sidoli, L., Paizis, A., 2014. Bright flares in supergiant fast X-ray transients. MNRAS 442, 2325–2330. https://doi.org/10.1093/mnras/stu1027.

Shakura, N.I., Sunyaev, R.A., 1973. Black holes in binary systems. Observational appearance. A&A 24, 337–355.

Shaw, S.E., Chernyakova, M., Rodriguez, J., Walter, R., Kretschmar, P., Mereghetti, S., 2004. INTEGRAL observations of the PSR B1259-63/SS2883 system after the 2004 periastron passage. A&A 426, L33–L36. https://doi.org/10.1051/0004-6361:200400077.

Shklovskii, I.S., 1970. Possible Causes of the Secular Increase in Pulsar Periods. Soviet Ast. 13, 562.

Shtykovskiy, P., Gilfanov, M., 2005. High-mass X-ray binaries in the Small Magellanic

Cloud: the luminosity function. MNRAS 362 (3), 879–890. https://doi.org/10.1111/j.1365-2966.2005.09320.x.

Sidoli, L., Esposito, P., Ducci, L., 2010. The longest observation of a low-intensity state from a supergiant fast X-ray transient: Suzaku observes IGRJ08408-4503. MNRAS 409, 611–618. https://doi.org/10.1111/j.1365-2966.2010.17320.x.

Sidoli, L., Esposito, P., Motta, S.E., Israel, G.L., Rodríguez Castillo, G.A., 2016. XMM-Newton discovery of mHz quasi-periodic oscillations in the high-mass X-ray binary IGR J19140 + 0951. MNRAS 460 (4), 3637–3646. https://doi.org/10.1093/mnras/stw1246.

Sidoli, L., Israel, G.L., Esposito, P., Rodríguez Castillo, G.A., Postnov, K., 2017. AX J1910.7 + 0917: the slowest X-ray pulsar. MNRAS 469, 3056–3061. https://doi.org/10.1093/mnras/stx1105.

Sidoli, L., Mereghetti, S., Sguera, V., Pizzolato, F., 2012. The XMM-Newton view of supergiant fast X-ray transients: the case of IGR J16418-4532. MNRAS 420, 554–561. https://doi.org/10.1111/j.1365-2966.2011.20063.x.

Sidoli, L., Paizis, A., 2018. An INTEGRAL overview of High-Mass X-ray Binaries: classes or transitions? MNRAS 481, 2779–2803. https://doi.org/10.1093/mnras/sty2428.

Sidoli, L., Paizis, A., Mereghetti, S., 2006. IGR J11215-5952: a hard X-ray transient displaying recurrent outbursts. A&A 450, L9–L12. https://doi.org/10.1051/0004-6361:20064940.

Sidoli, L., Paizis, A., Postnov, K., 2016. INTEGRAL study of temporal properties of bright flares in Supergiant Fast X-ray Transients. MNRAS 457, 3693–3701. https://doi.org/10.1093/mnras/stw237.

Sidoli, L., Postnov, K., Tiengo, A., Esposito, P., Sguera, V., Paizis, A., Rodríguez Castillo, G.A., 2020. NuSTAR observation of the supergiant fast X-ray transient IGR J11215-5952 during its 2017 outburst. A&A 638, A71. https://doi.org/10.1051/0004-6361/202038078.

Sidoli, L., Postnov, K.A., Belfiore, A., Marelli, M., Salvetti, D., Salvaterra, R., De Luca, A., Esposito, P., 2019. Supergiant Fast X-ray Transients uncovered by the EXTraS project: flares reveal the development of magnetospheric instability in accreting neutron stars. arXiv e-prints (1905.00897).

Sidoli, L., Romano, P., Ducci, L., Paizis, A., Cusumano, G., Mangano, V., Krimm, H.A., Vercellone, S., Burrows, D.N., Kennea, J.A., Gehrels, N., 2009. Supergiant Fast X-ray Transients in outburst: new Swift observations of XTE J1739-302, IGR J17544-2619 and IGR J08408-4503. MNRAS 397, 1528–1538. https://doi.org/10.1111/j.1365-2966.2009.15049.x.

Sidoli, L., Romano, P., Mangano, V., Pellizzoni, A., Kennea, J.A., Cusumano, G., Vercellone, S., Paizis, A., Burrows, D.N., Gehrels, N., 2008. Monitoring Supergiant Fast X-ray Transients with Swift. I. Behavior outside outbursts. ApJ 687, 1230–1235.

Sidoli, L., Romano, P., Mereghetti, S., Paizis, A., Vercellone, S., Mangano, V., Götz, D., 2007. An alternative hypothesis for the outburst mechanism in supergiant fast X-ray transients: the case of IGR J11215-5952. A&A 476, 1307–1315. https://doi.org/10.1051/0004-6361:20078137.

Sidoli, L., Tiengo, A., Paizis, A., Sguera, V., Lotti, S., Natalucci, L., 2017. XMM-Newton and NuSTAR Simultaneous X-Ray Observations of IGR J11215-5952. ApJ 838, 133. https://doi.org/10.3847/1538-4357/aa671a.

Sierpowska-Bartosik, A., Torres, D.F., 2008. Pulsar wind zone processes in LS 5039. Astroparticle Physics 30 (5), 239–263. https://doi.org/10.1016/j.astropartphys.2008.09.009.

Sina, R., 1996. Ph.D. thesis. Univ. Maryland.

Smith, A., Kaaret, P., Holder, J., Falcone, A., Maier, G., Pandel, D., Stroh, M., 2009. Long-Term X-Ray Monitoring of the TeV Binary LS I + 61 303 With the Rossi X-Ray Timing Explorer. ApJ 693 (2), 1621–1627. https://doi.org/10.1088/0004-637X/693/2/1621.

Smith, D.M., 1997. XTE J1739-302. IAU Circ. 6757, 2.

Smith, D.M., Heindl, W.A., Markwardt, C.B., Swank, J.H., Negueruela, I., Harrison, T.E., Huss, L., 2006. XTE J1739-302 as a Supergiant Fast X-Ray Transient. ApJ 638, 974–981. https://doi.org/10.1086/498936.

Smith, D.M., Markwardt, C.B., Swank, J.H., Negueruela, I., 2012. Fast X-ray transients towards the Galactic bulge with the Rossi X-ray Timing Explorer. MNRAS 422, 2661–2674. https://doi.org/10.1111/j.1365-2966.2012.20836.x.

Soffitta, P., 2017. IXPE the Imaging X-ray Polarimetry Explorer. Proc. SPIE. Society of Photo-Optical Instrumentation Engineers (SPIE) Conference Series 10397. pp. 103970I. https://doi.org/10.1117/12.2275485.

Soldi, S., Brandt, S., Garau, A.D., Grebenev, S.A., Kuulkers, E., Palumbo, G.G.C., Tarana, A., 2005. Discovery of a new X-ray transient IGR J16283-4838 with INTEGRAL. The Astronomer's Telegram 456, 1.

Staubert, R., Klochkov, D., Fürst, F., Wilms, J., Rothschild, R.E., Harrison, F., 2017. Inversion of the decay of the cyclotron line energy in Hercules X-1. A&A 606, L13. https://doi.org/10.1051/0004-6361/201731927.

Staubert, R., Klochkov, D., Wilms, J., Postnov, K., Shakura, N.I., Rothschild, R.E., Fürst, F., Harrison, F.A., 2014. Long-term change in the cyclotron line energy in Hercules X-1. A&A 572, A119. https://doi.org/10.1051/0004-6361/201424203.

Staubert, R., Kreykenbohm, I., Kretschmar, P., Chernyakova, M., Pottschmidt, K., Benlloch-Garcia, S., Wilms, J., Santangelo, A., Segreto, A., von Kienlin, A., Sidoli, L., Larsson, S., Westergaard, N., 2004. INTEGRAL/IBIS Observations of VELA X-1 in a Flaring State. In: Schoenfelder, V., Lichti, G., Winkler, C. (Eds.), 5th INTEGRAL Workshop on the INTEGRAL Universe. ESA Special Publication 552. pp. 259.

Staubert, R., Shakura, N.I., Postnov, K., Wilms, J., Rothschild, R.E., Coburn, W., Rodina, L., Klochkov, D., 2007. Discovery of a flux-related change of the cyclotron line energy in Hercules X-1. A&A 465 (2), L25–L28. https://doi.org/10.1051/0004-6361:20077098.

Staubert, R., Trümper, J., Kendziorra, E., Klochkov, D., Postnov, K., Kretschmar, P., Pottschmidt, K., Haberl, F., Rothschild, R.E., Santangelo, A., 2019. Cyclotron lines in highly magnetized neutron stars. A&A 622, A61. https://doi.org/10.1051/0004-6361/201834479.

Steiner, C., Eckert, D., Mowlavi, N., Decourchelle, A., Vink, J., 2005. IGR J01583+6713, a new hard X-ray transient discovered by INTEGRAL. The Astronomer's Telegram 672, 1.

Stella, L., White, N.E., Rosner, R., 1986. Intermittent Stellar Wind Acceleration and the Long-Term Activity of Population I Binary Systems Containing an X-Ray Pulsar. ApJ 308, 669. https://doi.org/10.1086/164538.

Stratta, G., (THESEUS Collaboration), 2018. THESEUS: A key space mission concept for Multi-Messenger Astrophysics. Advances in Space Research 62, 662–682. https://doi.org/10.1016/j.asr.2018.04.013.

Sturm, R., Haberl, F., Pietsch, W., Immler, S., 2011. IGR J05414-6858 detected in X-ray outburst with SWIFT. The Astronomer's Telegram 3537, 1.

Sturm, R., Haberl, F., Rau, A., Bartlett, E.S., Zhang, X.L., Schady, P., Pietsch, W., Greiner, J., Coe, M.J., Udalski, A., 2012. Discovery of the neutron star spin and a possible orbital period from the Be/X-ray binary IGR J05414-6858 in the LMC. A&A 542, A109. https://doi.org/10.1051/0004-6361/201219093.

Sugizaki, M., Mihara, T., Nakajima, M., Makishima, K., 2017. Correlation between the luminosity and spin-period changes during outbursts of 12 Be binary pulsars observed by the MAXI/GSC and the Fermi/GBM. PASJ 69 (6), 100. https://doi.org/10.1093/pasj/psx119.

Sugizaki, M., Mitsuda, K., Kaneda, H., Matsuzaki, K., Yamauchi, S., Koyama, K., 2001. Faint X-Ray Sources Resolved in the ASCA Galactic Plane Survey and Their Contribution to the Galactic Ridge X-Ray Emission. ApJS 134, 77–102. https://doi.org/10.1086/320358.

Sundqvist, J.O., Owocki, S.P., 2013. Clumping in the inner winds of hot, massive stars from hydrodynamical line-driven instability simulations. MNRAS 428 (2), 1837–1844. https://doi.org/10.1093/mnras/sts165.

Sundqvist, J.O., Owocki, S.P., Puls, J., 2018. 2D wind clumping in hot, massive stars from hydrodynamical line-driven instability simulations using a pseudo-planar approach. A&A 611, A17. https://doi.org/10.1051/0004-6361/201731718.

Sunyaev, R., Lutovinov, A., Molkov, S., Deluit, S., 2003. Possible new source IGR J17391-3021 or an outburst from XTE J1739-302. The Astronomer's Telegram 181, 1.

Sunyaev, R.A., Grebenev, S.A., Lutovinov, A.A., Rodriguez, J., Mereghetti, S., Gotz, D., Courvoisier, T., 2003. New source IGR J17544-2619 discovered with INTEGRAL. The Astronomer's Telegram 190, 1.

Swank, J., Remillard, R., Smith, E., 2004. Transient Pulsar V0332+53 in Outburst. The Astronomer's Telegram 349, 1.

Swank, J.H., Smith, D.M., Markwardt, C.B., 2007. RXTE PCA Pointed Observations of IGR J11215-5952. The Astronomer's Telegram 999, 1.

Taam, R.E., Fryxell, B.A., 1988. On Nonsteady Accretion in Stellar Wind–fed X-Ray Sources. ApJ 327, L73. https://doi.org/10.1086/185143.

Taani, A., Karino, S., Song, L., Al-Wardat, M., Khasawneh, A., Mardini, M.K., 2019. On the possibility of disk-fed formation in supergiant high-mass X-ray binaries. Research in Astronomy and Astrophysics 19 (1), 012. https://doi.org/10.1088/1674-4527/19/1/12.

Tarter, C.B., Tucker, W.H., Salpeter, E.E., 1969. The Interaction of X-Ray Sources with Optically Thin Environments. ApJ 156, 943. https://doi.org/10.1086/150026.

Tauris, T.M., Kramer, M., Freire, P.C.C., Wex, N., Janka, H.T., Langer, N., Podsiadlowski, P., Bozzo, E., Chaty, S., Kruckow, M.U., van den Heuvel, E.P.J., Antoniadis, J., Breton, R.P., Champion, D.J., 2017. Formation of Double Neutron Star Systems. ApJ 846, 170. https://doi.org/10.3847/1538-4357/aa7e89.

Tawara, Y., Yamauchi, S., Awaki, H., Kii, T., Koyama, K., Nagase, F., 1989. Discovery of 413.9-second X-ray pulsation from X 1722-36. PASJ 41, 473–481.

Thompson, T.W.J., Tomsick, J.A., in 't Zand, J.J.M., Rothschild, R.E., Walter, R., 2007. The Orbit of the Eclipsing X-Ray Pulsar EXO 1722-363. ApJ 661 (1), 447–457. https://doi.org/10.1086/513458.

Thompson, T.W.J., Tomsick, J.A., Rothschild, R.E., in't Zand, J.J.M., Walter, R., 2006. Orbital Parameters for the X-Ray Pulsar IGR J16393-4643. ApJ 649 (1), 373–381. https://doi.org/10.1086/506251.

Tjemkes, S.A., van Paradijs, J., Zuiderwijk, E.J., 1986. Optical light curves of massive X-ray binaries. A&A 154, 77–91.

Tomsick, J.A., Chaty, S., Rodriguez, J., Foschini, L., Walter, R., Kaaret, P., 2006. Identifications of Four INTEGRAL Sources in the Galactic Plane via Chandra Localizations. ApJ 647, 1309–1322. https://doi.org/10.1086/505595.

Tomsick, J.A., Chaty, S., Rodriguez, J., Walter, R., Kaaret, P., 2006. IGR J06074+2205 is a Be X-ray Binary. The Astronomer's Telegram 959, 1.

Tomsick, J.A., Chaty, S., Rodriguez, J., Walter, R., Kaaret, P., 2008. Chandra Localizations and Spectra of INTEGRAL Sources in the Galactic Plane. ApJ 685, 1143–1156. https://doi.org/10.1086/591040.

Tomsick, J.A., Heinke, C., Halpern, J., Kaaret, P., Chaty, S., Rodriguez, J., Bodaghee, A., 2011. Confirmation of IGR J01363+6610 as a Be X-ray Binary with Very Low Quiescent X-ray Luminosity. ApJ 728 (2), 86. https://doi.org/10.1088/0004-637X/728/2/86.

Tomsick, J.A., Lingenfelter, R., Corbel, S., Goldwurm, A., Kaaret, P., 2004. Two New INTEGRAL Sources: IGR J15479-4529 and IGR J16418-4532. The Astronomer's Telegram 224, 1.

Torrejón, J.M., Negueruela, I., Smith, D.M., Harrison, T.E., 2010. Near-infrared survey of high mass X-ray binary candidates. A&A 510, A61. https://doi.org/10.1051/0004-6361/200912619.

Torres, D.F., Rea, N., Esposito, P., Li, J., Chen, Y., Zhang, S., 2012. A Magnetar-like Event from LS I +61 303 and Its Nature as a Gamma-Ray Binary. ApJ 744 (2), 106. https://doi.org/10.1088/0004-637X/744/2/106.

Townsend, L.J., Coe, M.J., Corbet, R.H.D., Hill, A.B., 2011. On the orbital parameters of Be/X-ray binaries in the Small Magellanic Cloud. MNRAS 416 (2), 1556–1565. https://doi.org/10.1111/j.1365-2966.2011.19153.x.

Townsend, L.J., Coe, M.J., Corbet, R.H.D., McBride, V.A., Hill, A.B., Bird, A.J., Schurch, M.P.E., Haberl, F., Sturm, R., Pathak, D., van Soelen, B., Bartlett, E.S., Drave, S.P.,

Udalski, A., 2011. The orbital solution and spectral classification of the high-mass X-ray binary IGR J01054-7253 in the Small Magellanic Cloud. MNRAS 410 (3), 1813–1824. https://doi.org/10.1111/j.1365-2966.2010.17563.x.

Tsyganhov, S.S., Doroshenko, V., Mushtukov, A.A., Lutovinov, A.A., Poutanen, J., 2018. On the magnetic field of the first Galactic ultraluminous X-ray pulsar Swift J0243.6+6124. MNRAS 479, L134–L138. https://doi.org/10.1093/mnrasl/sly116.

Tsyganhov, S.S., Doroshenko, V., Mushtukov, A.eA., Suleimanov, V.F., Lutovinov, A.A., Poutanen, J., 2019. Cyclotron emission, absorption, and the two faces of X-ray pulsar A 0535+262. MNRAS 487 (1), L30–L34. https://doi.org/10.1093/mnrasl/slz079.

Tsyganhov, S.S., Krivonos, R.A., Lutovinov, A.A., 2012. Broad-band observations of the Be/X-ray binary pulsar RX J0440.9+4431: discovery of a cyclotron absorption line. MNRAS 421 (3), 2407–2413. https://doi.org/10.1111/j.1365-2966.2012.20475.x.

Tsyganhov, S.S., Lutovinov, A.A., Churazov, E.M., Sunyaev, R.A., 2006. V0332+53 in the outburst of 2004-2005: luminosity dependence of the cyclotron line and pulse profile. MNRAS 371, 19–28. https://doi.org/10.1111/j.1365-2966.2006.10610.x.

Tsyganhov, S.S., Lutovinov, A.A., Churazov, E.M., Sunyaev, R.A., 2006. V0332+53 in the outburst of 2004-2005: luminosity dependence of the cyclotron line and pulse profile. MNRAS 371 (1), 19–28. https://doi.org/10.1111/j.1365-2966.2006.10610.x.

Tsyganhov, S.S., Lutovinov, A.A., Churazov, E.M., Sunyaev, R.A., 2007. 4U 0115+63 from RXTE and INTEGRAL data: Pulse profile and cyclotron line energy. Astronomy Letters 33 (6), 368–384. https://doi.org/10.1134/S1063773707060023.

Tsyganhov, S.S., Lutovinov, A.A., Doroshenko, V., Mushtukov, A.A., Suleimanov, V., Poutanen, J., 2016. Propeller effect in two brightest transient X-ray pulsars: 4U 0115+63 and V 0332+53. A&A 593, A16. https://doi.org/10.1051/0004-6361/201628236.

Tsyganhov, S.S., Lutovinov, A.A., Serber, A.V., 2010. Completing the puzzle of the 2004-2005 outburst in V0332+53: the brightening phase included. MNRAS 401 (3), 1628–1635. https://doi.org/10.1111/j.1365-2966.2009.15791.x.

Tsyganhov, S.S., Mushtukov, A.A., Suleimanov, V.F., Poutanen, J., 2016. Propeller effect in action in the ultraluminous accreting magnetar M82 X-2. MNRAS 457, 1101–1106. https://doi.org/10.1093/mnras/stw046.

Tsyganhov, S.S., Rouco Escorial, A., Suleimanov, V.F., Mushtukov, A.A., Doroshenko, V., Lutovinov, A.A., Wijnand s, R., Poutanen, J., 2019. Dramatic spectral transition of X-ray pulsar GX 304-1 in low luminous state. MNRAS 483 (1), L144–L148. https://doi.org/10.1093/mnrasl/sly236.

Tuerler, M., Chenevez, J., Bozzo, E., Ferrigno, C., Tramacere, A., Caballero, I., Rodriguez, J., Cadolle-Bel, M., Sanchez-Fernandez, C., Del Santo, M., Fiocchi, M., Tarana, A., den Hartog, P.R., Kreykenbohm, I., Kuehnel, M., Paizis, A., Puehlhofer, G., Watanabe, K., Weidenspointner, G., Zhang, S., 2012. A new hard X-ray transient discovered by INTEGRAL: IGR J18179-1621. The Astronomer's Telegram 3947, 1.

Underhill, A.B., 1975. Circumstellar lines in the spectrum of Eta Canis Majoris. ApJ 199, 691–693. https://doi.org/10.1086/153738.

Vallée, J.P., 2002. Metastudy of the Spiral Structure of Our Home Galaxy. ApJ 566 (1), 261–266. https://doi.org/10.1086/337988.

van den Heuvel, E.P.J., 2019. High-Mass X-ray Binaries: progenitors of double compact objects. arXiv e-prints. arXiv:1901.06939

van den Heuvel, E.P.J., Heise, J., 1972. Centaurus X-3, Possible Reactivation of an Old Neutron Star by Mass Exchange in a Close Binary. Nature Physical Science 239, 67–69. https://doi.org/10.1038/physci239067a0.

Vasilopoulos, G., Maitra, C., Haberl, F., Hatzidimitriou, D., Petropoulou, M., 2018. Identification of two new HMXBs in the LMC: an 2013 s pulsar and a probable SFXT. MNRAS 475, 220–231. https://doi.org/10.1093/mnras/stx3139.

Vinciguerra, S., Neijssel, C.J., Vigna-Gómez, A., Mandel, I., Podsiadlowski, P., Maccarone, T.J., Nicholl, M., Kingdon, S., Perry, A., Salemi, F., 2020. Be X-ray binaries in the SMC as (I) indicators of mass transfer efficiency. arXiv e-prints. arXiv:2003.00195

Voss, R., Ajello, M., 2010. Swift-BAT Survey of Galactic Sources: Catalog and Properties of the Populations. ApJ 721 (2), 1843–1852. https://doi.org/10.1088/0004-637X/721/2/1843.

Walter, R., Bodaghee, A., Barlow, E.J., Bird, A.J., Dean, A., Hill, A.B., Shaw, S., Bazzano, A., Ubertini, P., Bassani, L., Malizia, A., Stephen, J.B., Belanger, G., Lebrun, F., Terrier, R., 2004. 14 New Unidentified INTEGRAL Sources. The Astronomer's Telegram 229, 1.

Walter, R., Lutovinov, A.A., Bozzo, E., Tsyganhov, S.S., 2015. High-mass X-ray binaries in the Milky Way. A closer look with INTEGRAL. A&A Rev. 23, 2. https://doi.org/10.1007/s00159-015-0082-6.

Walter, R., Rodriguez, J., Foschini, L., de Plaa, J., Corbel, S., Courvoisier, T.J.-L., den Hartog, P.R., Lebrun, F., Parmar, A.N., Tomsick, J.A., Ubertini, P., 2003. INTEGRAL discovery of a bright highly obscured galactic X-ray binary source IGR J16318-4848. A&A 411, L427–L432. https://doi.org/10.1051/0004-6361/20031369.

Walter, R., Xu, M., 2017. Observations of Cygnus X-1 in the MeV band by the INTEGRAL imager. A&A 603, A8. https://doi.org/10.1051/0004-6361/201629347.

Walter, R., Zurita Heras, J., Bassani, L., Bazzano, A., Bodaghee, A., Dean, A., Dubath, P., Parmar, A.N., Renaud, M., Ubertini, P., 2006. XMM-Newton and INTEGRAL observations of new absorbed supergiant high-mass X-ray binaries. A&A 453, 133–143. https://doi.org/10.1051/0004-6361:20053719.

Wang, W., 2011. Long-term hard X-ray monitoring of 2S 0114+65 with INTEGRAL/IBIS. MNRAS 413 (2), 1083–1098. https://doi.org/10.1111/j.1365-2966.2010.18192.x.

Warwick, R.S., Norton, A.J., Turner, M.J.L., Watson, M.G., Willingale, R., 1988. A survey of the galactic plane with EXOSAT. MNRAS 232, 551–564. https://doi.org/10.1093/mnras/232.3.551.

Watson, M.G., Griffiths, R.E., 1977. Ariel V Sky Survey Instrument: extended observations of 3U 0900-40. MNRAS 178, 513–524. https://doi.org/10.1093/mnras/178.4.513.

Webster, B.L., Murdin, P., 1972. Cygnus X-1-a Spectroscopic Binary with a Heavy Companion ? Nature 235, 37–38. https://doi.org/10.1038/235037a0.

White, N.E., Nagase, F., Parmar, A.N., 1995. The properties of X-ray binaries. X-ray Binaries 1–57.

Wilson-Hodge, C.A., Malacaria, C., Jenke, P.A., Jaisawal, G.K., Kerr, M., Wolff, M.T., Arzoumanian, Z., Chakrabarty, D., Doty, J.P., Gendreau, K.C., Guillot, S., Ho, W.C.G., LaMarr, B., Markwardt, C.B., Özel, F., Prigozhin, G.Y., Ray, P.S., Ramos-Lerate, M., Remillard, R.A., Strohmayer, T.E., Vezie, M.L., Wood, K.S., NICER Science Team, 2018. NICER and Fermi GBM Observations of the First Galactic Ultraluminous X-Ray Pulsar Swift J0243.6+6124. ApJ 863 (1), 9. https://doi.org/10.3847/1538-4357/aace60.

Wolff, M.T., Becker, P.A., Gottlieb, A., Fuerst, F., Britton Hemphill, P., Marcu-Cheatham, D., Pottschmidt, K., Schwarm, F.-W., Wilms, J., Wood, K., 2016. The NuSTAR X-ray Spectrum of Hercules X-1: A Radiation-Dominated Radiative Shock. AAS/High Energy Astrophysics Division #15. pp. 120.24.

Wood, K., Bjorkman, J.E., Whitney, B.A., Code, A.D., 1996. The Effect of Multiple Scattering on the Polarization from Axisymmetric Circumstellar Envelopes. I. Pure Thomson Scattering Envelopes. ApJ 461, 828. https://doi.org/10.1086/177105.

Xing, Y., Wang, Z., Takata, J., 2017. Superorbital Modulation at GeV Energies in the γ-Ray Binary LS I + 61 303. ApJ 851, 92. https://doi.org/10.3847/1538-4357/aa9b36.

Xu, W., Stone, J.M., 2019. Bondi-Hoyle-Lyttleton accretion in supergiant X-ray binaries: stability and disc formation. MNRAS 488 (4), 5162–5184. https://doi.org/10.1093/mnras/stz2002.

Yamamoto, T., Sugizaki, M., Mihara, T., Nakajima, M., Yamaoka, K., Matsuoka, M., Morii, M., Makishima, K., 2011. Discovery of a Cyclotron Resonance Feature in the X-Ray Spectrum of GX 304-1 with RXTE and Suzaku during Outbursts Detected by MAXI in 2010. PASJ 63, S751–S757. https://doi.org/10.1093/pasj/63.sp3.S751.

Yamauchi, S., Aoki, T., Hayashida, K., Kaneda, H., Koyama, K., Sugizaki, M., Tanaka, Y., Tomida, H., Tsuboi, Y., 1995. New Transient X-Ray Source in the Scutum Region Discovered with ASCA. PASJ 47, 189–194.

Yang, J., Laycock, S.G.T., Christodoulou, D.M., Fingerman, S., Coe, M.J., Drake, J.J., 2017. A Comprehensive Library of X-Ray Pulsars in the Small Magellanic Cloud: Time Evolution of Their Luminosities and Spin Periods. ApJ 839 (2), 119. https://doi.org/10.3847/1538-4357/aa6898.

Yuan, W., Zhang, C., Ling, Z., Zhao, D., Wang, W., Chen, Y., Lu, F., Zhang, S.-N., Cui, W., 2018. Einstein Probe: a lobster-eye telescope for monitoring the x-ray sky. Proc. SPIE. Society of Photo-Optical Instrumentation Engineers (SPIE) Conference Series 10699. pp. 1069925. https://doi.org/10.1117/12.2313358.

Yudin, R.V., 2001. Statistical analysis of intrinsic polarization, IR excess and projected rotational velocity distributions of classical Be stars. A&A 368, 912–931. https://doi.org/10.1051/0004-6361:20000577.

Zamanov, R.K., Reig, P., Martí, J., Coe, M.J., Fabregat, J., Tomov, N.A., Valchev, T., 2001. Comparison of the Hα circumstellar disks in Be/X-ray binaries and Be stars. A&A 367, 884–890. https://doi.org/10.1051/0004-6361:20000533.

Zdziarski, A.A., Lubiński, P., Sikora, M., 2012. The MeV spectral tail in Cyg X-1 and optically thin emission of jets. MNRAS 423 (1), 663–675. https://doi.org/10.1111/j.1365-2966.2012.20903.x.

Zdziarski, A.A., Maitra, C., Frankowski, A., Skinner, G.K., Misra, R., 2012. Energy-dependent orbital modulation of X-rays and constraints on emission of the jet in Cyg X-3. MNRAS 426 (2), 1031–1042. https://doi.org/10.1111/j.1365-2966.2012.21635.x.

Zdziarski, A.A., Neronov, A., Chernyakova, M., 2010. A compact pulsar wind nebula model of the γ-ray-loud binary LS I +61˚ 303. MNRAS 403, 1873–1886. https://doi.org/10.1111/j.1365-2966.2010.16263.x.

Zdziarski, A.A., Pjanka, P., Sikora, M., Stawarz, Ł., 2014. Jet contributions to the broadband spectrum of Cyg X-1 in the hard state. MNRAS 442 (4), 3243–3255. https://doi.org/10.1093/mnras/stu1009.

Zhang, S., (eXTP Collaboration), 2019. The enhanced X-ray Timing and Polarimetry mission——eXTP. Science China Physics, Mechanics, and Astronomy 62, 29502. https://doi.org/10.1007/s11433-018-9309-2.

Zhang, S., Torres, D.F., Li, J., Chen, Y.P., Rea, N., Wang, J.M., 2010. Long-term monitoring of LS I +61˚ 303 with INTEGRAL. MNRAS 408, 642–646. https://doi.org/10.1111/j.1365-2966.2010.17152.x.

Zimmermann, L., Massi, M., 2012. Implications of the radio spectral index transition in LS I +61˚ 303 for its INTEGRAL data analysis. A&A 537, A82. https://doi.org/10.1051/0004-6361/201116706.

Zimmermann, L., Massi, M., 2012. Implications of the radio spectral index transition in LS I +61˚ 303 for its INTEGRAL data analysis. A&A 537, A82. https://doi.org/10.1051/0004-6361/201116706.

Zurita Heras, J.A., Chaty, S., 2008. INTEGRAL, XMM-Newton and ESO/NTT identification of AX J1749.1-2733: an obscured and probably distant Be/X-ray binary. A&A 489 (2), 657–667. https://doi.org/10.1051/0004-6361:20079097.

Zurita Heras, J.A., Chaty, S., 2009. Discovery of an eccentric 30 day period in the supergiant X-ray binary SAX J1818.6-1703 with INTEGRAL. A&A 493, L1–L4. https://doi.org/10.1051/0004-6361:200811179.

Zurita Heras, J.A., De Cesare, G., Walter, R., Bodaghee, A., Bélanger, G., Courvoisier, T.J.-L., Shaw, S.E., Stephen, J.B., 2006. IGR J17252-3616: an accreting pulsar observed by INTEGRAL and XMM-Newton. A&A 448, 261–270. https://doi.org/10.1051/0004-6361:20053876.

Zurita Heras, J.A., Walter, R., 2009. INTEGRAL and XMM-Newton observations of AX J1845.0-0433. A&A 494, 1013–1019. https://doi.org/10.1051/0004-6361:200810219.